

Characterization of temperature-sensitivity and its intragenic
suppression in *Saccharomyces cerevisiae* tRNA nucleotidyltransferase
mutants

Mark Goring

A

Thesis

in

The Department of

Biology

Presented in Partial Fulfillment of the Requirements

for the Degree of Master of Science (Biology)

at Concordia University

Montreal, Quebec, Canada

April 2011

©Mark Goring, 2011

CONCORDIA UNIVERSITY

School of Graduate Studies

This is to certify that the thesis prepared

By: Mark Goring

Entitled: Characterization of temperature-sensitivity and its intragenic suppression in *Saccharomyces Cerevisiae* tRNA nucleotidyltransferase mutants

and submitted in partial fulfillment of the requirements for the degree of

Master of Science (Biology)

Complies with the regulations of the University and meets the accepted standards with respect to originality and quality.

Signed by the final examining committee:

Dr. Dayanandan _____ Chair

Dr. Turnbull _____ Examiner

Dr. Zerges _____ Examiner

Dr. Storms _____ External Examiner

Dr. Joyce _____ Supervisor

Approved by _____ Selvadurai Dayanandan _____ Graduate Program Director

Brian Lewis _____ Dean of Faculty

Date April 12, 2011

ABSTRACT

Characterization of temperature-sensitivity and its intragenic suppression in *Saccharomyces cerevisiae* tRNA nucleotidyltransferase mutants

Mark Goring

ATP:CTP-specific tRNA nucleotidyltransferase enzymes catalyze the stepwise addition of one CMP, a second CMP, and finally an AMP as needed to generate the functional 3' termini of tRNA molecules. The following work concerns the structural and functional characterization of a temperature-sensitive variant E189F of tRNA nucleotidyltransferase from *Saccharomyces cerevisiae*, and two suppressor variants; R64WE189F and R64WE189K of this phenotype. Previous work has shown that E189K, E189F, and other variants of tRNA nucleotidyltransferase with substitution mutations at E189 are temperature-sensitive, and can exhibit enzymatic activity levels as low as 4% relative to that of native enzyme (Aebi *et al.*, 1990, Shan *et al.*, 2008). Moreover, E189F and E189K display almost identical levels of compromised thermal stability as compared to the native enzyme. Here, tRNA nucleotidyltransferase from recently isolated intragenic suppressor mutants of the temperature-sensitive phenotype are characterized in an effort to understand the development of the temperature-sensitive phenotype and its suppression. The suppressor strains R64WE189F and R64WE189K show a level of thermal stability that is comparable to E189F, or intermediate to E189F and E189 respectively. However, both suppressors display native-like levels of activity. It is evident that severely reduced activity is the major determining factor of the temperature-sensitive phenotype, not compromised thermal stability, and that a marked increase in specific activity is responsible for its suppression. Consequently, these data also suggest that the temperature-sensitive phenotype may be caused by an inability of temperature-sensitive variants to meet the demand for mature tRNA at the restrictive temperature.

Acknowledgments

I would first like to thank my supervisor Dr. Joyce for assigning me to such an interesting project, and express my gratitude for his support and availability throughout my program. I would also like to thank Pam for her excellent site-directed mutagenesis and growth work. Her cheerful presence helped make each day in the lab a sunny one. I would also like to say thank you to my committee members; Dr. Turnbull and Dr. Zerges, for their advice and guidance at various stages of my program. I would like to thank my external examiner; Dr. Storms, for his guidance and advice throughout my program. I would also like to express my special appreciation to Dr. Newman for her guidance, support, and teaching throughout my programs. Primarily, I would like to express my deepest appreciation to my family for their outstanding encouragement and support.

Mark E. Goring

Table of Contents

	page
Abstract.....	iii
Acknowledgments.....	iv
Table of Contents.....	v
List of Figures.....	ix
List of Tables.....	xi
List of Abbreviations.....	xii
1. INTRODUCTION.....	1
1.1 The nucleotidyltransferase superfamily.....	1
1.2 Class II tRNA nucleotidyltransferases.....	4
1.3 Properties and maturation of transfer RNA (tRNA).....	10
1.4 The mechanism of tRNA nucleotidyltransferase.....	11
1.5 <i>Saccharomyces cerevisiae</i> tRNA nucleotidyltransferase.....	16
1.6 Temperature-sensitive mutations and their suppression.....	17
1.7 The purpose of this study.....	21
2.0 MATERIALS AND METHODS.....	22
2.1 Strains, plasmids, growth media, solutions, and chemicals.....	22
2.2 Construction of protein expression vectors carrying wild-type or mutant tRNA nucleotidyltransferase.....	22
2.2.1 Generation of Polymerase Chain Reaction (PCR) products and their purification.....	22

2.2.2 Small scale isolation of plasmid DNA.....	25
2.2.3 Restriction digestion conditions.....	25
2.2.4 Agarose gel electrophoresis.....	25
2.2.5 Ligation conditions.....	26
2.2.6 Preparation of competent cells.....	26
2.2.7 <i>E.coli</i> transformations.....	27
2.3 Expression of GST-tRNA nucleotidyltransferase fusion protein and purification by GST-affinity chromatography (see Appendix for protocol).....	27
2.3.1 Expression of GST-tRNA nucleotidyltransferase fusion protein.....	27
2.3.2 Cell lysis.....	28
2.3.3 Column preparation.....	28
2.3.4 Purification and thrombin cleavage of GST-tRNA nucleotidyltransferase fusion protein.....	29
2.3.5 Protein concentration measurements.....	30
2.3.6 Sodium dodecyl sulphate polyacrylamide gel electrophoresis (SDS-PAGE).....	31
2.4 tRNA nucleotidyltransferase activity assays.....	32
2.4.1 Large scale plasmid isolation of G73 and pmBSDCCA from <i>E.coli</i>	32
2.4.2 Preparation of [$\alpha^{32}\text{P}$] GMP-labelled tRNA with N, NC, NCC, or NCCA 3'-ends by run-off transcription.....	33
2.4.3 Enzyme activity assays with [$\alpha^{32}\text{P}$] GMP-labelled tRNA prepared by run-off transcription.....	34
2.4.4 Denaturing polyacrylamide gels.....	35
2.5 Biophysical characterization of variant and native tRNA nucleotidyltransferase.....	36
2.5.1 Far-UV circular dichroism spectroscopy studies.....	36
2.5.2 Thermal denaturation studies by circular dichroism.....	37
2.5 Studies of intrinsic fluorescence at excitation wavelengths of 280 nm, and 295 nm.....	37

3.0 RESULTS.....	38
3.1 Plasmid construction.....	38
3.2 Over-expression and purification of GST-fusion proteins.....	39
3.3 Biophysical characterization of tRNA nucleotidyltransferase.....	42
3.3.1 Characterization of secondary structure by circular dichroism.....	42
3.3.2 Characterization of tertiary structure by fluorescence spectroscopy at excitation wavelengths of 280 nm and 295 nm.....	44
3.3.3 Temperature induced denaturation of native and variant enzymes monitored by circular dichroism spectroscopy.....	47
3.4 Run-off transcription activity assays.....	49
3.4.1 Digestion of G73 and pmBSDCCA plasmids by restriction enzymes.....	49
3.4.2 Enzyme activity assays with tRNA-N, tRNA-NC, or tRNA-NCC with ATP, CTP, or ATP and CTP at 22°C	50
3.4.3 Enzyme activity assays with tRNA-N, tRNA-NC, or tRNA-NCC under various NTP substrate availability conditions at 37°C.....	54
3.5 Growth data.....	56
4.0 DISCUSSION.....	58
4.1 Characterization of secondary and tertiary structure for the native and variant enzymes.....	58
4.2 Characterization of thermal stability of the native and variant enzymes.....	60
4.3 Characterization of enzyme activity of the native and variant enzymes.....	63
4.4 The salt bridge hypothesis of temperature-sensitive phenotype development.....	66
4.5 An alternative mechanism for development of the temperature-sensitive phenotype.....	67
4.6 Potential mechanism for suppression of the temperature-sensitive phenotype.....	72
5.0 CONCLUSIONS.....	75
6.0 FUTURE WORK.....	77
7.0 REFERENCES.....	80

8.0 APPENDIX.....	83
8.1 A GST-fusion protein purification protocol.....	83
8.2 Raw protein thermal denaturation profile data.....	86
8.3 Equation used to develop the ‘fraction unfolded vs. temperature’ protein thermal denaturation curve	87

List of Figures

Fig. 1-1 Motif A carries the signature sequence for all members of the NT superfamily.....	2
Fig. 1-2 General structure of the CCA-adding enzyme from <i>Bacillus stearothermophilus</i>	4
Fig. 1-3 Alignment of twelve class II tRNA nucleotidyltransferase sequences by clustalW.....	8
Fig. 1-4 The four tRNA nucleotidyltransferase crystal structures resolved to date.....	9
Fig. 1-5 Tertiary structure of yeast phenylalanine tRNA at 2.0 \AA resolution.....	10
Fig. 1-6 Illustration of the general tRNA processing pathway and acylation.....	11
Fig. 1-7 CCA-addition polymerization mechanism for the general two-metal ion-catalyzed reaction.....	13
Fig. 1-8 PYMOL representation of the <i>B. stearothermophilus</i> crystal structure (1MIV) showing the five catalytic domains; motif A to E (highlighted).....	15
Fig. 1-9 A cartoon representation of a model developed by PHYRE (http://www.sbg.bio.ic.ac.uk/~phyre/) of tRNA nucleotidyltransferase E189 from <i>Saccharomyces cerevisiae</i> (c1ou5A) based on the <i>H. sapiens</i> structure (1OU5).....	17
Fig. 1-10 Replica plating experiment of <i>S. cerevisiae</i> YPH500 E189, the temperature-sensitive mutants E189F and E189K, the double mutant suppressors R64WE189F and R64WE189K, the single mutant R64W, and with vector alone.....	19
Fig. 3-1 1% Agarose gel of PCR products used to make plasmid constructs.....	38
Fig. 3-2 SDS-PAGE of lysate from induced and non-induced E189, R64W, R64WE189F, and R64WE189K carrying strains (expression test).....	40
Fig. 3-3 SDS-PAGE of protein eluate for purification of E189.....	41
Fig. 3-4 SDS-PAGE of all purified proteins used in this study showing protein quality.....	41
Fig. 3-5 Far-UV Circular Dichroism spectra for the wild-type enzyme E189, and variant enzymes R64W, R64WE189F, R64WE189K, and E189F.....	43
Fig. 3-6 Fluorescence emission spectra for native and variant tRNA nucleotidyltransferases excited at 280 nm.....	45

Fig. 3-7 Fluorescence emission spectra for native and variant tRNA nucleotidyltransferases excited at 295 nm.....	46
Fig. 3-8 Overlaid thermal denaturation curves for E189, and each of the variant enzymes.....	48
Fig. 3-9 1% Agarose gel of digested G73, and pmBSDCCA plasmids.....	49
Fig. 3-10 Gel assay results for native and variant enzymes under various ATP and CTP availability conditions with tRNA-N.....	51
Fig. 3-11 Gel assay results for native and variant enzymes under various ATP and CTP availability conditions with tRNA-NC.....	52
Fig. 3-12 Gel assay results for native and variant enzymes under various ATP and CTP availability conditions with tRNA-NCC.....	53
Fig. 3-13 Gel assay results for native and variant enzymes under various ATP and CTP availability conditions with tRNA-N, tRNA-NC, or tRNA-NCC conducted at 37°C.....	55
Fig. 3-14 Replica plating experiment at 22°C and 37°C for testing of the ‘salt bridge hypothesis’ (Adapted from images provided by Dr. Pamela J. Hanic-Joyce).....	57
Fig. 4-1 PyMOL models of three crystallized tRNA nucleotidyltransferases illustrating hydrogen bond interactions that occur between the residue equivalent to position 189 and elements of the β -turn.....	69
Fig. 4-2 A cartoon representation of a model developed by PHYRE (http://www.sbg.bio.ic.ac.uk/~phyre/) of tRNA nucleotidyltransferase E189 from <i>Saccharomyces cerevisiae</i> (c1ou5A) based on the <i>H. sapiens</i> structure (1OU5).	70
Fig. 8-2: Raw protein thermal denaturation profile data.....	86

List of Tables

Table 2-1 Recipes for media and buffers.....	23
Table 2-2 chemical list.....	24
Table 3-1 Fluorescence emission maxima of native and variant proteins measured at 22°C and excited at 280 nm.....	45
Table 3-2 Fluorescence emission maxima of native and variant proteins measured at 22°C and excited at 295 nm.....	46
Table 3-3 The melting temperature (T_m), and percent remaining α -helicity at 37°C for E189 and each of the variant enzymes.....	48
Table 3-4 The counts for each product of activity assays conducted with tRNA-N and each of the five enzymes.....	51
Table 3-5 The counts for each product of activity assays conducted with tRNA-NC and each of the five enzymes.....	53
Table 3-6 The counts for each product of activity assays conducted with tRNA-NCC and each of the five enzymes.....	54
Table 3-7 The counts for each product of activity assays conducted at 37°C with tRNA-N, tRNA-NC, or tRNA-NCC substrate and each of the five enzymes.....	55
Table 4-1 Growth, activity, and biophysical parameters of the native protein and all of the variants characterized to date.....	61
Table 4-2 Four combinations of activity and thermal stability represented by the native (E189) and three variant proteins (E189F, R64WE189F, and E189H).....	66

List of Abbreviations

Amp: Ampicillin	SDS: Sodium dodecyl sulfate
AMP: Adenosine monophosphate	TBE: Tris-boric acid-EDTA
APS: Ammonium persulfate	TEMED: Tetramethylethylenediamine
ATP: Adenosine triphosphate	Tm: Melting temperature
BSA: Bovine serum albumin	ts: temperature-sensitive
CD: Circular dichroism	tRNA: Transfer ribonucleic acid
CTP: Cytidine triphosphate	tRNA NT: tRNA nucleotidyltransferase
dH ₂ O: Distilled water	UV: Ultraviolet
DNA: Deoxyribonucleic acid	YT: Yeast tryptone
EDTA: Ethylene diamine tetra-acetic acid	
EtBr: Ethidium bromide	
GST: Glutathione-S-transferase	
GTP: Guanosine triphosphate	
H-bond: Hydrogen bond	
IPTG: Isopropyl-β-D-Thiogalactopyranoside	
mdeg: Millidegrees	
NTP: Nucleoside triphosphate	
PBS: Phosphate-buffered saline	
PCR: Polymerase chain reaction	
PEG: Polyethylene glycol	
RNA: Ribonucleic acid	
rpm: Rotations per minute	

1.0 INTRODUCTION

ATP:CTP-specific tRNA nucleotidyltransferase enzymes catalyze the stepwise addition of one CMP, then a second CMP, and finally an AMP to generate functional 3' termini of tRNAs. The fact that this enzyme is essential in eukarya, archaea, and many eubacteria (Aebi *et al.*, 1990), as well as its remarkable activity to polymerize a specific nucleotide sequence without the use of a nucleic acid template, but with high fidelity, have made it the subject of much interest. The following work concerns the structural and functional characterization of temperature-sensitive variants of tRNA nucleotidyltransferase from *Saccharomyces cerevisiae*, and their corresponding suppressors. A temperature-sensitive yeast strain, unable to grow at 37°C, was isolated in 1990 (Aebi *et al.*, 1990). Subsequent work showed that this and other temperature-sensitive variants of tRNA nucleotidyltransferase with substitution mutations at amino acid 189 can exhibit enzymatic activity levels as low as 4% relative to that of native enzyme (Shan *et al.*, 2008). Here, recently isolated intragenic suppressor variants of the temperature-sensitive phenotype are characterized in an effort to understand the development of the temperature-sensitive phenotype and its suppression, in this strain.

1.1 The nucleotidyltransferase superfamily

This enzyme represents one member of the nucleotidyltransferase (NT) superfamily (Li *et al.*, 2002; Neuenfeldt *et al.*, 2008). The entire NT superfamily itself is defined only by a homologous polymerase domain, with a consensus active site sequence; G[SG][LIVMFY]xR[GQ]x_{5,6}D[LIVM][DE]-[CLIVMFY]₃₋₅ (Fig. 1-1) (Xiong *et al.*, 2003; Li *et al.*, 2002). This superfamily consists of enzymes capable of adding nucleotides to a remarkably diverse set of substrates; DNA, RNA, protein, and antibiotics (Xiong *et al.*, 2003). They are also involved in a wide range of processes, such as DNA replication, translation, telomere maintenance, transcription, DNA/RNA ligation, and RNA processing (Betat *et al.*, 2010).

bst_cca	(20)	YDAYFV GGAVRD LLLGRPIG--- DVD IATSA---
ec_cca	(1)	MKIYLV GGAVRD ALLGLPVK--- DRD WVVVG---
aae_a	(452)	LRAYIV GGVVRD ILLGKEVW--- DVD FVVEGNAIELAKELARRHGVNVHPFPEFGTAHLK
aae_cc	(35)	HYCFIV GGWVRD RILGEPVGYNI DVD FLTTADPVELAKNFAKRIGGHFFVFEKRGFLIKR
bsu_cca	(20)	HQAYFV GGAVRD SYMKRTIG--- DVD IATDA---
sce_cca	(60)	LTLRIT GGWVRD KLLGQGSH--- DLD IAINV---

MSGE(8aa) QQHYAKYGAKPHNIHKI

Fig. 1-1: Motif A carries the signature sequence for all members of the NT superfamily *B.stearothermophilus* (bst_cca), *E. coli* (ec_cca), *A. aeolicus* CC-adding enzyme (aae_cc), *A. aeolicus* A-adding enzyme (aae_a), *B. subtilis* (bsu_cca), *S. cerevisiae* (sce_cca). The boxed sequences are motif A. The two catalytic aspartic acids are highlighted at the right end of the boxed sequences (Li et al., 2002).

The polymerase β superfamily to which all tRNA nucleotidyltransferases belong shows the broadest substrate and reaction spectrum of all of the nucleotidyltransferase subfamilies. The amino acid signature sequence shared by this family is $hG[GS]x(9,13)Dh[DE]h$ (x = any amino acid; h = a hydrophobic amino acid), and resides inside a consensus fold composed of a five strand antiparallel β -sheet, with two flanking α -helices (Betat *et al.*, 2010). Also, two highly conserved carboxylates (DxD or DxE), which serve to coordinate two catalytically essential divalent metal ions are found within the β -sheet sequence (Betat *et al.*, 2010).

The polymerase β superfamily is further subdivided into two subgroups; class I nucleotidyltransferases and class II nucleotidyltransferases, based on additional sequence elements. However, these two groups essentially have only the signature motifs described above in common. In fact, phylogenetic studies suggest that either the two classes separated very early in evolution, or this polymerase activity arose twice during evolution (Betat *et al.*, 2010; Xiong *et al.*, 2003).

Aside from the NT signature sequence, class I nucleotidyltransferases are a very large and rather heterogenous group, in terms of sequence and activity. In fact, class I nucleotidyltransferases bear little sequence similarity even to other enzymes within the class. Notable members of this class include the eukaryotic DNA polymerase β (pol β), archeal tRNA nucleotidyltransferases, eukaryotic poly (A)

polymerases, the polymerase X family, terminal deoxynucleotidyltransferases (TdT), antibiotic nucleotidyltransferases, and protein nucleotidyltransferases (Xiong *et al.*, 2003; Betat *et al.*, 2010).

The class II nucleotidyltransferases represent a much smaller group of different enzyme activities than do the class I nucleotidyltransferases, consisting solely of bacterial and eukaryotic tRNA nucleotidyltransferases, as well as bacterial poly (A) polymerases (Betat *et al.*, 2010). Members of this class exhibit high homogeneity along the entire N-terminal 25 kDa region, with several conserved active site motifs (Betat *et al.*, 2010).

While tRNA nucleotidyltransferases belong to a specific subgroup of nucleotidyltransferases including terminal deoxynucleotidyltransferases (TdT), terminal uridyltransferase, and poly (A) polymerase (Betat *et al.*, 2010) that are capable of adding nucleotides to a nucleic acid primer (DNA or RNA), independent of any nucleic acid template, tRNA nucleotidyltransferase displays the most sophisticated activity, adding the C-C-A sequence to the 3'-end of immature tRNA molecules that are missing all, or just part of the trinucleotide sequence (Betat *et al.*, 2010). By comparison, TdT adds any of the four deoxynucleotides available (dATP, dCTP, dGTP, or dTTP) to the 3'-end of its DNA substrate, while poly (A) polymerase synthesizes long poly-adenylate tails at the 3'-ends of its mRNA primary substrates, and uridylyl transferase adds only UMP to mRNA, and other small transcripts (Betat *et al.*, 2010).

Several crystal structures from both classes of nucleotidyltransferases have been resolved. These resolved enzymes include pol β , KNT, and eukaryotic PAP from class I, as well as eukaryotic and eubacterial tRNA nucleotidyltransferases from class II (Betat *et al.*, 2010). It is evident from these structures that all members of the NT superfamily share at least two common structural traits (Xiong *et al.*, 2003): (1) all members of the NT superfamily carry a homologous polymerase domain, with the β -sheet motif described above, with an embedded NT signature sequence, and (2) all members carry additional domains, with different structures suited to different functions. For example, the thumb

domain of polymerase β (pol β) is required to bind a double stranded DNA primer, whereas the body and tail regions of class II tRNA nucleotidyltransferases serve a tRNA binding function.

1.2 Class II tRNA nucleotidyltransferases

The structure of tRNA nucleotidyltransferase has been likened to that of a sea-horse (Li *et al.*, 2002); consisting of a head, neck, body, and tail region (Fig.1-2). The active site is located in the head region, and the other regions are involved either directly or indirectly in NTP and/or tRNA binding.

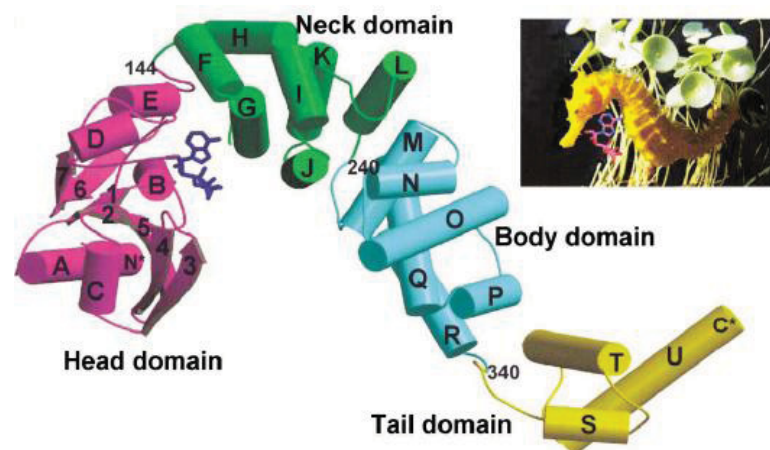


Fig. 1-2: General structure of the CCA-adding enzyme from *Bacillus stearothermophilus* (Li *et al.*, 2002).

Class II CCA-adding enzymes differ from class I CCA-adding enzymes in terms of their primary sequence, overall architecture, catalytic strategy for template-independent nucleotide incorporation, and evolutionary conservation (Betat *et al.*, 2010). In contrast to class I enzymes, only the head domain contains a β -sheet, with high α -helical content distributed throughout the rest of the protein (Betat *et*

al., 2010). The head domain is homologous to the palm domain of DNA polymerase β , although it does not carry a thumb domain that is required for the binding of a double-stranded DNA primer (Betat *et al.*, 2010).

Additionally, class II enzymes show high conservation of five individual catalytic core motifs, designated A to E (Fig. 1-3) (Betat *et al.*, 2010). Several of these motifs have defined roles and are involved in metal ion binding, catalysis, ribose recognition, nucleotide selection, and templating (Betat *et al.*, 2010). Motif A is located in the head domain, and contains the general NT signature motif carrying the two metal-binding carboxylates. There is no sequence similarity between class I and II tRNA nucleotidyltransferases beyond this motif (Betat *et al.*, 2010).

CLUSTAL 2.0.12 multiple sequence alignment

TM	-----	
AA	-----	
EC	-----	
PA	-----	
SC	-MLRSTISLLMNSAAQKMTNSN-----	22
CG	-MFKAIRRVT-----	10
KL	-MFKMV-----	5
AT	MRLSSLPIN-TLINLP--KSLFLISPFRNRNLNRSLTVASRISSLLRVSGVSSRPCGYW	57
LA	MRLSFKTVTNTVVVLPGRTRSIINFILFPTITSNLVLHP-----LLRTPKTPS-----FH	51
HS	MHHHHHHSSGLVPRGSGMKTAAKFERQHMDSPDLGTDD-----	40
MM	-MQSVLYP--WHRQVLRCWSRLCLLKRYLF-----	29
BS	-----	
TM	-MQIFRDVS KLLVERVDPKILNLFRLLKGFGDEVN-----MPV	37
AA	-MVGQIAKEMG-----LRA	13
EC	-----MKI	3
PA	-----MQI	3
SC	-FVLNAPKITLTKEQNICONLLNDYTDLYNQKYHNKPEPLTL	63
CG	-MIPRIQLTEKETRICCNLLKDYTAHYNSLHYGQ-EPLTL	47
KL	-ASKIQLNKVESEICLTKEFCSHYNKANAET-EPLVA	41
AT	FSTNAAMTNVGEEDKQSIPSIELKENIELTDKERKIFDRLLSTLRYCN-----LDTQL	110
LA	SSLSSPMSSHKVRDNIQLSDVEKRIFDRLLATLRFFN-----LQTHL	93
HS	DDKMKLQSPEFQSLFTEGLKSLSLTEL FVK-----ENHEL	73
MM	-MKLQSPEFQSLFTEGLKSLSLTEL FAK-----ENHEL	59
BS	-MKPPFQEALGIIQQLQHQG-----YDA	22
Motif A		
TM	YVVGGFVRDLLLGIKNLDIDIVVEGNA-----LEFAEYAKRFLP-----GKLV	80
AA	YIVGGAVVRDILLGKEVWDVDFVVEGNA-----IELAKELARRHG-----VN VH	56
EC	YLVGGAVVRDALLGLPVKDRDWVVVG-----STPQEMLDAGYQ-----QVGR	44
PA	YKVGGA VRD RLL GRPVTDIDWVVVG-----ASSDEMLARGYR-----PVGA	44
SC	RITGGWVRDKLLGQGSHDL DIA IN VMSGE QFAT GLNE YLQQHYAKYGA KPHNIH KID KNP	123
CG	RITGGWVRDKLLGQGSHDL DIA IN VMSGE QFAT GLNE YLQQHYAKYGA KPHNIH KID KNP	107
KL	RITGGWVRDKLLGQGSHDL DIA IN VMSGE QFAT GLNE YLQQHYAKYGA KPHNIH KID KNP	97
AT	RVAGGVVRD KLL GKE CYD IDIA LD KMMG TEF VDKV RE LLS I-----DEEVQGD TVIER N	166
LA	RVAGGVVRD KLL GKE CYD IDIA LD KMMG TEF VDKV RE LLS I-----GEEAQGV C VIES N	149
HS	RIAGGA VRD L L NGVK P QD ID FATT ATP-----TQMKE MFQSAG-----IRMIN	116
MM	RIAGGA VRD L L NGVK P QD ID FATT ATP-----TQMKE MFQSAG-----IRMIN	102
BS	YFVGGA VRD L L GRPI GDV DIAT S ALP-----EDVMA IFPKT-----IDVGS	64
	*** * * * * *	.
Motif B		
TM	KHDKFMTASLFLKGGLRIDIATARLEYYESPAKLPDVE-MSTIKKDLYRRDFTINAMA IK	139
AA	PFPEFGTAHLKIG-KLKLEFAT TARRETYPRPGAYPKV-E-PASLKE DLI RR DFTINAMA IS	114
EC	DFFPVFLHPQTH EYALAR TERKS GSG YT G-----FTCYA AP-DVTLEDDLKRRDLTINA LAQ	100
PA	DFFPVFLHPQSGEEY ALAR TERKS GSG YT G-----FTFHASP-EVTLEEDL T RRD LTINA MAE	100
SC	EKSKHLETATTKLFGVEVDFVNLRSEKYTELSRIPKVC-FGTPEE DALRRD ATLNALFYN	182
CG	EKSKHLETATTKLFGVEVDFVNLRSEKYTELSRIPKVC-FGTPEE DALRRD ATLNALFYN	166
KL	SKSKHLETCTT KLF DV PFDV FNLRSE EY TME SRIPKVC-FGTPEY DDAMRRD ATLNAMFYN	156
AT	DQSKHLETAKL RIYD QWID FVN LRSE EY TENS R IPT MK-FGTAKK DAF RRD LTINS LFYN	225
LA	DQSKHLETARMRL FDM WID FVN LRSE EY TD NSRIPSMQRFGTPEE DAY RRD LTINS LFYN	209
HS	NRGEKHGTITARLHEENFEITT LR-IDVTTDGRHAEVEFTTDWQKDAERRDLTINS MFLG	175
MM	NKGEKHGTITARLHEENFEVTT LR-IDVTTDGRHAEVEFTTDWQKDAERRDLTINS MFLG	161
BS	KHGTVVVHKG KAYEVTTFKTDGDYEDYR RPESVTFVR-SLEEDLKRRDFTMNAIAMD	121
	.* *** *;:::	
Motif C		
TM	LNP KDF GLL ID FFG-GYR DLKEGVIR VLHTL-SFVDD PTR IL RAI RFE QR-FDF RI	192
AA	VNLEDY GTL IDY FG-GLRDLKDKVIR VLHPV-SFIEDP VRL RALRFAGR-LNF KL	167
EC	--DDNGEI ID PYN-GLGDLQNRLLRH VSP-AFGEDPLRVL RVARFAARYAH LGF RI	152
PA	--DEQGRV ID PYG-GQADLEAR LL RH VSP-AFAEDPLRVL RVARFAARYAG LGF RV	152
SC	--IH KGEVEDFTKRG LQDLKDGVLRTPLPAKQTFLDDPLRVL RLI RFAS R-FNFT I	235
CG	--IQQDAVE DFTKRG WQDLQDGVLRTPLPARQTFLDDPLRVL RLI RFAS R-FN FNI	219
KL	--ITEKIEDFTKKGFQDLNDGILRTPLPPRQTFIDDPLRVL RLI RFAS R-FN FQ I	209
AT	--INSGA VEDLTERGIDDLKSGKIVTPLPAKATFLDDPLRVL RAVRFGAR-FGFT L	278
LA	--INTDSVEDFTKRGISDLKSGKIVTPLPPKATFLDDPLRVR VAI RF GAR-FEFT L	262

	Motif C	Motif D	
HS	----FDGTLFDYFN--GYEDLKNKKVRFVGAKQRIQEDYLRLRLRYFRFYGR---IVDKP	226	
MM	----FDGTLFDYFN--GYADLKNKKVRFVGAKQRIQEDYLRLRLRYFRFYGR---IVDRP	212	
BS	----EYGTIIDPFG--GREAIRRRIIRTVGEAEKRFREDALRMMRAVRFVSE---LGFAL	172	
	: * : . : Motif E : : * * ; * ** . :		
TM	EETTERLLK-QAVEEGYLERTTGPRLRQELEKILEEKNPLKSIRRMAQFDVIKHLFPKTY	251	
AA	SRSTEKLK-QAVNLGLLKEAPRGRLINEIKLALREDRFLIELEYRKYRVLEEEIEGFQ	226	
EC	ADETLTLMR-EMTHAGELEHLTPERVKETENALTTTRNPQVFQVLRDCGALRVLPEID	211	
PA	AAETLALMR-QLAESGELQALTPERSWKEISRALMPEPNPEVFIQVQLHDCGALAEIPEVE	211	
SC	DPEVMAEMGDPQINAVFSKISRERGVEMEKILVGPPTPLALQLIQRAHLENVIFFWHN	295	
CG	EAGVLKEMHDPEINEAFNFKISRERIGVEMEKILVGPNPILGLKLQIQRTHLENVIFLWHD	279	
KL	DPQTYQAMRDPGIHQSFNKHISKGRVYTEMHKTLTSANPFYALDLIQGAHLSRVIFTTNE	269	
AT	DEELKEAASSEEVRVALGEKISRERIGNEIDLMISSNGNPVSAVTYLSDLKLFSVVFALPS	338	
LA	DEDLKQAAACDEVKDALAAKISRERIGTEIDLMISSNGNPVKAATYICDLTIFWIVFSLPP	322	
HS	GDHDHETLEAIAENAKLAGISGERIWEVKLKVGNHVNHЛИYDLDVAPYIGL PAN	286	
MM	GDHDHETLEAIAENAKLAGISGERIWEVKLKVGNHVNHЛИYDLDVAPYIGL PAN	272	
BS	APDTEQAIV--QNAPLLAHISVERMTMEMEKLLGGPFAARALPLLAETGLNAYLPGLAG	229	
	* * : . : :		
TM	YTPSMDEKMENLF-----RNIPWVEENFG--EVDRFYAV	283	
AA	WNEKVLQKLYALR-----KVVDWHALEFSEERIDYGWL	260	
EC	ALFGVPAPAPARWHP-----EIDTGIHTLMTLSMAAMLSQ	245	
PA	ALFGVPQPAAHHP-----EIDTGVHVLSQLQCARHRQP	245	
SC	DSSVVKFNEENCQDMKDINKHVNNDN--ILNSHLKS--FIELYPMFLEKLPILREKIG-RS	350	
CG	DQSVIEYNRKNWPQTKDVEDIYKKG--IFNHHLKN--FIHHYKDFLSRYLKLQAIETKD	335	
KL	SS-----PEIESIYEN--LDQHLKS--VVETIPKLLKSHTTFASVFP---	307	
AT	SAEPSPPENCGSLSQSYLEAMMSLL--KTPRPGKFSGEQRRRLALYAAMFLPFRKTVYKDT	396	
LA	TFEPAISDGCRCLCISQLDISWNLI--HLLGKTTFTDEQRRLTLYAAMFLPLRNNTIYREK	380	
HS	AS-----LEEFDKVSKNVDG-----FSPKPVTLLASLFKVQDDVTKLD	324	
MM	AN-----LEEFNKVSKNVEG-----FSPKPMTLLASLFKVQDDVTKLD	310	
BS	KE-----KQLRLAAAYRPWLAAREER	251	
TM	LHVFLEFYDDESWKEVRDRYSLRRNLINEIRHVEKSAPALLEMLSERVPASFVYPLVKGV	343	
AA	LLILISNLNDYERGKHFLEEMSAPSWSVRETYKFMKFLGSLKEELKAKENYEVYRLLKPL	320	
EC	VDVRFTTLCHDLGKLTPELWPRHHGPGAVKL--VEQLCQRLRVPNEIRDALARLVAEF	304	
PA	LSVRWACLLHDLGKGLTSEADWRPHIAHEARGVPL-IDAVNQRFRVPRDCQELARLVGEY	304	
SC	PGFQQNFILSAILSPMANLQIIGNPKKKINNLVSVTESIVKEGLLKSNDAAVIAKTVDS	410	
CG	KSFQQNFLLASILIPMADLKIALPKKKLNNTLPVSESESIVREGLKFNKASSIVVARCVEN	395	
KL	-GMQEPLILSVLSGFKGLK--GPDPAKPKNSIPLAGVITKEGLNFPNTQVDNVIACVES	364	
AT	KGKSIPVVNHIFKFSMKRKTSDAETVMNIHQTTFRSLIPSLEVKKDVELDEL TWAADI	456	
LA	KAKKVPVVNYIFRESLKRKAKDPTVLDLHRSASNFKLSLIPCLVSNEDVQIVGHDWMTEL	440	
HS	LRLKIAKEEKNLGLFIVKNRKDLIKATDSSDPLKPYQDFVIDSREP DAT-----	373	
MM	LRLKISKEEKNLGLFIVKNRKDLIKATDSSDPLKPYQDFVIDSREP DAT-----	359	
BS	WALLHALGVQESRPFLRAWKLPNKVVDEAGAILTALADIPRPEAWTNEQLFSAGLERAL	311	
TM	SNE-----TICHFLAYLSGEKEGLFKSYLLKKIKNTKLEKINGEYLIR-----	385	
AA	H-----TSVLLLLMLLEEELKEKIKLYLEELRKVKLPKEKIEELKK-----	360	
EC	HD-----LIHTFPMLNPKTIVKLFDSIDAWRKPVQRVEQLALTSEAD-----	345	
PA	HT-----HAHRALELRPNTLLELLQSFDVYRRPQRFEEFVAASEMD-----	345	
SC	ICSYEEILAK--FADRSQKKSEIGIFLRFNNGEWEATAHFASLSDAFLKIPKLETKIEL	468	
CG	IAAYNSMVEK--YLGSGDLKRSEVGTFRLRELRGDWIEVHYVSLMDQYLYKISRKDNVNM	452	
KL	EDSYHNLVK--NGKSMKRSLELGKLNQWQMVHFYNLCDYLRHGDEP-----	413	
AT	LEHWKSITLNDPVIATSKIRVLTGFLRLKDFWRVSLTSLLSATVDGSNDHQDIGQ	516	
LA	ID-----VPVSSRVRVLTGFLRLRDFWRVALLISILLHP-ID-VNDEDE--	485	
HS	-----TRVCELLKYQGEHCLLKEMQQWSIPPFP-----	401	
MM	-----ARVCELLKYQGEHGLLKEMQQWSVPPFP-----	387	
BS	S-----VETVRAFTGAPPGPWHEKLRRRFASLPIKTKG-----	345	
TM	-----KGITSGKIIIGEVLEK-----ILMKKLDGDTRD---EEEILEE	419	
AA	-----QGLK-GKELGERIEE-----LKREIMN-----	381	
EC	-----VRGRTGFESADYPQGRWLREAWEVAQSPTKAVV---EAGFKGV	386	
PA	-----ARGRGLEQRDYPQAAYLGAQAARAVSVKPLV---EKGLKGA	386	
SC	-----LFQNYNEFYSYIFDNNLNNCHELKPIVDGKQMAKLLQMKGPG-WLGTKINNEAI	520	
CG	-----IIDKYDRFWNYIQEQNLQDSDKMVPIIDGKRMVKILETKPGP-WLGTKINDEVI	504	
KL	-----IPHYDEFYKHVDCKLDDVYTLKHIINGKELAKLLDRKPGI-WMGETLDRIL	464	

AT	LDFQLERMRETYLTVEATIHEGLDKIWDAKPLVNNGREIMQIAELKGGSRLLREWQQKLL	576
LA	-SSQLSKRRDLFNTVENVIKLGLEKVWDVKQLINGKDVMCSVLQLKGGP-MVKEWLDKAM	543
HS	-----VSGHDIRKVG---ISSGKEIGALLQQLREQ-----	428
MM	-----VSGHDIRKVG---ISSGKEIGALLQQLREQ-----	414
BS	-----ELAVNGKDVIEWVGKPGPWWKEALDAIWRRAVNN-----	379
TM	VLASLETEGKLAAALEHHHHHH-----	441
AA	-----KIKLAAALE-----	390
EC	EIREELTRRRRIAAVASWKEQRCPKPE---	412
PA	ELGEALKRARLAALKAYKEERGKA-----	410
SC	RWQFDNPTGTDQELITHKAILPKYL---	546
CG	LWQFDHPQGTEQELISFIKSILPNYLQ--	531
KL	IWQLDNPDISKETFIENLNDIVHLP-----	489
AT	TWQLAYPNGTAECKEWMRDIKAKRQRIE	605
LA	ACNLPIP-----QELQRNVLIG-----	560
HS	-WKKSGYQMEKDELLSYIKKT-----	448
MM	-WKKSGYRMEKDELLSYIKKT-----	434
BS	-GEVENEKERIYAWLMERNRTREKNC---	404

Fig. 1-3: Alignment of twelve class II tRNA nucleotidyltransferase sequences by ClustalW (Larkin *et al.*, 2007). *Thermotoga maritima*, TM (3H38_A); *Aquifex aeolicus*, AA (1VFG_A); *Escherichia coli*, EC (NP_289631); *Pseudomonas aeruginosa*, PA (YP_788757); *Saccharomyces cerevisiae*, SC (NP_011095); *Candida glabrata*, CG (XP_449283); *Kluyveromyces lactis*, KL (AAG00316); *Arabidopsis thaliana*, AT (NP_173680); *Lupinus albus*, LA (AAB03077); *Homo sapien*, HS (10U5_A); *Mus musculus*, MM (NP_081572); *Bacillus stearothermophilus*, BS (Q7SIB1). Accession numbers are bracketed above.(*) are amino acids conserved in all presented sequences, (:) conservation of highly similar amino acids, (.) conservation of slightly similar amino acids. The conserved Motifs A-E are delineated by a line (Li *et al.*, 2002). The amino acids corresponding to E189 are revealed by (→). The amino acids corresponding to R64 are revealed by (↗). The essential catalytic acidic residues are revealed by (↘).

To date, the crystal structures of four class II tRNA nucleotidyltransferases have been resolved. Three are from the domain eubacteria; *Bacillus stearothermophilus* (Li *et al.*, 2002), *Thermotoga maritima* (Toh *et al.*, 2009), and *Aquifex aeolicus* (Tomita *et al.*, 2004), as well as one from the domain Eukarya; *Homo sapiens* (Augustin *et al.*, 2003) (Fig. 1-4). Examination of these available crystal structures clearly show the overall “seahorse” -like shape with four distinguishable domains; head, neck, body, and tail. Also, apparent in these crystals, is the single β-sheet found in the head domain, which is the hallmark of all nucleotidyltransferases (Betat *et al.*, 2010).

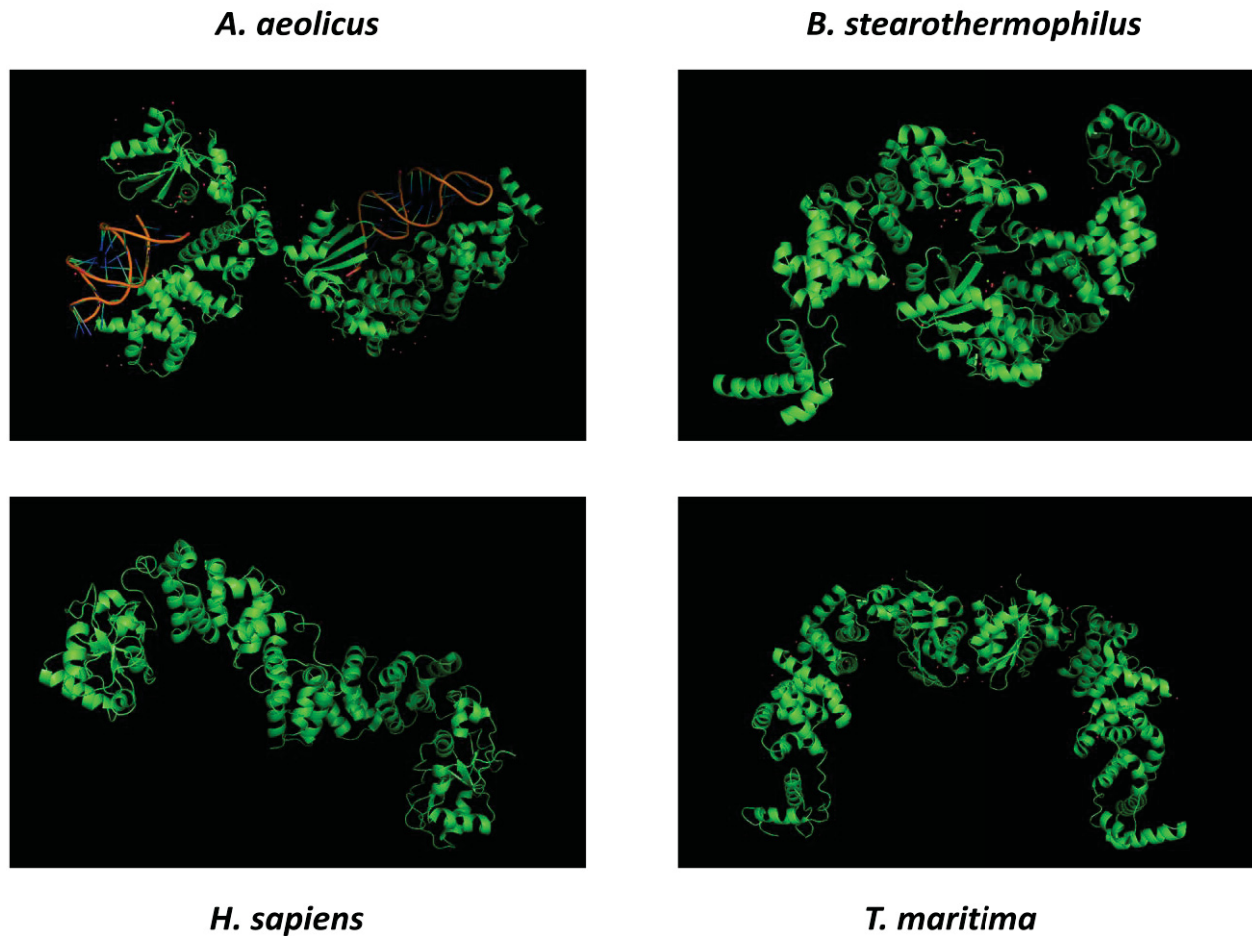


Fig 1-4: The four tRNA nucleotidyltransferase crystal structures resolved to date. Above are PYMOL cartoon representations of tRNA nucleotidyltransferases from four different organisms; *A. aeolicus* (Tomita *et al.*, 2004; PDB ID: 1VFG), *B. stearothermophilus* (Li *et al.*, 2002; PDB ID: 1MIW), *H. sapiens* (Augustin *et al.*, 2003; PDB ID: 1OU5), and *T. maritima* (Toh *et al.*, 2009; PDB ID: 3H37).

1.3 Properties and maturation of transfer RNA (tRNA)

The adapter molecule function of tRNAs to convert nucleic acid sequence information to polypeptide sequence information during the translation process is well characterized (Voet and Voet, 2004). Mature tRNA exists in a secondary structure with a characteristic cloverleaf-like fold brought about by many intramolecular Watson-Crick base-pairing interactions (Voet and Voet, 2004).

The tertiary structure has a characteristic L shaped conformation achieved when all of the loop and stem structures are folded back on each other, except for the anti-codon loop and acceptor-stem structure (Voet and Voet, 2004) (Fig. 1-5). Both of these structures project away from the body at a 90° angle to each other, establishing the characteristic L-shape (Voet and Voet, 2004).

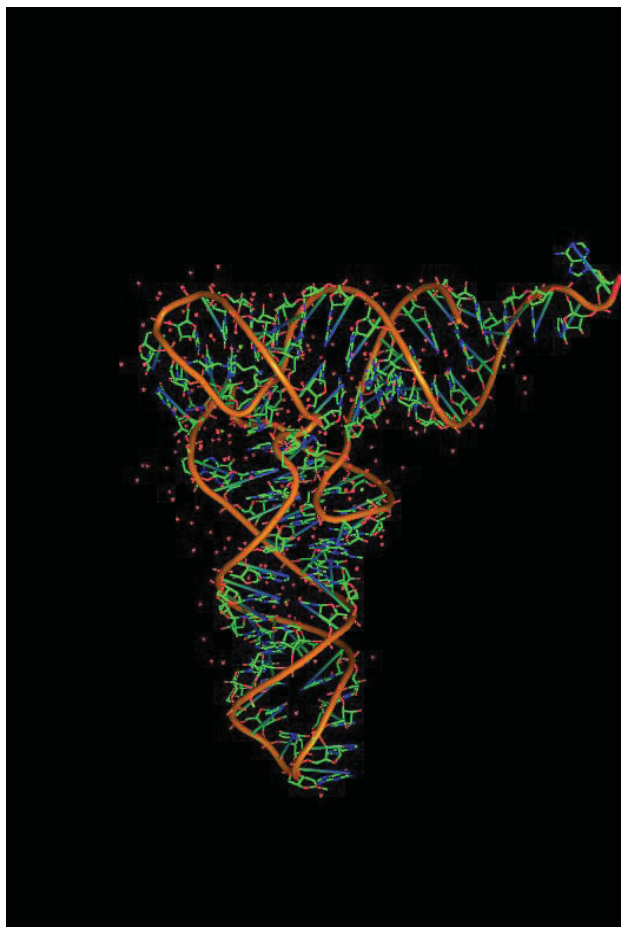


Fig.1-5: Tertiary structure of yeast phenylalanine tRNA at 2.0 Å resolution (PDB:1evv), from (<http://www.rcsb.org/pdb/home/home.do>).

A tRNA molecule is first transcribed as a precursor with a 5' end leader, and a 3' end trailer (fig. 1-6). Following this transcription, RNase P endonucleolytically cleaves the tRNA at the 5' end; +1 position. tRNase Z endonucleolytically cleaves the precursor near the 3' end, at the discriminator base (N); +73 position (Levinger *et al.*, 2004). Introns are also removed if they occur in the transcript (Levinger *et al.*, 2004). tRNA nucleotidyltransferase adds the CCA trinucleotide sequence to the discriminator base at the new 3' end that was produced by tRNase Z (Levinger *et al.*, 2004). tRNA must also undergo further specific modifications, such as nucleotide methylations, by other enzymes in order to become fully mature and able to facilitate protein biosynthesis most effectively (Voet and Voet, 2004). This modified tRNA is now mature, and ready to be charged with its cognate amino acid by a specific aminoacyl-tRNA synthase (aaRS) (Levinger *et al.*, 2004).

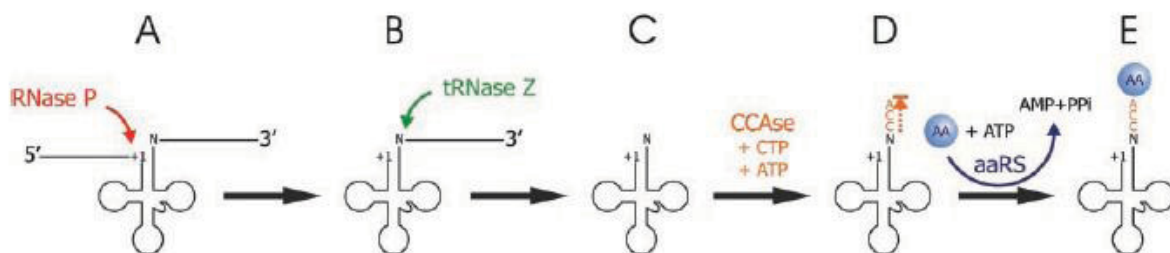


Fig. 1-6: Illustration of the general tRNA processing pathway and acylation. (A) tRNA precursor with 5'-end leader, and 3'-end trailer. (B) 5'-end leader cleaved off by RNase P endonuclease at +1 (C) 3'-end trailer cleaved off by tRNase Z endonuclease at +73; discriminator base N (D) tRNA nucleotidyl transferase added CCA to 3'-end (E) tRNA charged with amino acid by an aminoacyl-tRNA synthase (aaRS) (Adapted from Levinger *et al.*, 2004).

1.4 The mechanism of tRNA nucleotidyltransferase

Although the mechanism of CCA addition has been studied for decades (Deutscher *et al.*, 1972, 1982; Yue *et al.*, 1996; Steitz *et al.*, 1998), the precise molecular events that result in the addition of each

nucleotide, beginning with the addition of a C to the N73 discriminator base, is not known. However, it is clear that a number of mechanistic hurdles (listed below) must be overcome in order for polymerization to occur (Betat *et al.*, 2010).

- (i) **Substrate recognition:** The correct immature tRNA (those possessing part or none of the CCA trinucleotide sequence), ATP, and CTP must be recognized, and other forms of RNA, UTP, and GTP must be discriminated against.
- (ii) **Templating:** Once two C residues have been added consecutively to the 3'-end of the tRNA, the enzyme must immediately switch to adding an A residue, and each of these additions must occur independent of any nucleic acid template.
- (iii) **Polymerization termination:** Polymerization must be terminated immediately after the full C-C-A sequence has been constructed on the immature tRNA substrate.

Previous research on the *B. stearothermophilus* and Archaeal enzymes (Xiong *et al.*, 2003; Weiner *et al.*, 2004) has established that the catalytic mechanism for CCA-addition is characterized by a number of properties:

- (1) Nucleotide addition is catalyzed by a general two-metal ion mechanism common to all polymerases,
- (2) CCA mostly recognizes the acceptor stem, and the T ψ C stem-loop of tRNA,
- (3) There is no translocation of tRNA relative to the enzyme during polymerization,
- (4) There is a single catalytic domain with homology to the catalytic site of DNA pol β ,
- (5) A ‘protein template’ serves as a single nucleotide binding site for both CTP and ATP.

In addition, it is apparent that the catalytic mechanism is essentially the same for each single addition reaction. Each addition is carried out by a single active site containing the two well-conserved carboxylates (DxD), located in the most N-terminal element; motif A. Both of these carboxylates have

been demonstrated to be absolutely essential for CTP and ATP addition (Steitz TA *et al.*, 1998). This critical importance is attributed to their function in coordinating two divalent metal ions; preferably Mg^{2+} , on which catalysis depends. The reaction occurs by the same general two-metal ion-catalyzed mechanism that was originally attributed to DNA polymerases, but is now known to be common to all polymerases (Steitz *et al.*, 1998). The two metal ions are positioned in the active site in such a way that allows multiple coordinations between them, the NTP substrate, and the 3'-end of the tRNA substrate. Metal ion A is responsible for deprotonating the 3'-OH group of the tRNA's terminal ribose, thereby producing a suitable nucleophile for attacking the α -phosphate of the bound NTP (Fig. 1-7) (Betat *et al.*, 2010). In turn, multiple coordinations between the triphosphate moiety and metal ion B make the β,γ pyrophosphate a good leaving group. Both metal ions thereby serve a role in binding the triphosphate moiety of the incoming NTP. Also, both metal ions promote the transition state by enhancing its stability (Betat *et al.*, 2010).

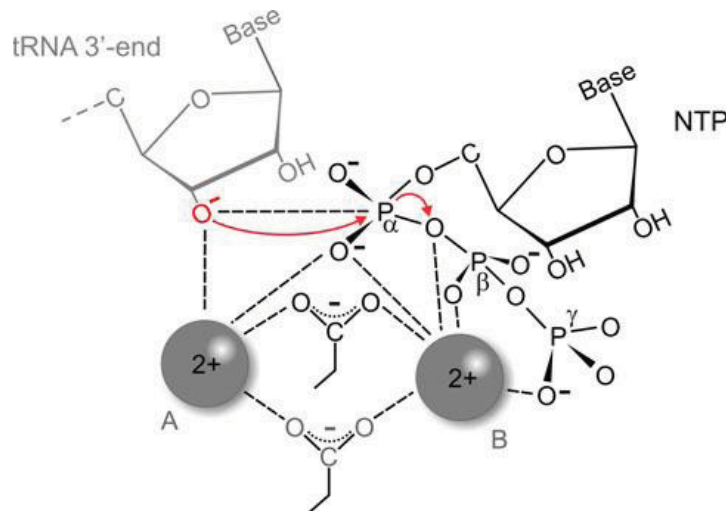


Fig. 1-7: CCA-addition polymerization mechanism for the general two-metal ion-catalyzed reaction (Betat *et al.*, 2010).

Motif B is essential for discriminating between NTPs and dNTPs (Betat *et al.*, 2010). This is achieved by the guanidinium group of the central arginine in a highly conserved RRD sequence located in motif B (Fig. 1-8) (Betat *et al.*, 2010). It is responsible for recognizing the 2'-OH group of sequestered NTP substrates by forming a single hydrogen bond with it. Motif D forms the single nucleotide binding pocket located in the neck domain, and is responsible for the specific recognition and binding of both CTP and ATP nucleotide substrates, to the exclusion of UTP and GTP (Betat *et al.*, 2010). This important and fascinating function is achieved by a sequence of three conserved amino acids; EDxxR (Betat *et al.*, 2010). Remarkably, these three amino acids were shown to form Watson-Crick-like hydrogen bonds to the nitrogenous bases of bound CTP or ATP substrates (Betat *et al.*, 2010). This segment of polypeptide thereby serves a true templating function by mimicking base pairing interactions common to nucleic acid, while possessing the unique ability to switch between the base-pairing properties required for binding CTP, or ATP. Also, the head and neck domain together form a positively charged cleft that interacts with the 3'-end of the tRNA primer, and the NTP substrates. The roles of Motif C and E have yet to be assigned, however Motif E is believed to be involved in stabilizing a helix-turn structure in motif D and/or in tRNA binding (Betat *et al.*, 2010).

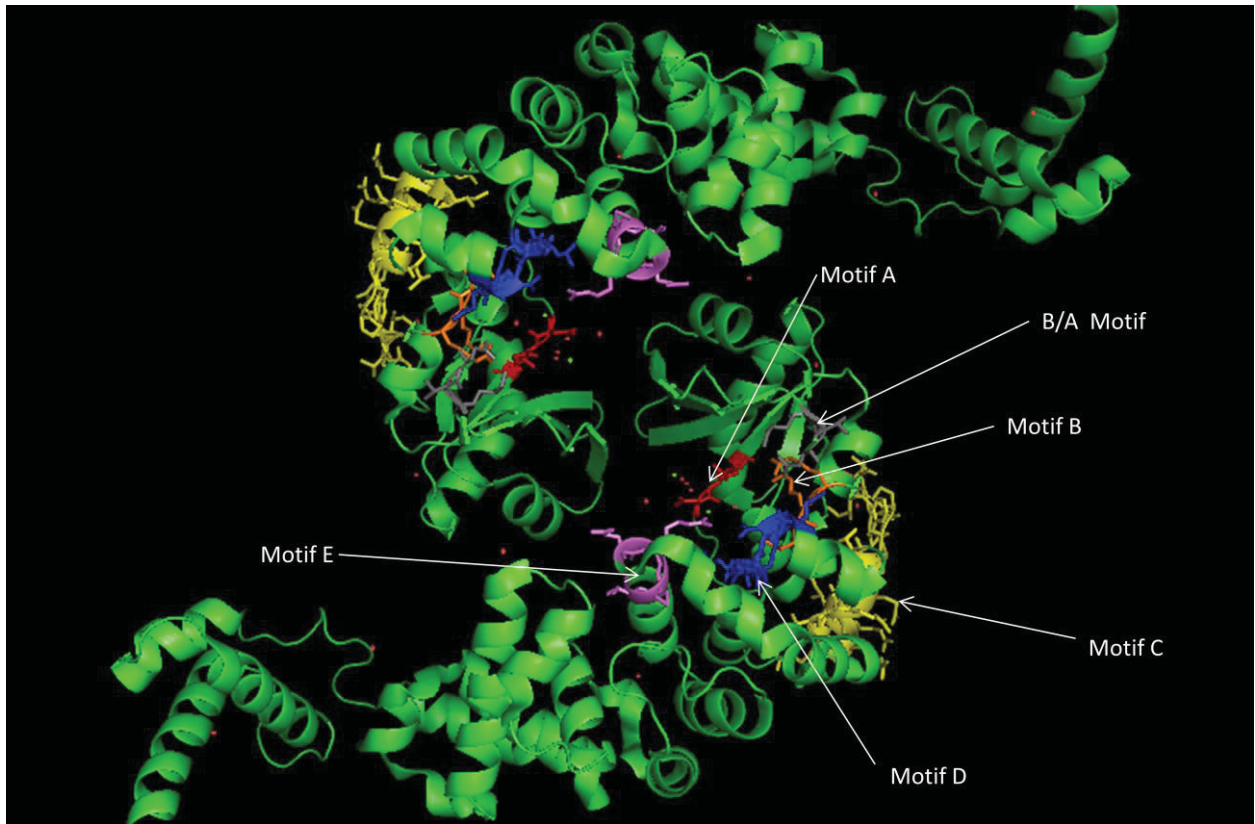


Fig. 1-8: PYMOL representation of the *B. stearothermophilus* crystal structure (1MIV) showing the five catalytic domains; motif A to E (highlighted). Motif A (red), motif B (orange), motif C (yellow), motif D (blue), motif E (indigo), and the B/A motif in grey.

The tertiary structure achieved by the enzyme allows each of the motifs described above to be located relatively close to one another. Consequently, the resulting active site configuration is able to bring the NTP and tRNA substrates into close proximity with each other, and with the catalytically critical metal ions, in an orientation that facilitates catalysis.

Aside from these five commonly recognized sequence motifs, there is another element that is usually not formally recognized as a conserved sequence element, but which is well conserved in class II CCA-adding enzymes, and carries-out an important proof-reading function. It is known as the basic/acidic motif (B/A motif), and is located between motif A and motif B (Betat *et al.*, 2010). The B/A motif is responsible for proof-reading tRNAs extended to the penultimate position. It does so by interacting with

this nucleotide, which should be a C (Betat *et al.*, 2010). If a nucleotide other than C was added at position 74 or 75, that particular tRNA is unlikely to be extended further. The basic amino acid in this B/A element is usually an arginine which hydrogen bonds to the O2 position of C75 to help bring its 3'-OH group into a position that will allow it to nucleophilically attack the α -phosphate of a bound ATP (Betat *et al.*, 2010).

The rest of the protein consists of a body and a tail domain responsible for the promiscuous recognition of the top-half of all tRNA primers, to serve an “anchoring function” (Betat *et al.*, 2010). This tRNA promiscuity is attributed to the fact that the body and tail domains of the enzyme interact mostly with sugar-phosphate backbone around the T-loop region located at the top half of tRNA, and with the anti-codon region projecting from the enzyme (Betat *et al.*, 2010).

1.5 *Saccharomyces cerevisiae* tRNA nucleotidyltransferase

Saccharomyces cerevisiae tRNA nucleotidyltransferase is a 546 amino acid enzyme with a molecular weight of 62 kDa. Currently little is known about this specific enzyme, and its crystal structure has yet to be resolved. However, a model developed by the Protein Homology/analogy Recognition Engine (PHYRE) computational software (Bennett-Lovsey *et al.*, 2008) produced a structure similar to that of the four crystal structures of class II CCA-adding enzymes determined to date (Fig. 1-9).



Fig.1-9: A cartoon representation of a model developed by PHYRE (<http://www.sbg.bio.ic.ac.uk/~phyre/>) of tRNA nucleotidyltransferase E189 from *Saccharomyces cerevisiae* (c1ou5A) based on the *H. sapiens* structure (1OU5). N-terminal 63 amino acids are colored orange, Arginine 64 is red, and glutamate 189 is yellow. This model was created by the PyMol viewing software (DeLano, 2009).

1.6 Temperature-sensitive mutations and their suppression

Temperature-sensitivity (ts) mutations have been discovered in a diverse spectrum of organisms, including *Arabidopsis thaliana* (Pickett *et al.*, 1996), *Saccharomyces cerevisiae* (Ben-Aroya *et al.*, 2008), *Neurospora crassa* (Dieterle *et al.*, 2010), *Drosophila melanogaster* (Peixoto *et al.*, 1998), *Homo sapiens* (Imamura *et al.*, 2000), and even viruses (Murphy *et al.*, 1980; Chou *et al.*, 1976). In fact, there is strong evidence in support of a role for temperature-sensitivity in some human diseases (Hashimoto *et al.*, 2005; Imamura *et al.*, 2000). A number of temperature-sensitive mutations are believed to be the root cause of some peroxisome biogenesis disorders including Zellweger syndrome, neonatal

adrenoleukodystrophy, and Infantile Refsum disease (Imamura *et al.*, 2000). Each displays an autosomal recessive mode of inheritance, and is caused by peroxisome assembly deficiency and peroxisome malfunction (Imamura *et al.*, 2000). The results of a study conducted on Infantile Refsum disease; the mildest form of peroxisome biogenesis disorder, demonstrated that temperature-sensitive peroxisome assembly is responsible for the mildness of its clinical features. In fact, the mutation leading to the phenotype was determined to be a frequent mutation in these patients, and resulted from a single missense mutation G→A at position 2528 in codon (GGT), which causes a glycine to aspartic acid substitution at position 843 in Pex1p. Pex1p is believed to be involved in the peroxisomal protein import process, and therefore protein structural configuration, trafficking kinetics, or stability may be affected (Imamura *et al.*, 2000). Imamura *et al.* (2000) have concluded that the temperature-sensitive phenotype link to this mutation is at least partially responsible for peroxisome deficiency in the cells of CG1 IRD patients.

Temperature-sensitive mutations have been of interest for decades mainly for their use in the genetic analysis of essential proteins, and are currently being used for the same purpose (Ben-Aroya *et al.*, 2008). In Arabidopsis, three *arrested development* mutations (*add*) 1, 2, and 3 were discovered in a screen designed to identify temperature-sensitive mutations that cause a conditional arrest of early shoot development (Pickett *et al.*, 1996). All three ts *add*-mutants segregate as recessive non-complementing mutants causing temperature-sensitive arrest, or delay of epicotyl development (Pickett *et al.*, 1996).

A temperature-sensitive mutation in the CCA1 gene coding for tRNA nucleotidyltransferase in *S. cerevisiae* was discovered during a screen conducted in 1990 to identify trans-acting factors involved in mRNA decay in *S. cerevisiae* (Aebi *et al.*, 1990). Subsequent studies have determined that this enzyme exhibits severely diminished nucleotidyltransferase activity at both 22°C and 37°C (Shan *et al.*, 2008).

Yeast cells carrying the temperature-sensitive mutation are unable to grow at the non-permissive temperature of 37°C, but clearly do so at the permissive temperature of 22°C (Fig. 1-10). It was also determined that a single missense mutation (G→A) at position 565 of the open reading frame, resulted in a codon change from GAA to AAA, and is solely responsible for this phenotype (Shan *et al.*, 2008). This single base pair change results in the substitution of a glutamate residue at position 189 for a lysine (Shan *et al.*, 2008).

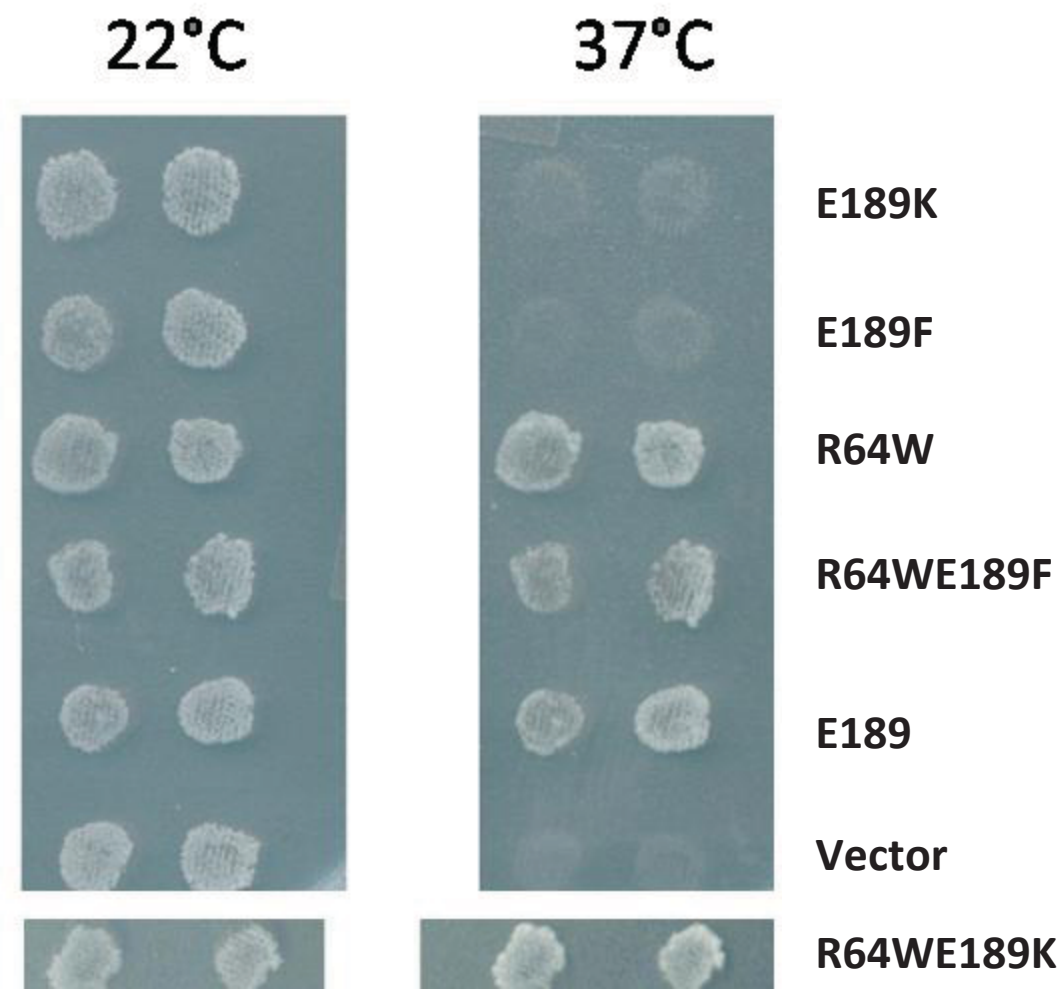


Fig. 1-10: Replica plating experiment of *S. cerevisiae* YPH500 E189, the temperature-sensitive mutants E189F and E189K, the double mutant suppressors R64WE189F and R64WE189K, the single mutant R64W, and with vector alone. At the permissive temperature of 22°C, and the restrictive temperature of 37°C (Adapted from images provided by Dr. Pamela J. Hanic-Joyce).

There are at least three other effects manifested by *Saccharomyces cerevisiae* carrying this temperature-sensitive mutation in the *CCA1* gene when grown at 37°C (Peltz *et al.*, 1992):

Protein synthesis is impaired. The incorporation of radiolabeled methionine dropped by approximately 20% within 5 minutes, and had been reduced to less than 10% native levels by 50 minutes.

Decay rates of mRNA are reduced. In fact, the rates of mRNA decay are comparable to those of cells treated with cycloheximide.

Polysome-to-monosome ratio increases. This result is generally interpreted to indicate a reduction in translation elongation rates.

The E189K mutation provides not only an opportunity to better understand the role that glutamate 189 plays in supporting tRNA nucleotidyltransferase activity, but also to better understand how a temperature-sensitive phenotype occurs in general. Also, to further address these questions, intragenic suppressors of the temperature-sensitive phenotype were recently generated spontaneously by UV induced mutagenesis (Joyce, unpublished). An intragenic substitution mutation converting arginine 64 to tryptophan was found to suppress the ts phenotype in *S. cerevisiae* carrying a tRNA nucleotidyltransferase with either the E189F or E189K mutations (Fig.1-10).

1.7 The purpose of this study

The purpose of this study was twofold: (1) To understand how the single E189F mutation causes the ts phenotype observed, and also (2) to understand how the R64W mutation works to suppress the ts phenotype. In order to meet these goals, the native enzyme and four variants; R64W, R64WE189K, R64WE189F, and E189F have been cloned, expressed, and purified. Circular dichroism and fluorescent spectroscopy have been used to characterize the secondary and tertiary structures respectively, for each. Also, thermal denaturation studies were conducted using circular dichroism in order to characterize the thermal stabilities of each protein in terms of melting temperature (T_m). Enzyme activity assays were conducted as well, in order to determine activity levels for each enzyme under various NTP substrate availability conditions, at 22°C and 37°C. The activity assays were conducted using radio-labelled tRNA transcripts produced by run-off transcription. The reaction products were resolved on a sequencing gel, and visualized by autoradiography.

2.0 MATERIALS AND METHODS

2.1 Strains, plasmids, growth media, solutions, and chemicals

The *E.coli* strain XL2-blue was used for transformations in the construction and propagation of all plasmids while BL21 (DE3) was used for protein expression and purification. The plasmid vector was pGEX-2T (GE Healthcare) modified (Shan *et al.*, 2008) to include a *Sall* restriction site downstream of the *BamHI* restriction site.

2.2 Construction of protein expression vectors carrying wild-type or mutant tRNA nucleotidyltransferase

2.2.1 Generation of Polymerase Chain Reaction (PCR) products and their purification

Oligonucleotides were purchased from BioCorp. Inc. (Montreal). The PCR products were generated with the following two oligo nucleotide primers; primer FJ7787/B130: 5'-ACTAGTGGATCCATGACGAA-3', and primer FH6114/B947: 5'-ATCGATGTCGACTACTACAG-3', which carried the *BamHI* and *Sall* restriction sites, respectively. The PCR reactions contained 10 pmol of each primer, 200 ng of template DNA, each dNTP at 200 μ M, 5 μ l of 10x MBI reaction buffer, 8 mM MgSO₄, and distilled water in a final volume of 50 μ l. Samples were layered with mineral oil and PCR was carried out as follows in a PERKIN ELMER DNA thermal cycler: start; 95°C for 1 minute, 50°C for 1 minute, 72°C for 4 minutes. Amplification; 95°C for 30 seconds, 50°C for 1 minute, 72°C for 4 minutes-35 cycles. Termination; 95°C for 30 seconds, 50°C for 1 minute, 72°C for 10 minutes-1 cycle.

Table 2-1: Recipes for media and buffers

YT (Sambrook <i>et al.</i> , 1989)	0.5% (w/v) Yeast extract, 0.8% (w/v) Tryptone, 0.5% (w/v) NaCl
1 x Phosphate buffered saline (PBS) pH 7.3	8 g NaCl, 0.2 g KCl, 1.44 g Na ₂ HPO ₄ , 0.24 g KH ₂ PO ₄
10 x Tris/borate/EDTA (TBE) 2L	120 g Tris, 62 g Boric acid, 40 ml of 0.5 M EDTA (pH 8.0)
Protein purification cell lysis buffer (Modified from Shan, 2008)	1 x PBS pH 7.4, 1 mM EDTA, 0.01% Lysozyme, 50 µl Amresco protease inhibitor per 4 g wet cell pellet
30% acrylamide solution [29:1], (Sambrook <i>et al.</i> , 1989)	29.2 g acrylamide, 0.8 g bis-acrylamide, 100 mL distilled water
5 x SDS Running Buffer (Modified from Sambrook <i>et al.</i> , 1989)	72 g/L glycine, 15 g/L Tris-HCl, 5 g/L sodium dodecyl sulfate (SDS)
13% SDS-Polyacrylamide resolving gel (Sambrook <i>et al.</i> , 1989)	4.3 ml 30% acrylamide, 3 ml distilled water, 2.5 ml 1.5 M Tris-HCl (pH 8.8), 100 µl 10% sodium dodecyl sulfate, 100 µl 10% (v/v) ammonium persulfate (APS), 10 µl TEMED
SDS-Polyacrylamide stacking gel (Sambrook <i>et al.</i> , 1989)	1.3 ml 30% acrylamide solution, 6.1 ml distilled water, 2.5 ml 0.5 M Tris-HCl (pH 6.8), 100 µl 10% sodium dodecyl sulfate, 100 µl 10% ammonium persulfate (APS), 10 µl TEMED
SDS-PAGE staining solution A (Wong <i>et al.</i> , 2000)	0.05% (v/v) Coomassie brilliant blue, 25% (v/v) isopropanol, 10% (v/v) acetic acid
SDS-PAGE staining solution B (Wong <i>et al.</i> , 2000)	0.005% (v/v) Coomassie brilliant blue, 10% (v/v) isopropanol, 10% (v/v) acetic acid
SDS-PAGE destaining solution D (Wong <i>et al.</i> , 2000)	10% (v/v) isopropanol, 10% (v/v) acetic acid
Peatties loading buffer (Peattie, 1979)	10 M urea, 5 mM Tris-borate (pH 8.3), 0.1 mM EDTA, 0.05% (v/v) xylene cyanol, 0.05% (v/v) bromophenol blue
12% (20%) Polyacrylamide 7M Urea denaturing gel	11.4 g acrylamide, 0.6 g (1.0 g) bis-acrylamide, 42 g urea, 650 µl 10% ammonium persulfate, 20 µl TEMED, brought to 100 ml with distilled water

Table 2-2: Chemical list

CHEMICAL	GRADE	MANUFACTURER
[α^{32} -P] guanosine triphosphate (GTP) (10 μ Ci/ μ L, 3000 Ci/mmol)		Perkin Elmer
Acetic Acid	Lab	Fisher Scientific
Acrylamide	Ultra Pure	Bioshop
Agar		Sigma-Aldrich
Agarose	Biotechnology	Bioshop
Ammonium Persulfate (APS)	Electrophoresis	Bioshop
Ampicillin (Amp)	Biotechnology	Bioshop
Bio-tryptone	Bacteriological	Bioshop
Bis-acrylamide	Bio Ultra Pure	Bioshop
Boric acid	Biotechnology	Bioshop
Bovine serum albumin acetylated		Fermentas
Bradford reagent		Bio-Rad
Calcium chloride ($CaCl_2$) dihydrate	Molecular Biology	Bioshop
Coomassie brilliant blue R-250	Ultra Pure	Bioshop
D-glucose	Reagent grade	Bioshop
Ethanol		Commercial Alcohols Inc.
Ethidium bromide (EtBr)		MP Biomedicals
Ethylenediaminetetraacetic acid (EDTA)	Biotechnology	Bioshop
Glycerol	Enzyme	Fisher Scientific
Glycine	Biotechnology	Bioshop
Isopropanol		Fisher Scientific
Isopropyl- β -D-thiogalactopyranoside (IPTG)		Gold biotechnology
Magnesium Chloride Hexahydrate		EM Science
Nuclease-free water		Integrated DNA Technologies, Inc.
Polyethylene glycol (PEG)	Biotechnology	MP Biomedicals
Potassium chloride (KCl)		Bioshop
Potassium phosphate monobasic		Anachemia
Protease inhibitor Cocktail	Bacterial	Amresco
Sodium Chloride	Biological	Fisher Scientific
Sodium dodecyl sulphate (SDS)	Ultra pure	MP Biomedicals
Sodium phosphate dibasic, heptahydrate	ACS	Bioshop
Sucrose	Ultra pure	Bioshop
Tetramethylethylenediamine (TEMED)	> 99.0 %	Bioshop
Tris	Bio ultra pure	Bioshop
Urea	Bio ultra pure	Bioshop
Yeast Extract		Bioshop

2.2.2 Small scale isolation of plasmid DNA

A single colony was selected and used to inoculate 5 ml of YT containing 50 µg/ml ampicillin. After overnight incubation at 37°C with shaking, cells were pelleted by repeated centrifugation of 1.5 ml aliquots in an Eppendorf centrifuge at 16 000 xg, for 5 minutes, at 4°C. The GeneJet Plasmid Miniprep Kit (Fermentas) was then followed according to the manufacturer's instructions. Plasmid DNA was eluted in two 50 µl aliquots into autoclaved Eppendorf tubes, and all 100 µl were stored at -20°C until needed.

2.2.3 Restriction digestion conditions

*Bam*HI (10 U/µl) and *Sal*I (10 U/µl) restriction enzymes along with their appropriate digestion buffers were used to digest isolated plasmids. Restriction digestions were typically carried out by incubating the mixtures for 1.5 hours at 37°C, and then adding 0.5 µl (0.5 U) of Calf Intestine Alkaline Phosphatase (CIAP, MBI), before incubating the mixtures for another 30 minutes.

2.2.4 Agarose gel electrophoresis

Agarose gels were typically 1% *i.e.*, 0.5 g of agarose was dissolved in 50 ml of 1xTBE, and 5 µl of 10 mg/ml ethidium bromide was added before the gel was allowed to solidify. For each of the samples, 6x loading dye was added prior to loading. Electrophoresis was typically carried out at 100 Volts for 45 minutes to 1 hour in 1xTBE. The gel was then placed on a FluorChem FC2 ultraviolet light box developed by Alpha Innotech, in order to view the DNA bands. If the products were to be used further, they were gel extracted and cleaned using the GFX PCR product cleanup kit (GE Healthcare), as directed by the accompanying instructions.

2.2.5 Ligation conditions

A typical ligation mixture consisted of 2 µl T4 ligase 10x buffer (Fermentas), 0.5 µl (0.2 U) of T4 ligase (Biolabs), 10 ng of *Bam*HI/*Sal*I digested vector, 50 ng of *Bam*HI/*Sal*I digested insert, 0.5 µl of 10 mM ATP, and 9 µl of sterile water. The mixtures were incubated overnight at 4°C, and subsequently used to transform XL2 blue (section 2.2.7).

2.2.6 Preparation of competent cells (Modified from Sambrook *et al.*, 1989)

A single colony of XL2 blue cells was selected from a YT agar plate containing 50 µg/ml ampicillin, and inoculated into 5 ml of YT medium with 50 µg/ml ampicillin. The culture was grown overnight in a Lab-Line Orbital Shaker at 37°C and 225 rpm. This overnight culture was subsequently subcultured by 80-fold dilution into a 1 l flask containing 400 ml of fresh YT medium and 50 µg/ml ampicillin. The inoculum was then allowed to grow in a New Brunswick Scientific Innova 4330 Refrigerated Incubator Shaker set at 37°C and 225 rpm until an OD₆₀₀ of 0.5-0.6 was reached. The culture was then chilled on ice for 40 minutes, and the cells collected by centrifugation in a JA-10 rotor at 4400 xg and 4°C for 10 minutes, followed by decanting of the supernatant. The cell pellet was then resuspended in cold sterile 50 mM CaCl₂ solution, and chilled on ice for 15 minutes. The cells were pelleted once again by centrifugation at 4400 xg and 4°C for 10 minutes, the supernatant decanted, and the cell pellet resuspended in sterile cold 50 mM CaCl₂ containing 15% (v/v) glycerol. The XL2 blue cells were then transferred in 0.5 ml aliquots to sterile 1 ml Eppendorfs, and stored at -80°C until needed.

2.2.7 *E. coli* transformations

A 100 µl aliquot of competent XL2-blue cells was transferred to a pre-chilled sterile 1.5 ml Eppendorf tube along with 2-5 µl of the appropriate DNA. After 45 minutes on ice the cells were heat shocked at 42°C for 45 seconds, and then chilled on ice for 5 min. Finally, 50 µl of YT medium were added to the suspension before placing it in a 37°C incubator for 1 hour. All 150 µl of cell suspension was then spread over a single YT agar plate containing 50 µg/ml ampicillin, and the plate incubated at 37°C for 24 hours.

2.3 Expression of GST-tRNA nucleotidyltransferase fusion protein and purification by GST-affinity chromatography (see Appendix for protocol)

2.3.1 Expression of GST-tRNA nucleotidyltransferase fusion protein

Three 5 ml cultures of YT and 100 µg/ml ampicillin were each inoculated with a single colony of transformed BL21 cells, and allowed to grow overnight in a Lab-line Orbital Shaker at 37°C and 225 rpm. Each 5 ml overnight culture was diluted into a Fernbach Flask containing 1.3 l of YT and 50 µg/ml ampicillin. All three subcultures were then incubated in a New Brunswick Scientific Innova 4330 Refrigerated Incubator Shaker at 37°C and 225 rpm, until an OD₆₀₀ of 0.4-0.5 was reached. At this point IPTG was added to each subculture to a final concentration of 1 mM, before incubation in a New Brunswick Scientific Innova 4330 Refrigerated Incubator Shaker at 18°C and 225 rpm for 16 hours. At the end of this induction phase, the cell suspensions were immediately placed on ice. The cultures were then centrifuged at 4400 xg for 15 minutes using a JA-10 rotor in order to pellet the cells, and the resulting cell pellet was stored at -80°C until needed.

2.3.2 Cell lysis

All manipulations were carried out at 4°C or on ice where possible. The frozen cell pellets (section 2.3.1) were thawed on ice for 0.5-1 hour, and resuspended in cold lysis buffer (1 ml/ 1 g cell pellet). Then, 50 µl of Amresco protease inhibitor for every 4 g of wet pellet mass was added to the cell suspension. The cell suspension was then loaded into a French®Pressure cell press from ThermoSpectonic that was previously chilled on ice, and pressed through in a dropwise fashion at 1500 psi, in order to lyse the cells. This cell lysate was then loaded onto the French®Pressure cell press again, and cell lysis repeated. The lysate was then centrifuged at 39 000 xg for 40 minutes in a JA-20 rotor. A 10 ml glass pipette was used to carefully transfer the supernatant only, to a clean centrifuge tube immediately after the 40 minute spin was completed. The 40 minute centrifugation was repeated for a second time under the same conditions, and the supernatant carefully transferred to a clean centrifuge tube in the same fashion. This clarified supernatant was then loaded into a purification column.

2.3.3 Column preparation

The Glutathione Fast Flow 4B chromatography resin from GE Healthcare was used for all purifications. Fresh resin slurry was slowly poured into an empty, clean 1.5 cm x 10 cm Bio-Rad column and allowed to settle by the force of gravity until a bed volume of 3 ml had been achieved. At least 10 bed volumes of distilled water were used to rinse the resin, before it was equilibrated with 10 bed volumes of 1 x PBS (pH 7.4). Regeneration of used resin was achieved by washing the column sequentially with two bed volumes of 6 M guanidine-HCl, two bed volumes of 10 mM reduced glutathione in 1 x PBS (pH 7.4), two bed volumes of 1% (v/v) Triton X-100, and two bed volumes of 70% (v/v) ethanol. However, the column was rinsed with 10 bed volumes of 1 x PBS (pH 7.4) after each of the

washes with different solutions noted above. The regenerated columns were then used immediately, or stored in 20% (v/v) ethanol at 4°C for future use.

2.3.4 Purification and thrombin cleavage of GST-tRNA nucleotidyltransferase fusion protein

After loading of the clarified supernatant (section 2.3.2), the column was plugged, sealed with parafilm, fastened to a Barnstead rotisserie, and left overnight at 4°C. The column was then placed upright, the beads allowed to settle by the force of gravity for 30 minutes, and the supernatant drained. Approximately 10 ml of 1 x PBS (pH 7.3) was added to the column before the column was attached to a Pharmacia LKB P-1 peristaltic pump. At least 500 ml of 1xPBS (pH 7.3) was passed through the column at a rate of 3 ml/min in order to wash the beads. Aliquots of wash buffer were collected every 50 ml for the purpose of determining wash effectiveness using SDS-PAGE, at the end of the wash stage. When the wash samples showed no detectable protein, the remaining wash buffer was pumped out of the column using a rubber bulb, and approximately 20 ml of elution/cleavage buffer (50 mM Tris-HCl, 140 mM NaCl, 15 mM glutathione, 2.5 mM CaCl₂, pH 8.0) was added. 16 ml of eluate were pushed through the column using a rubber bulb, and collected in 1 ml fractions. Aliquots of 16 µl were taken from fractions 1, 3, 5, 7, 9, 11, 13, and 16 for SDS-PAGE analysis. Also, Bradford assays were used to quantify at least the first ten fractions (section 2.3.5). Several of the most concentrated fractions were pooled, transferred to a 6-8 kDa dialysis bag, and a determined amount of thrombin (Amersham Biosciences) was added to the pooled sample before it was allowed to dialyse in 4 l of cold Tris-HCl/NaCl buffer (50 mM Tris-HCl, 140 mM NaCl, pH 8.0) overnight at 4°C. SDS-PAGE was used to verify sufficient fusion protein cleavage before transferring the pooled sample to a 50 kDa Spectra/Por6 dialysis tube for dialysis overnight in 4 l of 1xPBS (pH 7.3), at 4°C. The dialysis tube was then transferred to 4 l of fresh 1xPBS (pH 7.3), and the dialysis repeated overnight at 4°C. The beads were regenerated (section 2.3.3), the dialyzed pooled

protein was then added to the regenerated beads in the column, and slowly cycled through the column 5-15 times manually. SDS-PAGE was used to determine the degree to which GST was removed, and the overall purity of the pooled protein. Glycerol was then added to the protein pool to a final concentration of 10% (v/v), before the protein was stored at -80°C in small aliquots of 50-200 µl.

2.3.5 Protein concentration measurements

Bradford assays were conducted in order to determine protein concentrations according to the procedures provided with the Bio-Rad kit. Standard curves were prepared at 0, 2, 4, 6, 8, and 10 µg/ml concentrations with BSA as determined by OD₂₈₀, and this was subsequently used to quantify the concentration of protein in samples. These measurements were made at OD₅₉₅.

A standard BSA stock solution at approximately 0.1 mg/ml was prepared by first weighing out 1.0 mg of BSA in a 1.5 ml Eppendorff tube. 1 ml of 1xPBS (pH 7.3) was then added to the Eppendorff tube, and the BSA pipetted and vortexed until it was fully dissolved. The absorbance (OD₂₈₀) of this BSA solution was then measured, and the Beer-Lambert law ($A = \epsilon lc$; $\epsilon = 0.58 M^{-1}cm^{-1}$, $l = 1.0 cm$) was used to calculate the protein concentration more accurately. After establishing the protein concentration in this manner, the solution of BSA was diluted with 1 x PBS (pH 7.3) to a final concentration of 0.1 mg/ml. The final concentration of this diluted BSA solution was determined by measuring its OD₂₈₀ and using the Beer-Lambert law once again. The standard BSA stock solution was then diluted in 1x Bradford dye to prepare standard solutions at 2.0, 4.0, 6.0, 8.0, and 10.0 µg/ml. The Absorbances (OD₅₉₅) of these solutions were also determined, and an Absorbance (OD₅₉₅) versus BSA protein concentration (µg/ml) standard curve was generated.

2.3.6 Sodium dodecyl sulphate polyacrylamide gel electrophoresis (SDS-PAGE)

(Modified from Sambrook *et al.*, 1989)

A 13% resolving gel was prepared first by adding 4.3 ml of 30% (29:1 acrylamide/bisacrylamide) polyacrylamide solution, 3.0 ml of distilled water, 2.5 ml of Tris-HCl (pH 8.8), 100 µl 10% sodium dodecyl sulphate, and 100 µl of 10% ammonium persulfate to a small beaker and mixing. Polymerization was initiated by adding 10 µl of TEMED to the solution before it was briefly mixed by swirling and pipetted between the glass plates of an assembled Bio-Rad apparatus, leaving space for the stacking gel. This space was immediately filled with 60% isopropanol, and the gel left to polymerize. After polymerization had occurred, the isopropanol solution was removed. To prepare the stacking gel layer, 1.3 ml of 30% (29:1 acrylamide/ bisacrylamide) polyacrylamide solution, 6 ml of distilled water, 2.5 ml of Tris-HCl (pH 6.8), 100 µl of 10% (w/v) sodium dodecyl sulphate, and 100 µl of 10% (w/v) ammonium persulfate were added to a small beaker. Polymerization was initiated by adding 10 µl of TEMED to the mixture before it was swirled and used to fill the space above the resolving gel. A comb was then inserted into the stacking gel, before it was allowed to polymerize. The apparatus was then assembled with the casted gels, and submerged in 1x SDS running buffer. 4 µl of protein gel sample loading buffer (http://openwetware.org/wiki/Main_Page) was added to each of the samples, which were boiled for 2 minutes, and then cooled on ice for at least 3 minutes before loading. The samples were electrophoresed through the stacking gel for 15 minutes at 80 volts; before the voltage was increased to 200 volts for separation through the resolving gel, until the dye had completely run off the gel. The gel was removed from the electrophoresis apparatus and stained by the following procedure. In brief, the gel in 50 ml of solution A (Wong *et al.*, 2000), was microwaved for 1 minute and 20 seconds. The container was then shaken gently on an orbital shaker for at least 5 minutes at room temperature. Solution A was decanted from the container, before 50 ml of solution B (Wong *et al.*, 2000) was added.

The container was then microwaved and shaken under the same conditions again, before solution B was decanted and solution D (Wong *et al.*, 2000) added to the container, along with a Kimwipe folded in half twice. The microwaving and shaking steps were repeated once more in the same fashion, the Kimwipe was discarded along with solution D, and the gel was rinsed with distilled water. The gel was then sealed between two membranes of cellophane (BioDesign Inc. of New York) and allowed to dry overnight.

2.4 tRNA nucleotidyltransferase activity assays

2.4.1 Large scale plasmid isolation of G73 and pmBSDCCA from *E. coli*

Plasmids G73 and pmBSDCCA were originally constructed by Cho *et al.* (2002), and Oh and Pace (1994) respectively. However, we received both plasmids from Dr. Alan Weiner (University of Washington). Both plasmids encode for a tRNA^{Asp} gene from *B. subtilis* modified to contain restriction sites at its 3'-end that allow for the production of tRNA^{Asp} of various lengths. Each plasmid was separately transformed into XL2-blue, and a single colony used to inoculate 5 ml cultures of YT containing 100 µg/ml ampicillin. An aliquot (0.5 ml) of the resulting culture was then used to inoculate 500 ml of YT with 100 µg/ml ampicillin in a Fernbach flask. These cultures were then incubated at 37°C and 225 rpm overnight in a New Brunswick Scientific Innova 4330 Refrigerated Incubator Shaker. The cell suspensions were then centrifuged at 4400 xg and 4°C for 15 minutes in order to pellet the cells, and the supernatant discarded. From this point forward the Eppendorf Perfectprep Plasmid XL kit was used as recommended in the accompanying procedures.

2.4.2 Preparation of [α^{32} P] GMP labelled tRNA with N, NC, NCC, or NCCA 3'-ends by run-off transcription

The plasmids were digested with specific restriction enzymes in order to linearize them and produce templates that could be used for run-off transcription to generate tRNA with specific 3'-ends. Run-off transcription was carried out with *FokI* (New England Biolabs) digested plasmid G73, in order to generate tRNA ending with the discriminator base (-N) while digestions of plasmid pmBSDCCA, with *FokI* (New England Biolabs), *BpI* (Fermentas), or *Bst*O*I* (Promega) produced transcripts ending in C74, C75, and A76, respectively. Run-off transcription was carried out in 1.5 ml Eppendorf tubes containing 20 μ l of 5x transcription buffer, 5 μ l of 10 mM UTP, 5 μ l of 10 mM CTP, 5 μ l of 10 mM ATP, 5 μ l of 1 mM GTP, 50 μ Ci [α^{32} P] GTP at (10 μ Ci/ μ l, 3000 Ci/mmol), at least 1 μ g of linearized DNA template, 60 units of T7 RNA polymerase (Fermentas), and enough RNase-free water to bring the total reaction volume to 100 μ l. The reactions were incubated at 37°C for 3 hours and terminated with 200 μ l of phenol, 5 μ l of 0.5 mM EDTA, 75 μ l of RNase free water, and 18 μ l of 3 M NaOAc (pH 4.6). The terminated reactions were then vortexed briefly, centrifuged at 16 000 xg and 4°C for 5 minutes, and two volumes of 99% ethanol were used to precipitate the transcription products by incubating the terminated reactions at -80°C for 1-24 hours. The ethanol precipitated samples were then centrifuged at 16 000 xg and 4°C for 30 minutes, before the supernatant was removed and the pellets dried by desiccation for 20 minutes. The samples were then prepared for denaturing gel separation by resuspending the pellet in 8 μ l of RNase-free water and 8 μ l of Peattie's loading buffer, incubating them at 65°C for 10 minutes, and cooling them on ice. These were then loaded onto a 4 x 10 cm 20% polyacrylamide/7M urea denaturing gel, and electrophoresis was carried out for 3 hours at 200 volts. The gel was subsequently removed from the apparatus, wrapped in plastic, and aligned on a phosphor screen grid in a cassette (Amersham Biosciences). The cassette was closed with the phosphor screen for 10 minutes of exposure. The plastic wrapped gel was then removed from the cassette, the phosphor screen image developed by a Typhoon

Trio multi-mode imager (GE Healthcare), and the autoradiograph printed out. The gel was then unwrapped and realigned on the phosphor screen grid, with the plastic wrap between the gel and the grid. The autoradiograph and the grid below the gel were used to estimate the locations of the appropriate bands. Sections of gel encapsulating these bands were then extracted and transferred to 1.5 ml Eppendorf tubes. The grid was then blanked, the gel rewrapped with plastic, and placed back in the cassette, and a second autoradiograph produced in order to verify that the correct bands were indeed extracted. To each band was added 400 µl of phenol before the gel slices were crushed with a clean glass rod. After crushing the gel slice 26.7 µl of 7.5 M NH₄OAc, 8 µl 50 mM EDTA, 4 µl of 1 M Mg(OAc)₂ and 361.3 µl of RNase-Free water were added to each sample, the Eppendorf tubes were sealed with parafilm, set on a rotisserie, and allowed to mix overnight at 4°C. The samples were then centrifuged at 16 000 xg at 4°C for 5 minutes, and the supernatant transferred to a new Eppendorf tube. Two equivalent volumes of 99% ethanol were then added to each sample, which were then incubated for 1 hour at -80°C to precipitate the RNA. The samples were centrifuged at 16 000 xg and 4°C for 30 minutes, and the supernatant discarded. Then 26.7 µl of 7.5 M NH₄OAc, 373.3 µl of RNase-free water, and 1 ml of 99% ethanol were added to each sample, before the RNA pellet was resuspended, and incubated at -80°C for 1 hour. The samples were centrifuged once again for 30 minutes at 16 000 xg and 4°C, the supernatant discarded, and the pellet desiccated for 20 minutes. The RNA pellet was then resuspended in 50 µl of RNase-free water and stored at -20°C.

2.4.3 Enzyme activity assays with [α^{32} -P]GMP labelled tRNA prepared by run-off transcription

The minimum amount of transcript required for viewing by autoradiography was determined after separating 10-fold and 100-fold dilutions of the labelled transcripts on a small 8.3 cm x 7.3 cm polyacrylamide/urea gel for 1 hour. Each enzyme assay was prepared by adding 1 µl of 1 M glycine (pH

9.0), 1.0 μ l of 100 mM MgCl₂, 1 μ l of 4 mM CTP, 1 μ l of 10 mM ATP, an appropriate amount of diluted or undiluted labelled transcript, and RNase free water, such that when the enzyme (100 ng/1.64 μ l) was added, the total volume was 10 μ l. The reactions were carried out at either 22°C, or 37°C as noted. The reactions were initiated by adding enzyme to a 1.5 ml Eppendorf containing all of the reagents specified above, and mixing very briefly with the same tip. The reactions were then immediately incubated for 2 min at 22°C, or 37°C as indicated. The reaction was then terminated by adding 10 μ l of Peattie's loading buffer to each reaction vessel, dipping the Eppendorf tube into boiling water for 5-10 seconds, placing it in a heating block set at 65°C for at least 10 minutes and allowing it to cool to room temperature. The reactions were subsequently electrophoresed on a 12% polyacrylamide/urea denaturing gel for 6 hours to determine post-assay transcript lengths, or stored at -80°C for electrophoresis at a later time (section 2.4.4). After electrophoresis, a Geiger counter was used to determine the location of the RNA transcripts, the gel was sliced well above this region, and a pick-up film (old used film) applied to remove the transcript containing gel slice. This gel slice was then wrapped in plastic along with the pick-up film. A new Fuji Medical X-ray (Super RX) film was then cut to fit the gel slice, and placed on top of the plastic wrapped gel in a cassette. The cassette was then incubated at -80°C for at least one day of exposure time. A Kodak X-OMAT 1000A film processor was then used to develop the film. The gel was subsequently placed on a phosphor screen grid in a cassette (Amersham Biosciences), and exposed for 1-24 hours. The phosphor screen image was then developed by a Typhoon Trio multi-mode imager (GE Healthcare) and analyzed using IMAGEQUANT software (GE).

2.4.4 Denaturing polyacrylamide gels

A Sequi-Gen GT Nucleic Acid Electrophoresis Cell with 38 cm x 50 cm integral plate chamber (IPC) was used to determine all activity assay results. The lower polyacrylamide/urea plug was prepared first

by mixing 20.0 ml of 30% polyacrylamide/bisacrylamide solution with 16.82 g of urea, and filling to 40 ml with 1xTBE. This solution was then heated while stirring until the solution was clear. The resulting solution was polymerized relatively quickly by adding 240 μ l of 10% APS and 100 μ l of TEMED. Then, 150 ml of 12% polyacrylamide/urea denaturing gel solution was prepared by mixing 39.9 ml of 45% stock polyacrylamide/bisacrylamide solution, 15 ml of 10x Tris/Borate/EDTA (TBE) buffer, 63 g of urea, with 42.15 ml distilled water while stirring and heating in a fume hood until the solution was clear. This solution was then allowed to cool to room temperature, before degassing for at least 20 minutes. To polymerize the gel slowly, 975 μ l of 10% APS and 20 μ l of TEMED were used. A 32 well forming 0.4 mm plastic comb was used for all experiments. The gel was then allowed to solidify overnight, the apparatus assembled, filled with 1xTBE running buffer, and the comb removed. The wells were then rinsed with the 1xTBE running buffer before conducting a 1 hour pre-run at 1200 volts in order to warm the system. All samples were loaded onto the gel, and electrophoresis was carried out at 1900 volts for 6 hrs.

2.5 Biophysical characterization of variant and native tRNA nucleotidyltransferase

2.5.1 Far-UV circular dichroism spectroscopy studies

Circular dichroism studies were performed on all proteins, in the 200-280 nm far-UV region, at 22°C using a JASCO 815 spectropolarimeter. All of the protein concentrations were adjusted to 61 μ g/ml in these experiments. The experiments were conducted using a 0.2 cm quartz cuvette. The sensitivity was set to standard (100 mdeg), with a data pitch of 0.2 nm. The scan speed was set to 20 nm/min, a band width of 1 nm, and a response time of 1 second. Five accumulations were collected. The 1 x PBS buffer (pH 7.3) was scanned under identical conditions in order to establish the base line, which was

subsequently subtracted from each spectrum in order to reveal the protein spectra alone. It is important to note that the voltage values were well below 700 mV for all of these scans.

2.5.2 Thermal denaturation studies by circular dichroism

The JASCO 815 spectropolarimeter was also used to conduct thermal denaturation studies for the 20-70°C temperature range, using a 0.2 cm cuvette. The concentration of each variant was adjusted to 61 µg/ml, and a 500 µl aliquot was added to the cuvette. Protein unfolding was followed by monitoring the change in ellipticity at 222 nm. The data pitch was set to 0.2°C, with a 2 second delay time. The temperature slope was set to 30°C/hour, with sensitivity at 100 mdeg, and a 0.25 second response time. The band width in these studies was also set at 1 nm.

2.5 Studies of intrinsic fluorescence at excitation wavelengths of 280 nm, and 295 nm

A Varian Carey Eclipse Fluorescence spectrophotometer was used for all fluorescence studies. The samples were monitored in a 1.0 cm quartz cuvette. Fluorescence was induced at excitation wavelengths of 280 nm, and 295 nm, over a range of 300-400 nm. Scans (10) were collected for each spectra in ‘CAT MODE’, at a ‘FAST’ scan speed. The slit width for both excitation and emission were set at 5 nm. The voltage was set to ‘MED’, and the temperature control was set to 22°C. The protein concentrations used were 61.0 µg/ml and 21.3 µg/ml for studies conducted at excitation wavelengths of 280 nm and 295 nm respectively.

3.0 RESULTS

3.1 Plasmid construction

Inserts for the wild-type and mutant *CCA1* genes of *S. cerevisiae* were PCR amplified from vector pDK200 (or derivative) using *Bam*HI and *Sal*I restriction site-generating primers. A 5 µl aliquot of the resulting products was analyzed by electrophoresis on a 1% agarose gel in order to determine product size and estimate concentration. The results indicated that all of the products were similar in size to that of the open reading frame of *CCA1*; 1557 bp (Fig. 3-1). All PCR products were then gel extracted, and restriction digested with *Bam*HI and *Sal*I. The digested products were then cleaned once more, and ligated into a modified pGEX-2T vector (Shan *et al.*, 2008) previously digested with *Bam*HI and *Sal*I. *E.coli* transformants were generated from the ligation mixtures, and screened by restriction analysis. The inserts of appropriate size were then verified by DNA sequencing.

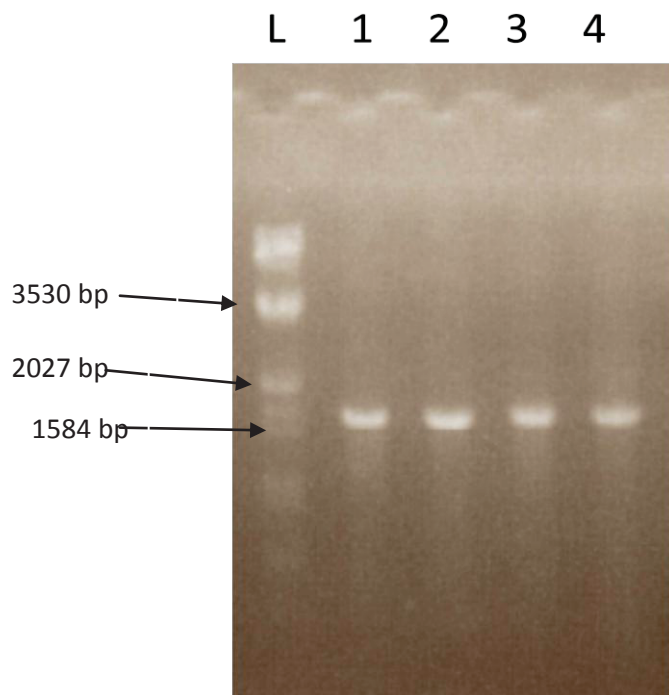


Fig. 3-1: 1% Agarose gel of PCR products used to make plasmid constructs. Lane L, λ DNA/*Eco*RI digested with *Hind*III ladder; lane 1, R64W; lane 2, R64WE189K; lane 3, E189; lane 4, R64WE189F.

3.2 Over-expression and purification of GST-fusion proteins

Over-expression of all five GST-fusion proteins (E189, R64W, R64WE189F, R64WE189K, and E189F) was achieved by IPTG induction (Fig. 3-2). Following induction, the proteins were purified according to the GST-fusion protein purification protocol (section 2.3). SDS-PAGE of total extracts from induced and non-induced cells revealed a prominent band at ~84 kDa (the size expected for this GST-tRNA nucleotidyltransferase fusion protein) in the induced lanes as compared to the non-induced lanes (Fig. 3-2).

The protein eluted from the glutathione column with 15 mM glutathione after washing showed high purity according to SDS-PAGE results, with the exception of remaining free GST (Fig. 3-3). The fractions showing the greatest amount of GST-tRNA nucleotidyltransferase were collected and subjected to thrombin protease treatment, dialyzed a few times, and loaded back onto the regenerated column to remove free GST tag, and any undigested GST-fusion protein. Elution from the glutathione column after off-column cleavage in this manner generally resulted in protein at approximately 90% purity which was used in all subsequent experiments (Fig. 3-4).

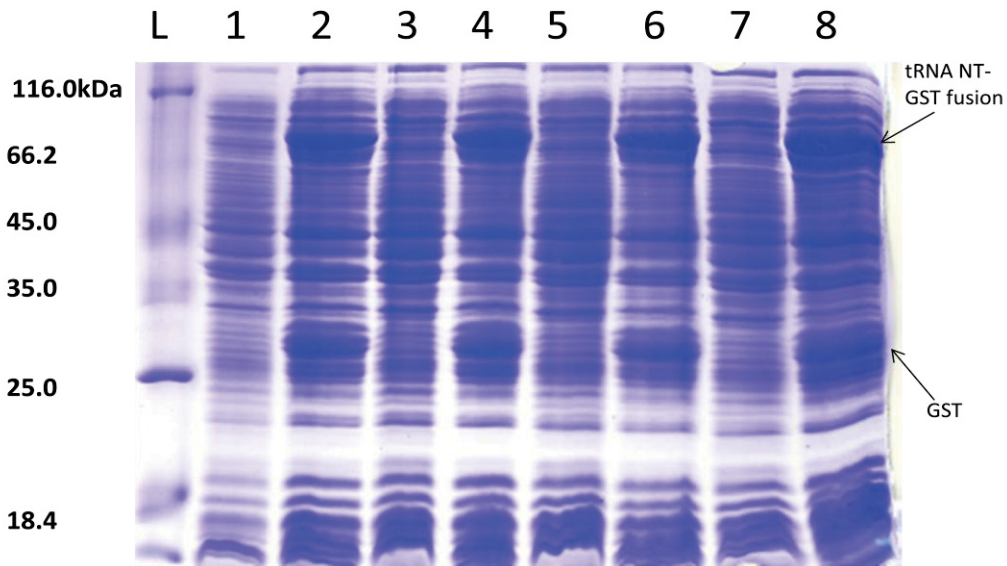


Fig. 3-2: SDS-PAGE of lysate from induced and non-induced E189, R64W, R64WE189F, and R64WE189K carrying strains (expression test). Cultures of BL21 carrying one of the constructs were grown with and without IPTG during the protein purification induction period, passed through the French pressure cell, and the lysates were resolved by SDS-PAGE. Lane L, molecular weight ladder (molecular weight values are shown adjacent to the ladder); lane 1, R64W (non-induced); lane 2, R64W (induced); lane 3, R64WE189K (non-induced); lane 4, R64WE189K (induced); lane 5, R64WE189F (non-induced); lane 6, R64WE189F (induced); lane 7, E189 (non-induced); lane 8, E189 (induced). The positions of tRNA nucleotidyltransferase-GST fusion protein (tRNA NT-GST fusion), and free GST are indicated.

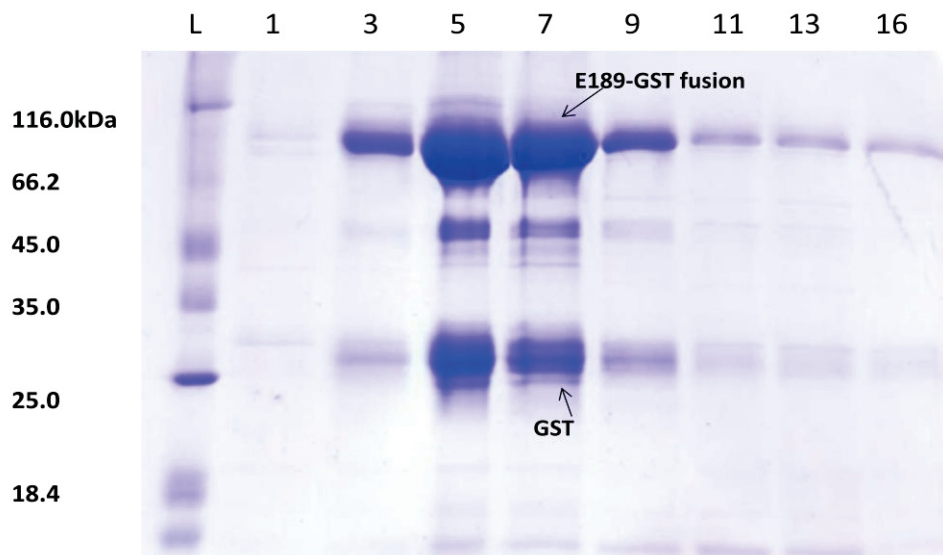


Fig. 3-3: SDS-PAGE of protein eluate for purification of E189. After 1 ml fractions of 15 mM glutathione eluate were collected from the GST-column, 16 µl from fractions 1, 3, 5, 7, 9, 11, 13, and 16 were resolved by SDS-PAGE. Lane L signifies the molecular weight ladder, and molecular weight values can be found adjacent. The positions of the E189-GST fusion protein, and free GST are marked.

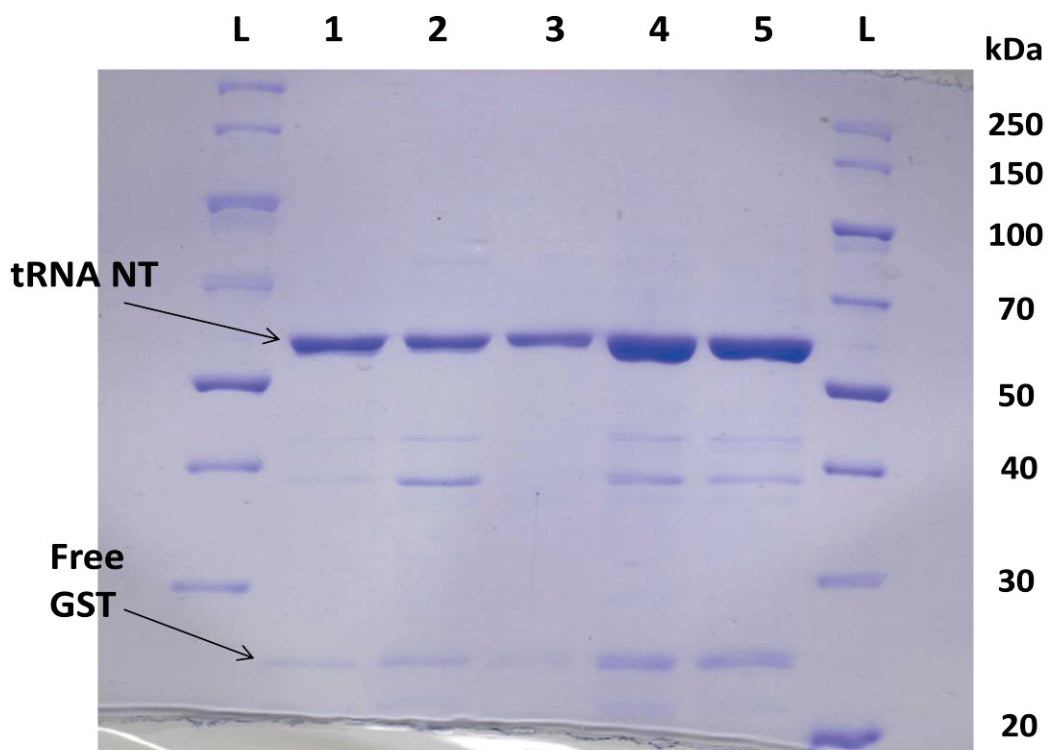


Fig. 3-4: SDS-PAGE of all purified proteins used in this study showing protein quality: 16 µl of each purified protein from the freezer stock was added per lane. Lane L, PageRuler™ unstained Broad Range Protein Ladder #SM1881; lane 1, E189 at 75.0 µg/ml; lane 2, E198F at 72.0 µg/ml; lane 3, R64W at 61.0 µg/ml; lane 4, R64WE189F at 195.0 µg/ml; lane 5, R64WE189K at 108.5 µg/ml.

3.3 Biophysical characterization of tRNA nucleotidyltransferase

3.3.1 Characterization of secondary structure by circular dichroism

Ellipticity (θ) is mainly affected by symmetrical features of the peptide backbone at the level of secondary structure. Accordingly, the symmetry found in α -helix and β -sheet structures contribute most to the shape of recorded spectra. The native enzyme, and each of the four variant enzymes, were subjected to far-UV circular dichroism (CD) at 22°C in order to determine the secondary structural features achieved by the peptide backbone at room temperature. All of the spectra are dominated by essentially the same double-trough features (Fig. 3-5) that are the hallmark of α -helices with characteristic minima values at 208 nm and 222 nm (Creighton *et al.*, 1998). This suggests that each protein is dominated by α -helical content as is expected from analysis of the available crystal structures for class II tRNA nucleotidyltransferases and the PYHRE generated model of tRNA nucleotidyltransferase from *Saccharomyces cerevisiae* (Fig. 1-9).

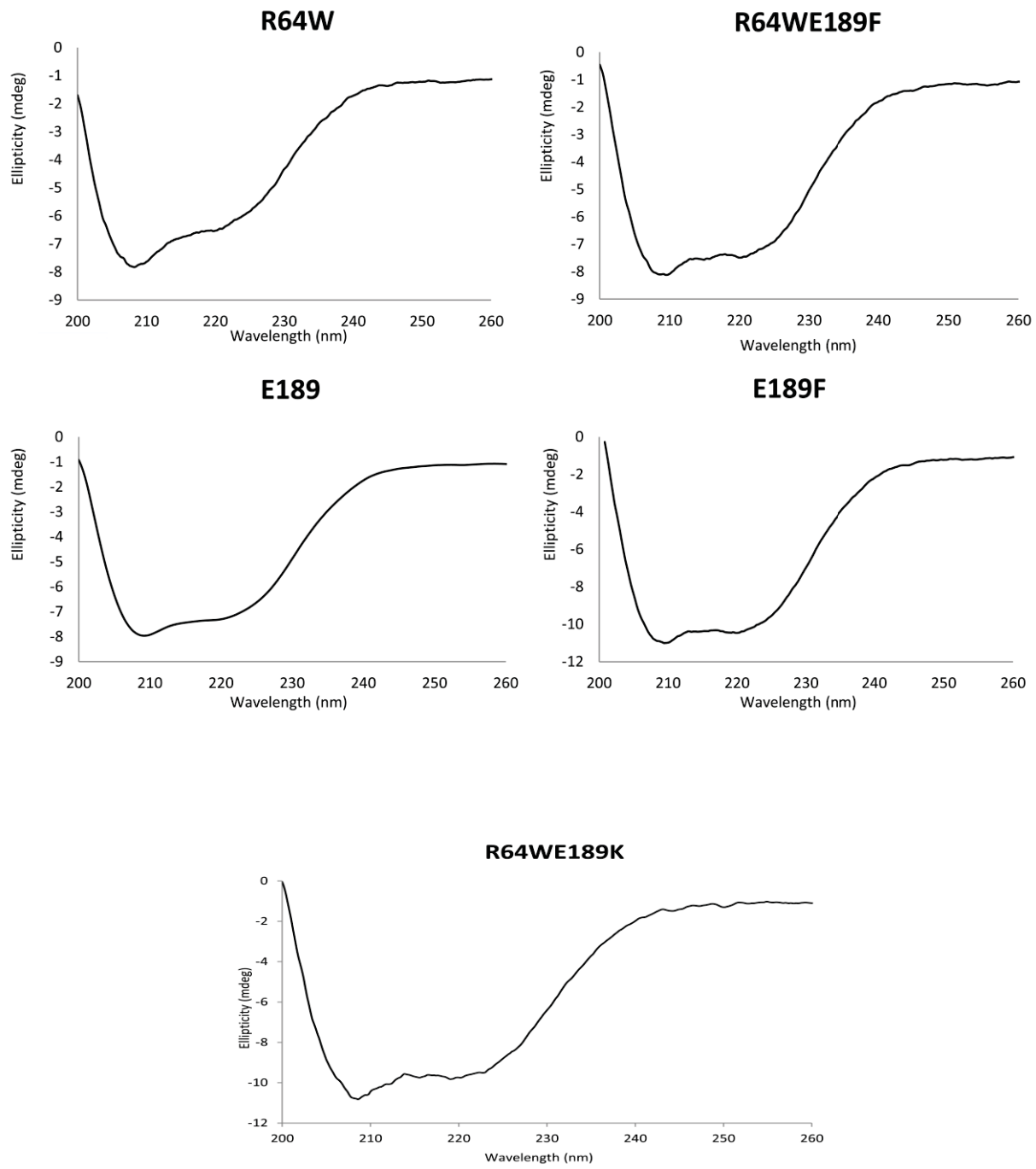


Fig. 3-5: Far-UV Circular Dichroism spectra for the native enzyme E189, and variant enzymes R64W, R64WE189F, R64WE189K and E189F. All enzyme samples were dissolved in 1 x PBS at pH 7.3, and scans were conducted at 5 accumulations.

3.3.2 Characterization of tertiary structure by fluorescence spectroscopy at excitation wavelengths of 280 nm and 295 nm

Fluorescence studies were conducted at excitation wavelengths of 280 nm and 295 nm in order to characterize the tertiary structure of each of the enzymes. Excitation at 280 nm induces fluorescence in the three amino acid chromophores in the following order of decreasing intensity; tryptophan > tyrosine > phenylalanine, while excitation at 295 nm induces fluorescence of tryptophan residues exclusively (Creighton *et al.*, 1998).

At an excitation wavelength of 280 nm the R64WE189F variant shows a maximum signal intensity that is approximately 20% higher than those of the E189, R64W, and E189F variants, and 10% higher than R64WE189K (Fig. 3-6). This increase in fluorescence intensity may be due to the incorporation of two additional chromophores; W and F, in that double mutant enzyme.

The fluorescence intensity maxima of each of the variants are redshifted relative to the native enzyme; which shows a fluorescence maximum at 323 nm (Table. 3-1). R64W has a fluorescence maximum at 326 nm, followed by R64WE189K at 327 nm, while R64WE189F and E189F both have identical fluorescence maxima at 330 nm.

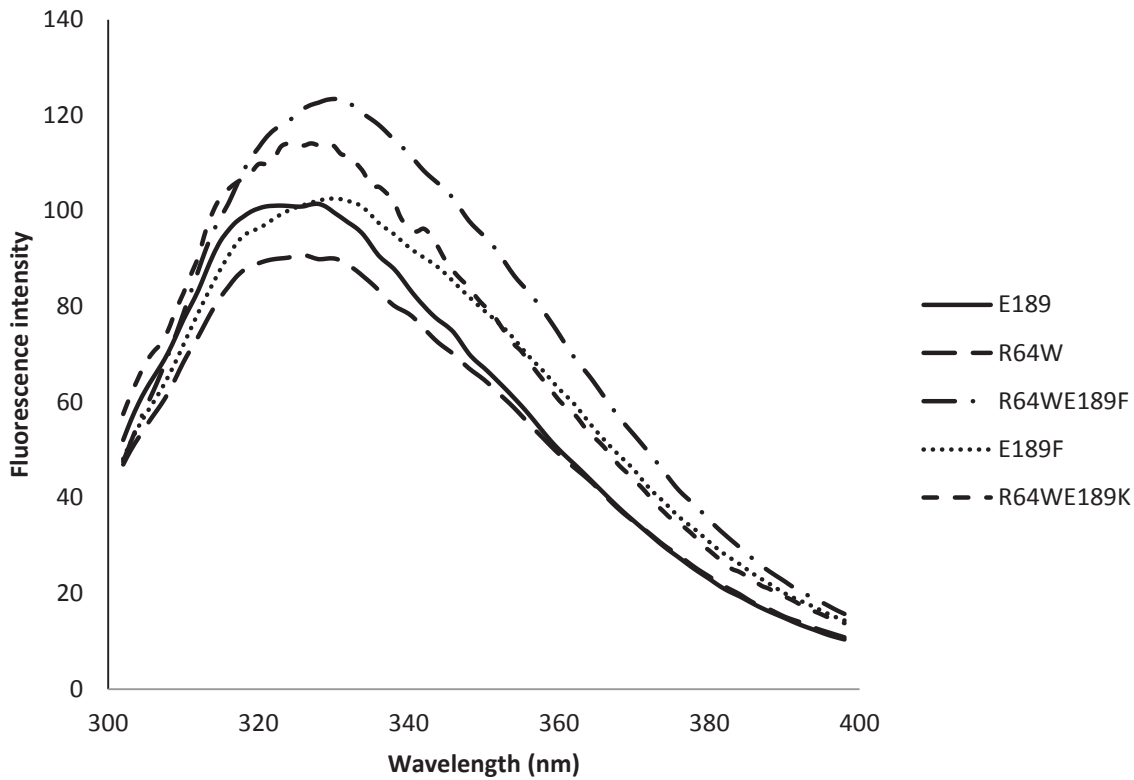


Fig. 3-6: Fluorescence emission spectra for native and variant tRNA nucleotidyltransferases excited at 280 nm. The fluorescence emission for each enzyme was measured at 22°C in the range of 300-400 nm.

Protein	Fluorescence maxima (λ_{\max}) at an excitation wavelength of 280 nm measured at 22°C
E189	323
R64W	326
R64WE189K	327
R64WE189F	330
E189F	330

Table. 3-1: Fluorescence emission maxima of native and variant proteins measured at 22°C and excited at 280 nm.

When fluorescence studies were conducted at an excitation wavelength of 295 nm (Fig. 3-7), the proteins showed an increase in fluorescence intensity in the following order; native, R64W, R64WE189K, R64WE189F, and E189F, which is different from that seen when the enzymes were excited at 280 nm. However, as was seen when the samples were excited at 280 nm, the emission maxima for R64W,

R64WE189F, and E189F are redshifted relative to the native enzyme which shows a fluorescence maximum at 329 nm (Table. 3-2). Notably, R64WE189K does not show a redshift at an excitation wavelength of 295 nm, but instead shares a λ_{\max} of 329 nm with the native enzyme.

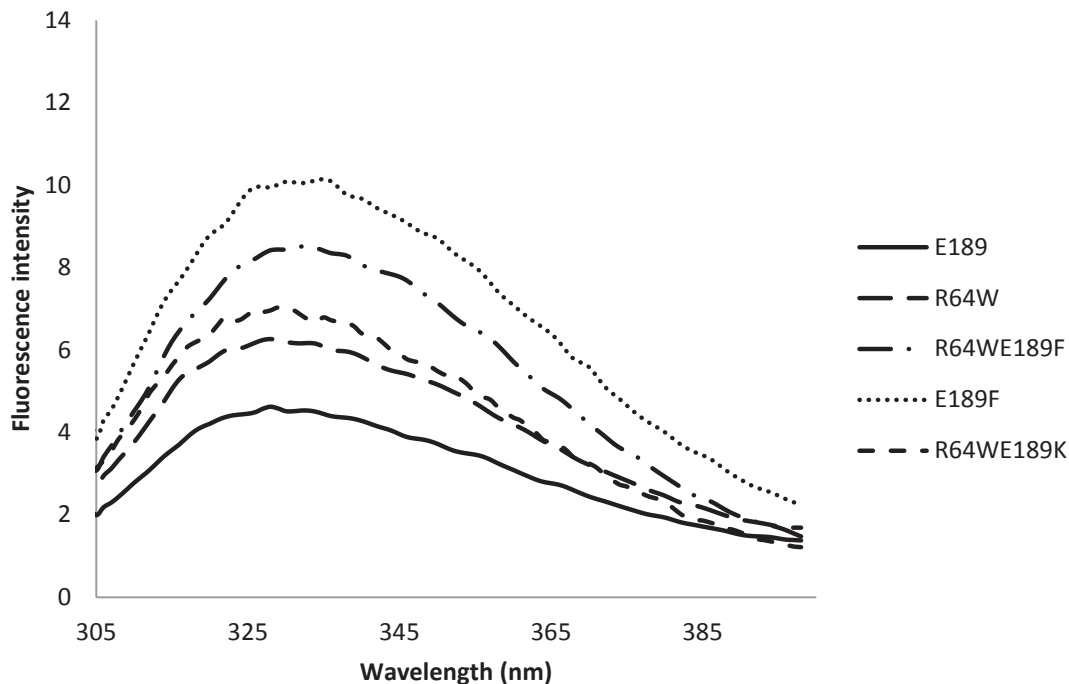


Fig. 3-7: Fluorescence emission spectra for native and variant tRNA nucleotidyltransferases excited at 295 nm. The fluorescence emission for each enzyme was measured at 22°C in the range of 300-400 nm.

Protein	Fluorescence maxima (λ_{\max}) at an excitation wavelength of 295 nm measured at 22°C
E189	329
R64WE189K	329
R64W	330
R64WE189F	332
E189F	333

Table. 3-2: Fluorescence emission maxima of native and variant proteins measured at 22°C and excited at 295 nm.

3.3.3 Temperature induced denaturation of native and variant enzymes monitored by circular dichroism spectroscopy

The thermal stability of the native and variant enzymes was accessed by monitoring the change in α -helical content as a function of increasing temperature using circular dichroism spectroscopy. Increasing temperature at a slow, and constant rate causes dissolved protein to undergo thermally-induced denaturation, which eventually results in the loss of all secondary structure. Since total α -helical content is responsible for most of the peak minima which occurs at 222 nm, it is the preferred wavelength for monitoring total α helical content throughout the thermal denaturation process.

Two properties are used to access thermal denaturation profiles; melting temperature (T_m), and percent remaining α -helicity at 37°C. T_m is defined as the temperature at which 50% of the initial amount of secondary structure is lost. Percent remaining α -helicity at 37°C is the fraction of remaining ellipticity at 37°C, relative to the initial amount of ellipticity at 22°C. The native and R64W enzymes display the highest level of thermal stability, whereas E189F and R64WE189F define the lowest level of thermal stability (Fig. 3-8). R64WE189K exhibited an intermediate level of thermal stability. While E189F and R64WE189F have both lost approximately 40% of their α -helical content at 37°C, R64W, E189, and R64WE189K have lost less than 20% of their initial α -helical content at 37°C (Table. 3-3).

Each complete thermal denaturation profile was resolved for 90 minutes, which meant exposing the protein to high temperatures for an extensive period. A CD scan was conducted at the end of each thermal denaturation experiment, and in each case such scans revealed that the protein had been completely denatured (data not shown). This conclusion was supported by the appearance of white protein precipitate in the cuvette at the end of each run, even after the cuvette had been allowed to cool to room temperature. Together, these data suggest that thermal denaturation is not reversible once a maximum thermal scan temperature of 70°C has been reached.

Thermal denaturation curves

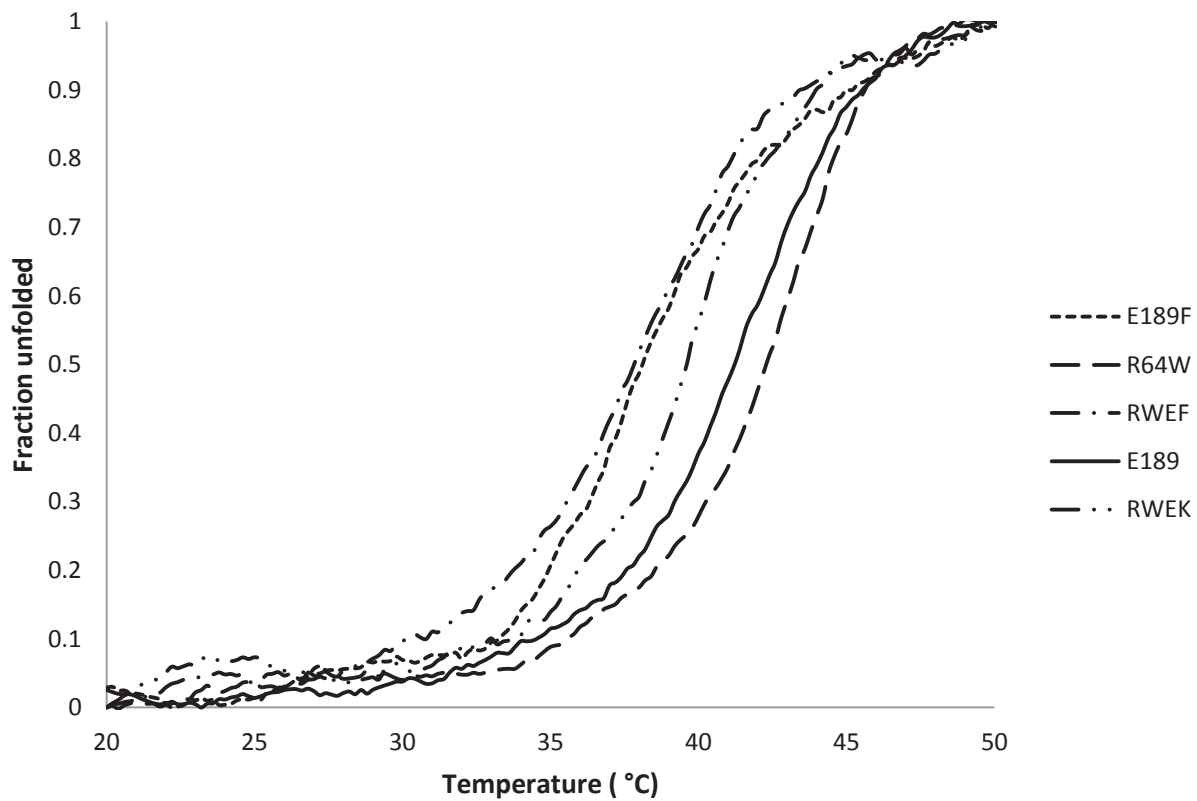


Fig. 3-8: Overlaid thermal denaturation curves for E189, and each of the variant enzymes.

Protein	Tm (°C)	% of θ_{222} at 37°C as compared to 22°C
E189	41.2	82.6
R64W	42.3	86.0
R64WE189F	37.8	61.0
R64WE189K	39.6	80.3
E189F	38.1	62.7

Table. 3-3: The melting temperature (T_m), and percent remaining α -helicity at 37°C for E189 and each of the variant enzymes.

3.4 Run-off transcription activity assays

3.4.1 Digestion of G73 and pmBSDCCA plasmids by restriction enzymes

The G73 and pmBSDCCA plasmids encoding a *B. subtilis* Asp-tRNA^{GUC} gene were digested by specific restriction enzymes to generate templates for run-off transcription (Fig. 3-9). Run-off transcription of the appropriate templates allowed the generation of four specific products which differed at their 3' ends; producing either N, N-C, N-CC, or N-CCA, where 'N' indicates the discriminator base at position 73. Each of these transcripts could then be used as substrates in activity assays, or together to provide products of expected size for a ladder.

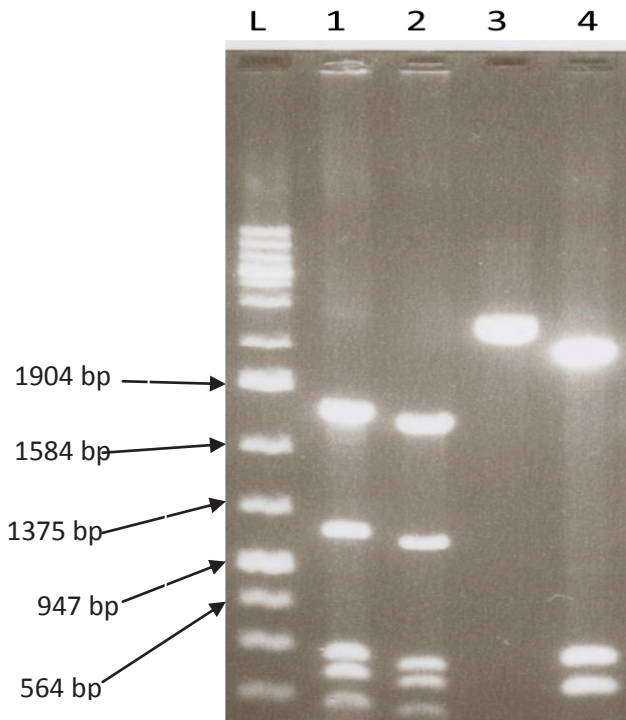


Fig. 3-9: 1% Agarose gel of digested G73, and pmBSDCCA plasmids. Lane L, λ DNA/EcoRI digested with HindIII ladder; Lane 1, G73 digested with *FokI*; lane 2-4, pmBSDCCA digested with *FokI*, *Bpi*, and *BstOI* respectively.

3.4.2 Enzyme activity assays with tRNA-N, tRNA-NC, or tRNA-NCC with ATP, CTP, or ATP and CTP at 22°C

In each of the following assays the indicated enzymes and NTPs were added to the standard reaction mixtures, and the reaction was allowed to proceed for 2 minutes at 22°C (section 2.4.3).

When tRNA-N is provided as the tRNA substrate in the presence of both ATP and CTP, or with CTP alone, E189, R64W, R64WE189F, and R64WE189K each produce a 76 nucleotide addition product (Fig. 3-10, Table 3-4).

With the same 73 nucleotide template, when ATP is the only nucleotide provided, nucleotide addition product length is different for each enzyme. E189 produces nucleotide addition products of 75 and 76 nucleotides. R64W produces 74 and 75 nucleotide addition products, with the double addition product of 75 nucleotides as the major product. R64WE189F produces a 75 nucleotide addition product alone, and R64WE189K produces 74 nucleotide and 75 nucleotide addition products, with approximately equimolar stoichiometry.

These data indicate that all enzymes other than E189F can carry out at least two consecutive additions of CMP or AMP when either is present alone, and that tRNA-N is extended by three nucleotides when both CTP and ATP are present together.

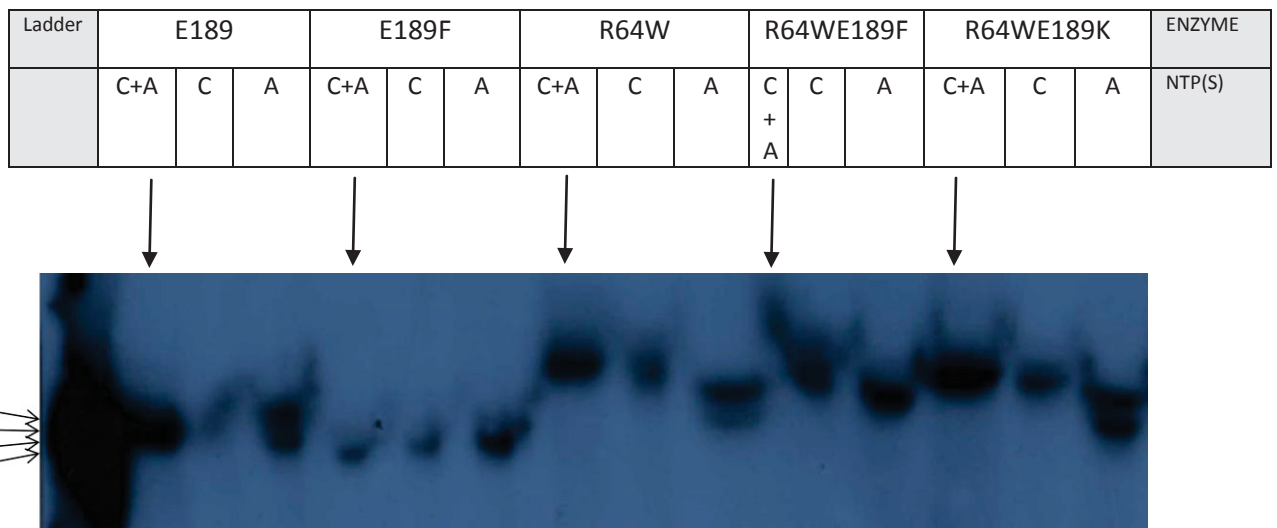


Fig. 3-10: Gel assay results for native and variant enzymes under various ATP and CTP availability conditions with tRNA-N. Template was mixed with ATP and/or CTP along with each enzyme and allowed to react for 2 min before the reactions were terminated by addition of an equal volume of Peattie's loading buffer. Samples were subsequently resolved by 12% acrylamide denaturing gels.

ENZYME	E189			E189F			R64W			R64WE189F			R64WE189K		
NTP(S)	C+A	C	A	C+A	C	A	C+A	C	A	C+A	C	A	C+A	C	A
COUNTS 76 nt	178.06	47.64	75.74	—	—	—	74.91	51.09	—	52.65	46.52	—	110.39	51.84	—
COUNTS 75 nt	—	—	48.49	—	—	—	—	—	54.84	—	—	62.57	—	—	58.12
COUNTS 74 nt	—	—	—	—	—	—	—	—	37.12	—	—	—	—	—	48.79
COUNTS 73 nt	—	—	—	45.42	43.89	63.83	—	—	—	—	—	—	—	—	—

Table. 3-4: The counts for each product of activity assays conducted with tRNA-N and each of the five enzymes. The counts reflect the band intensities as determined by the peak height parameter for the 73, 74, 75, and 76 nucleotide products (nt) using IMAGEQUANT software (GE).

When the 74 nucleotide tRNA-NC template is used as the tRNA substrate, E189, R64W, R64WE189F, and R64WE189K each produce a 76 nucleotide product as the major addition product with either ATP and CTP supplied together, or CTP supplied alone (Fig. 3-11, Table. 3-5).

Once again, when only ATP is present, the nucleotide addition product length is different for each enzyme. E189 appears to have added one AMP producing a 75 nucleotide product as the major product, and two AMPs to produce a 76 nucleotide product in high quantities as well. R64W added one AMP to

produce a 75 nucleotide addition product. R64WE189F appears to have added two AMPs to produce a 76 nucleotide major product, whereas R64WE189K has added one AMP to produce a 75 nucleotide major addition product. E189F appears not to have added any nucleotides to the original tRNA-NC substrate when both CTP and ATP were present together, or when each was present alone. This confirms that 4% activity (Shan *et al.*, 2008) is beneath the threshold of visibility when gel assays are prepared in this fashion. According to these data, E189, R64W, and the double variant enzymes are each capable of extending the immature substrate; tRNA-NC, by two CMP when CTP is present alone, or at least one AMP when only ATP is supplied. Also, each of the enzymes with the exception of E189F is capable of extending tRNA-NC to 76 nucleotides in the presence of both CTP and ATP together.

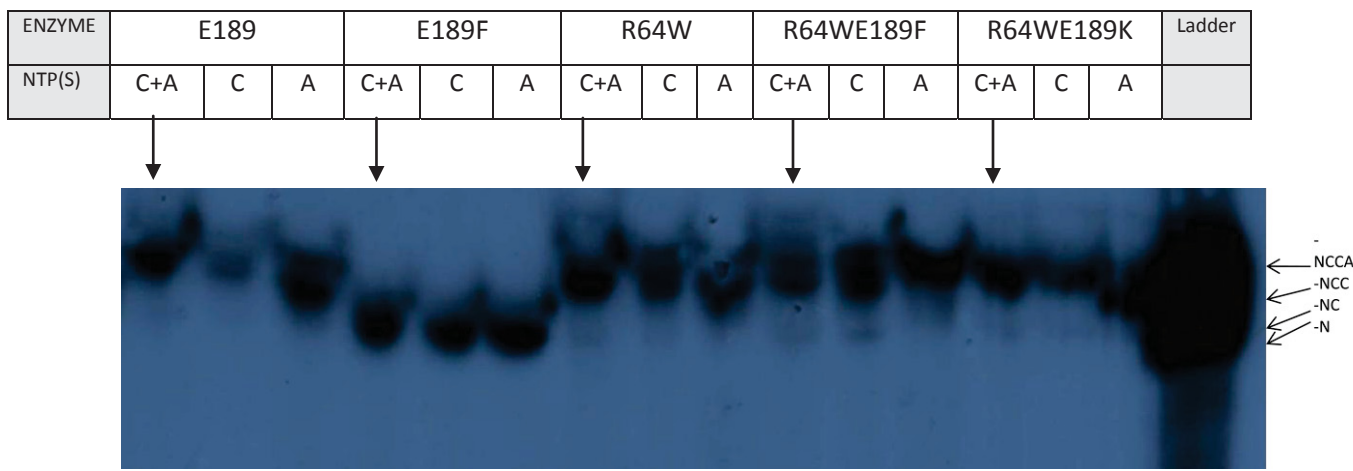


Fig. 3-11: Gel assay results for native and variant enzymes under various ATP and CTP availability conditions with tRNA-NC. Template was mixed with ATP and/or CTP along with each enzyme and allowed to react for 2 min before the reactions were terminated by addition of an equal volume of Peattie's loading buffer. Samples were subsequently resolved by 12% acrylamide denaturing gels.

ENZYME	E189			E189F			R64W			R64WE189F			R64WE189K		
NTP(S)	C+A	C	A	C+A	C	A	C+A	C	A	C+A	C	A	C+A	C	A
COUNTS 76 nt	100.79	42.88	60.58	—	—	—	142.38	61.81	—	70.88	72.92	240.81	141.98	100.41	—
COUNTS 75 nt	—	—	84.07	—	—	—	—	—	65.62	—	—	—	—	—	126.44
COUNTS 74 nt	—	—	—	96.55	99.8	131.93	—	—	—	—	—	—	—	—	—

Table. 3-5: The counts for each product of activity assays conducted with tRNA-NC and each of the five enzymes. The counts reflect the band intensities as determined by the peak height parameter for the 74, 75, and 76 nucleotide products (nt) using IMAGEQUANT software (GE).

When the 75 nucleotide tRNA-NCC template was used as the tRNA substrate, E189, R64W, R64WE189F, and R64WE189K each produced 76 nucleotide long major products with either CTP or ATP added separately, or together (Fig. 3-12, Table. 3-6). E189F did not show any visibly obvious addition products in the presence of CTP and ATP, either together or alone. These data indicate that R64W and the double mutant enzymes can add AMP to immature tRNA-NCC substrates, thereby producing mature tRNA-NCCA, at native-like levels, when ATP is supplied alone.

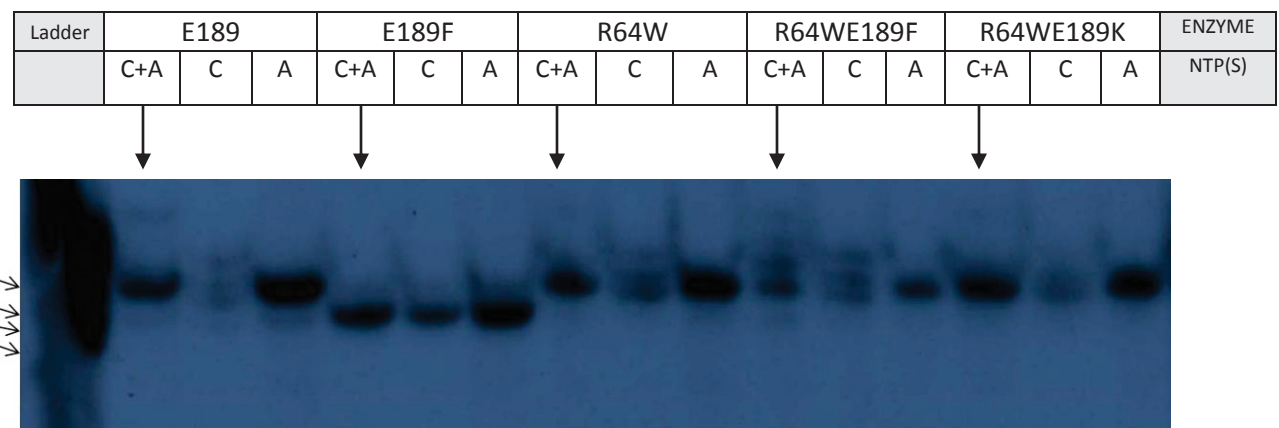


Fig. 3-12: Gel assay results for native and variant enzymes under various ATP and CTP availability conditions with tRNA-NCC. Template was mixed with ATP and/or CTP along with each enzyme and allowed to react for 2 min before the reactions were terminated by addition of an equal volume of Peattie's loading buffer. Samples were subsequently resolved by 12% acrylamide denaturing gels.

ENZYME	E189			E189F			R64W			R64WE189F			R64WE189K		
NTP(S)	C+A	C	A	C+A	C	A	C+A	C	A	C+A	C	A	C+A	C	A
COUNTS 76 nt	58.3	46.47	218.24	—	—	—	71.02	67.62	124.9	60.47	64.99	73.16	92.53	52.26	122.71
COUNTS 75 nt	—	—	—	108.05	74.36	146.92	—	—	—	—	—	—	—	—	—

Table. 3-6: The counts for each product of activity assays conducted with tRNA-NCC and each of the five enzymes. The counts reflect the band intensities as determined by the peak height parameter for the 75, and 76 nucleotide products (nt) using IMAGEQUANT software (GE).

3.4.3 Enzyme activity assays with tRNA-N, tRNA-NC, or tRNA-NCC under various NTP substrate availability conditions at 37°C

The following activity assays were conducted at 37°C with tRNA-N, -NC, and -NCC templates. For these particular assays CTP and ATP were supplied together with tRNA-N, the -NC assays were supplied with CTP alone, and -NCC assays were supplied with ATP alone. E189, R64W, R64WE189F, and R64WE189K each produced a 76 nucleotide addition product as the major product, under all of the various conditions described above (Fig. 3-13, Table. 3-7). E189F failed to produce any visible additions products. These data demonstrate that the single mutant suppressor; R64W, and the double mutants, can add CMP alone to the tRNA-NC substrate producing a tRNA-NCC product, and AMP alone to the tRNA-NCC substrate, producing the mature product; tRNA-NCCA, at 37°C. However, they also suggest that these additions take place at activity levels comparable to that of the native enzyme, even at 37°C. This is consistent with the results of growth studies conducted for the single mutant suppressor; R64W, and the double mutants that display wild-type like growth at 37°C (Fig. 1-10).

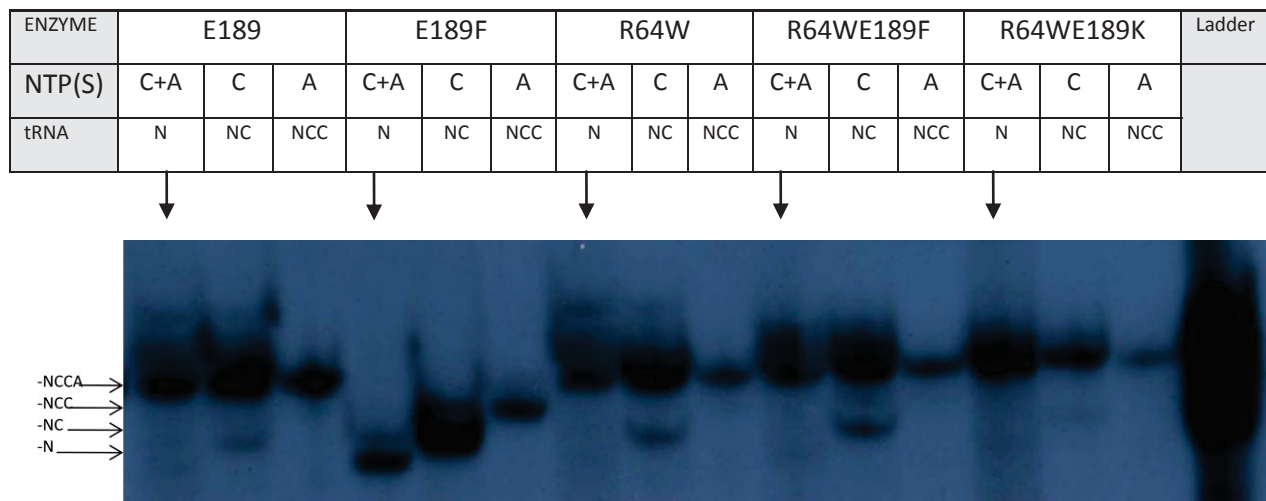


Fig. 3-13: Gel assay results for native and variant enzymes under various ATP and CTP availability conditions with tRNA-N, tRNA-NC, or tRNA-NCC conducted at 37°C. Each template was mixed with ATP and/or CTP along with each enzyme, and allowed to react for 2 min before the reactions were terminated with Peattie's buffer. Samples were subsequently resolved by 12% acrylamide denaturing gels.

ENZYME	E189			E189F			R64W			R64WE189F			R64WE189K		
NTP(S)	C+A	C	A	C+A	C	A	C+A	C	A	C+A	C	A	C+A	C	A
COUNTS 76 nt	124.07	185.36	114.92	—	—	—	87.75	161.51	77.59	74.37	220.24	118.63	267.07	143.00	77.18
COUNTS 75 nt	—	—	—	—	—	83.41	—	—	—	—	—	—	—	—	—
COUNTS 74 nt	—	—	—	—	270.42	—	—	—	—	—	—	—	—	—	—
COUNTS 73 nt	—	—	—	86.64	—	—	—	—	—	—	—	—	—	—	—

Table. 3-7: The counts for each product of activity assays conducted at 37°C with tRNA-N, tRNA-NC, or tRNA-NCC substrate and each of the five enzymes. The counts reflect the band intensities as determined by the peak height parameter for the 73, 74, 75, and 76 nucleotide products (nt) using IMAGEQUANT software (GE).

3.5 Growth data

E189F and E189K appear to be two of the most temperature-sensitive strains as judged by both liquid (Shan *et al.*, 2008), and solid media cultures (Fig. 1-10). On solid medium these cells show good growth at 22°C, but little or no growth at 37°C. However, the double mutants R64WE189F and R64WE189K show good growth at both 22°C and 37°C, demonstrating clear suppression of the temperature-sensitive phenotype caused by the E189F and E189K mutations respectively (Fig. 1-10). Mutant R64W shows good growth on solid medium at both 22°C and 37°C, suggesting that there are no deleterious effects caused by this single amino acid substitution alone (Fig. 1-10). E189 grows well at 22°C and 37°C as expected (Fig. 1-10), whereas cells bearing the vector alone grow well at 22°C, but show little or no growth at 37°C (Fig. 1-10).

E189R is another temperature-sensitive mutant; displaying good growth at 22°C, but little or no growth at 37°C on solid medium cultures (Fig. 3-14). Additionally, an R64E variant shows good growth at both the permissive and restrictive temperatures on solid media (Fig. 3-14). R64EE189F, R64EE189K, and R64EE189R also display the temperature-sensitive phenotype, demonstrating an inability of R64E to suppress the temperature-sensitive phenotype generated by E189F, E189K, and E189R respectively (Fig. 3-14).

22°C

37°C



E189R



R64E



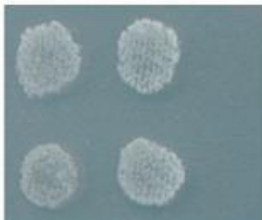
R64EE189R



R64EE189F



R64EE189K



E189K



E189F



E189

Fig. 3-14: Replica plating experiment at 22°C and 37°C for testing of the ‘salt bridge hypothesis’ (Adapted from images provided by Dr. Pamela J. Hanic-Joyce). The growth tests were conducted at the permissive temperature of 22°C, and the restrictive temperature of 37°C.

4.0 DISCUSSION

Temperature-sensitive mutants have been generated in a diverse spectrum of organisms, and are used extensively in research to help answer a wide variety of questions (section 1.6). However, relatively little research has been conducted on the mechanisms that give rise to temperature-sensitivity. Temperature-sensitive mutants should be better understood if they are going to be depended on so heavily. This work represents an effort to further our understanding of temperature-sensitivity and its intragenic suppression. More specifically, this work seeks to understand how the single E189F mutation causes the observed temperature-sensitive phenotype in *S. cerevisiae*, and how the intragenic R64W mutation works to suppress this temperature-sensitive phenotype.

4.1 Characterization of secondary and tertiary structure for the native and variant enzymes

As Shan *et al.*, (2008) showed no major differences in secondary structure for the native enzyme, and the E189K or E189F variant enzymes, it was not surprising that the far-UV circular dichroism of those native and variant enzymes characterized here, also showed no major changes (Fig. 3-5). All spectra were clearly dominated by an α -helix signal, characterized by a double dip at 208 nm and 222 nm feature (Creighton *et al.*, 1993). Contributions from β -sheets characterized by a dip at 215 nm in the scan range of 200-280 nm (Creighton *et al.*, 1993) were not apparent (Fig. 3-5). These results also support the model generated by PYHRE for the native and variant proteins (Fig. 1-9). The models predict that each of these enzymes is composed of 15 α -helices, and only two β -sheets; one major and one minor. This is reasonable considering that the four tRNA nucleotidyltransferases that have been crystallized to date display 33-54% α -helical content, and 5-10% β -sheet content (<http://www.rcsb.org/pdb/home/home.do>). Given that both glutamate 189 and arginine 64 are

predicted to occur in the major β -sheet, it is perhaps not surprising that no major changes were observed in α -helical content at 22°C. A more detailed analysis of the β -sheet structure by a technique such as Fourier Transform Infrared (FTIR) spectroscopy may be more informative. This technique is very sensitive to the differences in H-bonding patterns between α -helix and β -sheet regions of a protein, and the characteristic peaks are observed in different regions of the infrared spectrum (Creighton *et al.*, 1993).

Given that yeast tRNA nucleotidyltransferase contains 5 tryptophan residues and 15 tyrosine residues, it is an excellent candidate for fluorescence analysis. Previously, Shan *et al.*, (2008) had shown an 8 nm redshift in fluorescence when comparing the emission maxima of the native enzyme and E189F variant after excitation at 280 nm.

In order to probe changes in tertiary structure, fluorescence studies were conducted at excitation wavelengths of 280 nm and 295 nm for the native and variant enzymes at 22°C. When proteins are excited at 280 nm, all of the chromophoric amino acids; phenylalanine, tyrosine, and tryptophan are induced to fluorescence (Creighton *et al.*, 1989). However, excitation at 295 nm only induces the emission of tryptophans (Creighton *et al.*, 1989). The fluorescence spectra at each excitation wavelength has revealed that the lambda max (λ_{\max}) for the variant enzymes are redshifted relative to that of the native enzyme, by as much as 7 nm at 280 nm excitation, and 4 nm at 295 nm excitation (Table 3-1 and 3-2). These redshifts indicate that there are changes in the asymmetric polar environment of the chromophores brought about by altered protein conformation due to the amino acid substitution mutation(s) (Creighton *et al.*, 1989). Furthermore, these conformational changes have generally increased the exposure of chromophores to the water solvent, resulting in mild fluorescence quenching (Creighton *et al.*, 1989). This may mean that the tertiary structures of the variants are loosened relative to that of the native protein, although most of the tertiary structure is preserved. Typically, differences

in the amplitude of fluorescence intensity at λ_{\max} do not reliably indicate anything about protein structure, so little is revealed by this information in particular (Creighton *et al.*, 1989).

4.2 Characterization of thermal stability of the native and variant enzymes

Previous thermal denaturation studies conducted on tRNA nucleotidyltransferases from temperature-sensitive strains; E189F and E189K, as well as the native enzyme; E189, provided melting temperature (T_m) values of 36.5°C, 36.0°C and 42.5°C (Table 4-1), respectively (Shan *et al.*, 2008). The ~6°C range in T_m is small, but significant in terms of the proportion of tRNA nucleotidyltransferase that is induced to thermally denature *in vivo* when subjected to restrictive temperatures, because we may expect whole cell activity to decrease in direct proportion to percent denaturation. The E189 protein and the E189F variant displayed 17.4% and 37.3% thermally denatured protein at 37°C. This means that there is a greater than twofold difference in the amount of tRNA nucleotidyltransferase thermally induced to denature in the E189F mutant, compared to the wild-type at 37°C. The variants E189F and E189K display 47.1% and 48.6% thermally denatured protein at the restrictive temperature, respectively (Shan *et al.*, 2008), compared to only 10% thermally denatured protein for E189 at 37°C (Table 4-1). This almost 5-fold difference in the proportion of tRNA nucleotidyltransferase thermally induced to denature *in vivo* may cause significant deficits in the supply of mature tRNA for the cell at 37°C, and therefore could conceivably be responsible for the temperature-sensitive phenotype. This is especially true since we would expect there to be a concomitant increase in the demand for tRNA at increased temperatures as well, due to the higher rate of cell growth. This leads to the question of whether or not the thermal stability of tRNA nucleotidyltransferase is a major determining factor of the temperature-sensitive phenotype. The recent discovery of an intragenic suppressor of this temperature-sensitive phenotype

(R64W), provides us with an opportunity to access the role of thermal stability in the development of the temperature-sensitive phenotype, through suppressor analysis.

Enzyme	Enzyme Activity Level at 22°C relative to native enzyme	Thermal stability level relative to native enzyme	Growth phenotype	% reduction in α -helical content at 37°C relative to content at 22°C	% stability relative to native T_m (ℓ)	Melting temperature (T_m) in °C
E189	H	H	Wt	17.4 / 10*	100.0	41.2 / 42.5*
R64W	H	H	Wt	14.0	+135.5	42.3
R64WE189F	H	L	Wt	39.0	-9.7	37.8
R64WE189K	H	I	Wt	19.7	48.4	39.6
E189F	L	L	Ts	37.3 / 47.1*	0.0	38.1 / 36.5*
E189K	L	L	Ts	48.6*	-8.3	36.0*
E189H	L	H	Ts	12.0*	86.7	41.7*
E189Q	I	H	I	11.0*	+105.0	42.8*

Table. 4-1: Growth, activity, and biophysical parameters of the native protein and all of the variants characterized to date (Shan et al., 2008). These data illustrate a consistent correlation between the temperature-sensitive phenotype and enzyme activity. (H) high, (L) low, (I) intermediate, (Wt) wild-type, (Ts) temperature-sensitive, (*) values determined by Shan et al. (2008). (ℓ) In order to normalize T_m values derived from this study, as well as those from Shan et al. (2008), and compensate for differences in thermal stability measurement conditions between the two studies, a scale was developed for each of these studies. The E189F variant was used to define the lowest T_m range with 0% thermal stability, and E189 was used to define the normal upper T_m range for this study with 100% full thermal stability. The T_m values for all other variants used within this study were then represented as percentages on the thermal stability scale. T_m values above that of the native enzyme are designated with (+), and T_m values below that of E189F are designated with (-). The same procedure was performed for data provided by Shan et al. (2008).

As shown by Shan et al. (2008) the E189F temperature-sensitive variant displayed the lowest thermal stability, and therefore defined the lowest point in the T_m range for that study; 38.1°C (Table 3-3). The native protein showed significantly higher thermal stability, and its T_m can be regarded as the normal

melting temperature expected for tRNA nucleotidyltransferase from *Saccharomyces cerevisiae*, and therefore used to define the normal upper range (Table 3-3). In fact, the T_m for each of these proteins agreed well with those values established by Shan *et al.* (2008) for E189 and E189F (Table 4-1). Interestingly, the R64W variant shows the highest level of thermal stability recorded in this study; 42.3°C, which is 35.5% higher than even that of the native enzyme (Tables 3-3, and 4-1). Remarkably, the R64WE189F variant displays a thermal stability that is essentially identical to that of E189F, with very similar thermal denaturation profiles (Table 3-3, and Fig. 3-8). However, the R64WE189K variant displays a thermal stability that is intermediate to those of E189F and E189, with a T_m of 39.6°C (Fig. 3-8, and Table 3-3). R64W, E189, and R64WE189K lose 14 %, 17.4%, and 19.7% of their α -helical content respectively when the temperature is raised from permissive temperature (22°C) to restrictive temperature (37°C) (Table 3-3). However, R64WE189F and E189F lose 39% and 37% of their α -helical content respectively, when subjected to the same temperature change. Therefore, the thermally less stable R64WE189F and E189F variants are twice as likely to denature and lose approximately twice as much α -helix as the native enzyme, to thermal denaturation at 37°C. Yet E189F displays the temperature-sensitive phenotype, while R64WE189F does not. These data indicate that although the loss in secondary structure of R64WE189K and native enzyme are similar, suppression of temperature-sensitivity is not consistently associated with the restoration of thermal stability to native levels, and is therefore unlikely to be the direct cause of the temperature-sensitive phenotype alone. This is supported by data from Shan *et al.* (2008) with the E189H variant which displays a T_m value of 41.7°C, and a drop in α -helical content of 12% (Table 4-1). These values are virtually identical to those determined for the native enzyme E189 (T_m =42.5, and 10%), and the E189Q variant (T_m =42.8, and 11%). Yet E189H clearly exhibits the temperature-sensitive phenotype, showing little or no growth at 37°C, whereas E189Q grows at an intermediate level to those of E189 and E189F (Shan *et al.*, 2008). Although the temperature-sensitive strains; E189F and E189K, define the lowest levels of thermal stability, E189H

and E189Q share essentially the same level of thermal stability as E189, yet they exhibit the temperature-sensitive phenotype at a full and intermediate level, respectively. Therefore, the temperature-sensitive phenotype is not consistently associated with compromised thermal stability either.

Also, the native and variant enzymes display smooth thermal denaturation curves that possess a single inflection point, which suggests that unfolding is cooperative in each case (Creighton *et al.*, 1989).

4.3 Characterization of enzyme activity of the native and variant enzymes

Using standard *in vitro* enzyme assay conditions (section 2.4.3) all of the enzymes tested here with the exception of the E189F variant showed similar activity when supplied with any template (ending in –N, -NC, or –NCC) and ATP, or CTP, or ATP and CTP (Fig. 3-10 to 3-13). In contrast, under the same assay conditions the E189F variant appears to extend tRNA-N, tRNA-NC, or tRNA-NCC templates only to a small degree if at all, at either the permissive or restrictive temperature (Fig. 3-10 to 3-13).

Previous activity measurements with this enzyme were conducted using a precipitable-count based assay, and only indicated that incorporation of $\alpha^{32}\text{P}$ labeled AMP at position 76 is reduced to 4% and 5%, relative to the native enzyme, for E189F and E189K respectively (Shan *et al.*, 2008). These data do not preclude the possibility that the addition problem was restricted only to addition at the first, second, or third position. The possibility remained that CMP addition, which is known to be the default addition reaction for many class II tRNA nucleotidyltransferases (Hoffmeier *et al.*, 2010; Betat *et al.*, 2010), occurred relatively unimpeded and that the switch from CMP to AMP addition was defective. The assays performed here show that not only is AMP addition at position 76 affected (Fig. 3-12), but addition of CMP at positions 74 and 75 are also affected (Fig. 3-10 and 3-11). This indicates that for E189F at least,

the problem is not restricted to AMP addition, but does in fact severely reduce the rates of both CMP and AMP addition at all three positions, at both the permissive and restrictive temperatures. This suggests that the changes caused by the E189F substitution are such that addition of all three nucleotides has been severely reduced.

It is remarkable that the R64W substitution, from a basic hydrophilic residue to one that is very hydrophobic, does not appear to have a deleterious effect on the activity of the enzyme, or the viability of the cell, since it occurs in well-conserved motif A (Fig. 1-1). This is especially remarkable considering the fact that motif A represents the signature sequence for the nucleotidyltransferase superfamily, is located at the heart of the active site, and bears the two catalytic carboxylic acids essential for catalysis (Betat *et al.*, 2010). It appears that motif A is capable of accommodating such an amino acid substitution while sustaining native levels of specific activity.

The R64WE189F and R64WE189K variants clearly suppress the temperature-sensitive phenotype (Fig. 1-10), and their variant enzymes display native levels of activity as well (Fig. 3-10 to 3-13). Therefore, it is evident that the R64W substitution is capable of compensating for the effects caused by changing E189 to F or K. In the case of R64WE189F and R64WE189K, both of these variants show that suppression is consistently associated with native activity levels. In fact, R64W, R64WE189F and R64WE189K show that the wild-type phenotype is consistently associated with native levels of activity, and is independent of enzyme thermal stability (Table 4-1).

Furthermore the E189H variant studied by Shan *et al.*, (2008) also supports the correlation of the ts phenotype with low enzyme activity (4.0-7.6% relative to native enzyme activity), even at 22°C, irrespective of enzyme *in vitro* thermal stability (Table 4-1). The E189H variant shows a thermal denaturation curve similar to that of the native enzyme, but only 7.6% activity relative to the native enzyme, comparable to the activities of the E189F (4%) and E189K (5%) variants (Shan *et al.*, 2008).

Additionally, the liquid growth data shows the temperature-sensitive phenotype of E189H to be indistinguishable from either of the E189F and E189K temperature-sensitive mutants (Shan *et al.*, 2008). These findings also suggest that liquid cultures provide a more stringent and accurate test for comparing temperature-sensitive strains quantitatively. This is reasonable considering that generally more generations of growth are required in order to change turbidity in liquid culture, than is necessary to produce a visible colony on plates.

The E189H enzyme, along with E189F, R64WE189F, and E189 are of particular interest because they represent the four combinations of activity and thermal stability that are possible (Table 4-2). E189, which displays high specific activity and high thermal stability, produces the wild-type phenotype (Table 4-2). Alternatively, E189F shows low activity and low thermal stability, and displays the temperature-sensitive phenotype (Table 4-2). E189H displays low specific activity, comparable to E189F, and thermal stability comparable to that of the native protein, yet it too displays the temperature-sensitive phenotype (Table 4-2). However, R64WE189F which displays recovered activity, but compromised, low thermal stability is still capable of suppressing the temperature-sensitive phenotype to produce wild-type like growth on plates at 37°C (Table 4-2). Together, these four enzymes clearly illustrate a correlation of the temperature-sensitive phenotype with low specific activity, and its independence from enzyme thermal stability.

Enzyme	Enzyme Activity Level	Thermal Stability	Growth phenotype
E189	H	H	Wt
E189F	L	L	Ts
R64WE189F	H	L	Wt
E189H	L	H	Ts

Table. 4-2: Four combinations of activity and thermal stability represented by the native (E189) and three variant proteins (E189F, R64WE189F, and E189H). These four proteins illustrate the strong correlation of temperature-sensitivity with enzyme activity, but not with thermal stability. (H) high, (L) low, (Wt) wild-type, (Ts) temperature-sensitive.

The connection between enzyme activity (but not thermal stability) and the temperature-sensitive phenotype is further strengthened by the E189Q variant. This protein shows an intermediate level of activity (40% relative to native), and produces an intermediate temperature-sensitive phenotype (Table 4-1) displaying only ~40% growth at 21 hours, according to the more quantitative liquid growth tests (Shan *et al.*, 2008). This reinforces the predominant importance of enzyme activity in the development of the temperature-sensitive phenotype, because although it displays an intermediate level of activity, its thermal stability is equivalent to that of the native enzyme (Shan *et al.*, 2008). Therefore, even with a native level of thermal stability, 40% relative activity is not enough to recover wild-type levels of growth. Furthermore, these data appear to suggest that growth may be proportional to activity alone, at 37°C.

4.4 The salt bridge hypothesis of temperature-sensitive phenotype development

It was proposed that a salt bridge may form between glutamate 189 and arginine 64 in the native protein, and that this bridge might be important to thermal stability and/or activity such that its loss results in the temperature-sensitive phenotype. In order to explore this possibility an attempt was made to reconstruct the potential salt bridge by simply reversing the positions of the amino acids assumed to be involved. This can be done since E189R displays a clear temperature-sensitive phenotype as well (Fig.

3-14). To this end, an R64EE189R strain was constructed and tested for growth at 22°C and 37°C, along with R64E. The results indicate that although R64E does not appear to be deleterious to the cell by itself, it is unable to suppress the temperature-sensitive phenotype generated by E189R in the double mutant (Fig. 3-14).

Growth tests with the double mutants R64EE189F and R64EE189K also indicated that R64E is not able to suppress the temperature-sensitive phenotype generated by E189F or E189K either (Fig. 3-14). Although it is expected that temperature-sensitive suppression in R64EE189F could not arise by a salt bridge based mechanism between E64 and F189, since the side chain of phenylalanine is incapable of charge, this is not necessarily the case for R64EE189K. The N_ε of lysine is capable of being protonated, and with the proper orientation and distance can engage in salt bridge formation with the carboxylate group of a glutamate residue. R64EE189K thereby offers another opportunity for a salt bridge mechanism of suppression, yet suppression was not observed (Fig. 3-14). Although it can be argued that the salt bridge is replaced by a hydrophobic interaction in the R64WE189F variant, this does not explain suppression of the temperature-sensitive phenotype by the R64W substitution, in the R64WE189K variant.

4.5 An alternative mechanism for development of the temperature-sensitive phenotype

The apparent 20 to 25 fold increases in activity, as well as the compromised *in vitro* thermal stability observed for the R64WE189F and R64WE189K variants as compared to E189F, E189K, and E189, suggest that the severely reduced activity, displayed at both the permissive and restrictive temperatures, is more important for the development of the temperature-sensitive phenotype than is the small decrease in thermal stability as argued above. Furthermore, the data for the E189H and E189Q variants also make

the case against thermal stability, and for specific activity, as the predominant factor in the development of the temperature-sensitive phenotype. Although it cannot be completely excluded that compromised thermal stability contributes to development of the temperature-sensitive phenotype as well. Also, although there is an observed drop in activity from ~5% to approximately 2.5% for the E189K variant, and a similar 2 fold drop for the E189H variant at 37°C (Shan *et al.*, 2008) these 2 fold reductions in activity between the permissive and restrictive temperatures are not dramatic when compared to the 20 fold and 13 fold reduction in activity for E189K and E189H respectively, relative to native enzyme, that is even observed at permissive temperature (Shan *et al.*, 2008).

The predominant importance of the level of enzyme activity in defining the temperature-sensitive phenotype also is supported by the percent translation rate data for E189 and E189K conducted at 36°C, which shows a marked drop in overall translation within 30 min, for E189K (Peltz *et al.*, 1992). However, the cells continue to grow after 2 hrs at 36°C, and it is not until 5 hrs that the growth rates become negative, even though the translation data suggests that 0-10% translation is achieved after just 50 min (Peltz *et al.*, 1992). This indicates that although the general trend in the translation rate is reasonable, the translation rate values are not accurate. If the demand for mature tRNA is dramatically increased at 36°C, it is conceivable that large deficits, relative to the new demand rate, of one or more tRNA-activated amino acids can lower the rate of translation quickly, and result in the growth rate observed for the temperature-sensitive strain (Peltz *et al.*, 1992). Therefore, it appears that there may be a marked increase in the demand for mature tRNA at the restrictive temperature, and the inability of the temperature-sensitive variants to supply sufficient mature tRNA to meet this higher demand is responsible for the temperature-sensitive phenotype.

Also, the independence of temperature-sensitivity and its suppression, from enzyme thermal stability, makes a case against a misfolding induced heat-shock arrest based mechanism of temperature-

sensitivity (Trotter *et al.*, 2001). R64WE189F displays a high level of misfolding similar to that of E189F at 37°C, yet the former does not show the temperature-sensitive phenotype and the latter does (Table 4-1). Also, E189H shows low levels of misfolding that are comparable with that of the native enzyme, yet the E189H variant still displays the temperature-sensitive phenotype (Shan *et al.*, 2008).

Based on the available crystal structures, Shan *et al.* (2008) proposed that glutamate 189, which is located at the end of an outer β-strand, may hydrogen bond with other amino acids in the β-turn (Fig. 4-1), and that these interactions are important to enzyme structure and function.

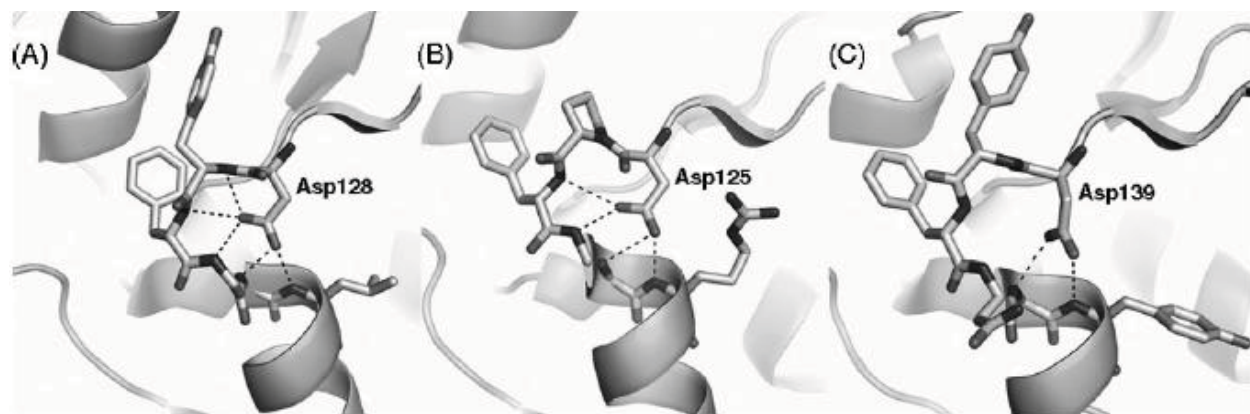


Fig. 4-1: PyMOL models of three crystallized tRNA nucleotidyltransferases illustrating hydrogen bond interactions that occur between the residue equivalent to position 189 and elements of the β-turn (Shan *et al.*, 2008). (A) *A. aeolicus*, (B) *B. stearothermophilus*, (C) *H. sapiens*, (-----) interatomic distances of $\leq 3.51 \text{ \AA}$.

I propose here that glutamate 189 may behave like a pin at the end of the β-strand, holding the highly conserved β-sheet in the proper conformation for activity and protein stability. Removal of this pin may contort the β-strand, to cause wide-spread misalignment effects that propagate through the β-sheet via the strand-to-strand hydrogen bonds, at least up to and including the β-strand containing arginine 64.

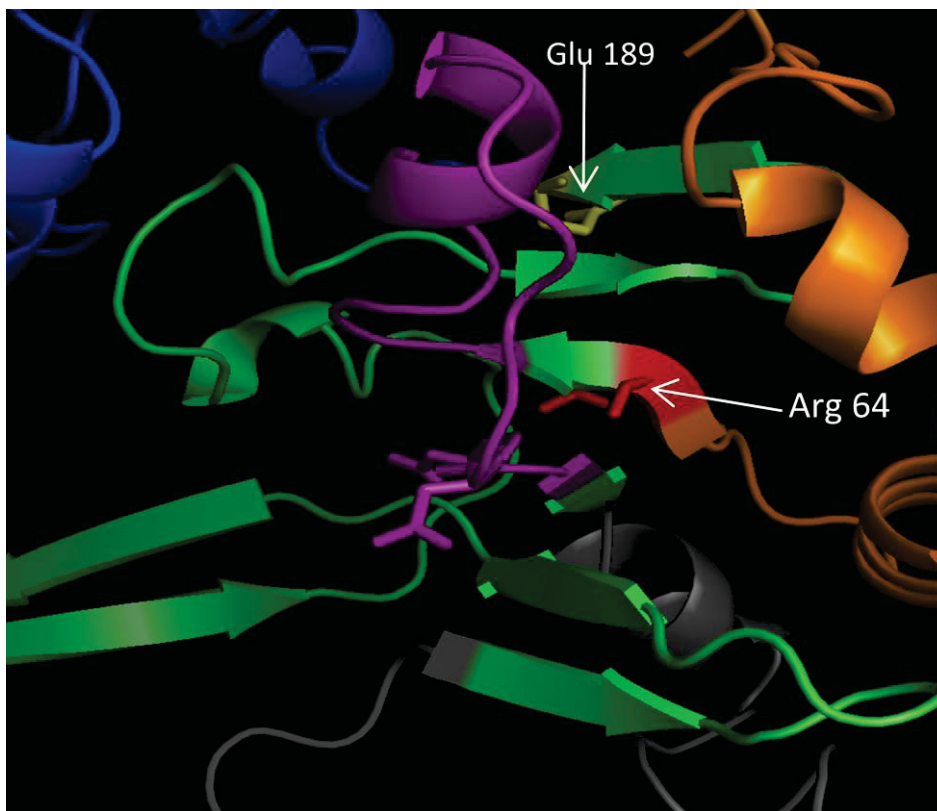


Fig.4-2: A cartoon representation of a model developed by PHYRE (<http://www.sbg.bio.ic.ac.uk/~phyre/>) of tRNA nucleotidyltransferase E189 from *Saccharomyces cerevisiae* (c1ou5A) based on the *H. sapiens* structure (1OU5). Shows proper alignment of the β -strands in the major β -sheet.

This contortion may move the β -strand bearing arginine 64 out of position, misaligning it from its proper position such that its dynamics may also be changed. The critically important motif A may be disturbed by these changes in a way that makes it unable to support its normal functions. These functions are likely to be vital since Motif A contains the carboxylate amino acids that are essential to chelate and activate the catalytic cations that are carried into the active site by the triphosphate moiety of the NTPs (Betat *et al.*, 2010). For instance, the ability for motif A to move the carboxylates into position to affect proper catalysis of any of the three nucleotidyltransferase reactions may be severely hindered. This would explain the greatly reduced capacity of E189F to add CMP or AMP to immature tRNA.

This contortion of the β -sheet may also explain how the redshift seen for R64WE189F and R64WE189K at 280 nm excitation is similar to that of E189F (Table. 3-1). The widespread β -sheet contortion may allow for increased solvent quenching to occur in the head-domain, and these contortions may only be slightly corrected in the double-variants.

The variants would also be expected to display similar CD spectra because the α -helical content would essentially remain high in the body and tail among the variants, and its intense signal would blind any changes which occurred in the β -sheet.

Furthermore, the loss in thermal stability may be due to the contortions of the β -sheet if it results in the weakening of non-covalent interactions between the strand bearing arginine 64 and the rest of the β -sheet. This may make it easier for the arginine 64-bearing β -strand, along with all of the residues N-terminal to position 64, to peel off from the rest of the protein, and thereby facilitate cooperative unfolding.

There are also functional implications for motif C generated by these data. The functional importance of motif C is not yet known (Betat *et al.*, 2010). Since glutamate 189 occurs in motif C however, the data suggest that motif C may play an indirect but important role in establishing the level of activity of tRNA nucleotidyltransferase, as well as in contributing to the thermal stability of the enzyme in the fashion delineated above.

There are alternative ts hypothesis that are not ruled out by the data that have been accumulated to date. It remains possible that temperature-sensitivity arises from a loss of fidelity in the polymerization reaction that may occur at restrictive temperatures but not at permissive temperatures.

Also, it has been proposed that temperature-sensitivity can be caused by changes in protein folding, proteolytic sensitivity, or altered protein-protein interactions (Chakshusmathi *et al.*, 2004). Although it is

known that small changes in tertiary structure do occur in the temperature-sensitive variants of tRNA nucleotidyltransferase, the double mutant suppressors show similar levels of change, and temperature-sensitivity has been demonstrated to occur independently of thermal stability. It is also possible that interactions between tRNA nucleotidyltransferase and other proteins have been changed as a result of the amino acid substitutions, or that oligomerization has been altered in a way that may result in the temperature-sensitive phenotype. Furthermore, a role for proteases in the development of temperature-sensitivity has not been explored. There is some indication that E189F and E189K do display an increased sensitivity to thrombin during protein purification (unpublished), therefore the possibility remains that increased sensitivity to cellular proteases, especially at the restrictive temperature, may result in the temperature-sensitive phenotype. However, this increased proteolytic sensitivity mechanism must be able to occur irrespective of enzyme thermal stability, in order to explain the E189H data. This potential mechanism of temperature-sensitivity may be explored by conducting a Western blot analysis of tRNA nucleotidyltransferase from wild-type and mutant cells, at both the permissive and restrictive temperatures.

4.6 Potential mechanism for suppression of the temperature-sensitive phenotype

Data for the R64WE189F and R64WE189K variants suggest that suppression of the temperature-sensitive phenotype is caused mainly by the restoration of specific activity to native-like levels (Tables 4-1 and 4-2). Although it is not unexpected that substitution mutations in motif A could alter specific activity, it is remarkable that the R64W substitution mutation results in an approximately 20-25 fold increase in specific activity over that of the corresponding E189F and E189K variants especially given that the R64W substitution alone does not appear to affect enzyme activity (Fig. 3-10 to 3-13). These

data support the hypothesis that motif A plays an important role in the catalytic mechanism (Betat *et al.*, 2010).

An attractive hypothesis is that there may be a hydrophobic pocket in the immediate vicinity of the side chain of arginine 64, and that tryptophan 64 is more capable of restoring the position and/or dynamics of motif A through hydrophobic interactions with this pocket. This is also supported by the fact that all of the tRNA nucleotidyltransferase sequences to date show that this equivalent position is occupied by either a tyrosine or an arginine. The R64W substitution may have proximal effects mostly restricted to the single β -strand and the rest of motif A, but not necessarily restoring much of the β -sheet alignment. However, the slightly improved T_m exhibited by the R64WE189K variant may suggest that more of the β -sheet is restored in this variant than in R64WE189F (Table 4-1). Also, this proposed hydrophobic pocket may accommodate tryptophan 64 well, and engage in enough hydrophobic interactions to explain how the R64W variant enzyme is thermally stabilized beyond that of even the native enzyme, with no apparent deleterious effect on the growth of the R64W mutant. However, it is somewhat surprising that the R64E substitution would be tolerated as well, since glutamate is a short, charged amino acid. Although arginine is also often charged, the charge is delocalized, and the long aliphatic R group may allow the charge to be positioned outside of the putative hydrophobic pocket.

Also, preliminary results suggest that an R64Q substitution mutation can suppress the temperature-sensitive phenotype as well (unpublished). The fact that a potentially hydrogen bond donating heteroatom is always located at the eta position for the native R64 enzyme, as well as R64W and R64Q, supports a potential role for hydrogen bond donation in suppression as well.

These data also support the possibility of indirect interaction between motif C and motif A, and suggest that the distorting effects originating from position 189 may reach at least as far as the motif A bearing β -strand in the β -sheet (Fig. 4-2). These data may implicate motif C in contributing to the

important role motif A plays in determining kinetic parameters (Betat *et al.*, 2010). This indirect interaction may allow for communication between motif C at the protein surface, and sites that more directly determine kinetic parameters e.g., active site residues, substrate binding regions, etc.

Also, other putative intragenic suppressors of the temperature-sensitive phenotype have been isolated recently (unpublished). Considering the increased thermal stability displayed by the R64W variant, these findings raise the intriguing question of whether or not it is possible to combine individual intragenic suppressor mutations to engineer enzymes with improved biophysical and kinetic properties.

5.0 CONCLUSIONS

The temperature-sensitive phenotype is associated with the severely reduced specific activity, and temperature-sensitivity suppression is associated with the restoration of specific activity to native-like levels for tRNA nucleotidyltransferase, irrespective of any changes observed in enzyme thermal stability *in vitro*. The severe reduction in specific activity appears to occur at each step of trinucleotide polymerization, and is therefore not caused by an inhibited capacity to switch from CMP addition to AMP addition. Although correlation does not imply causation, correlation is a necessary condition for causality. It is therefore possible that the temperature-sensitive phenotype may be brought about by a marked increase in the demand for mature tRNA which occurs between the permissive and restrictive temperatures, rather than through a much less marked loss in activity between those temperatures. According to this mechanism, it is the uncoupling of supply and demand that causes the reduced growth rates observed with temperature-sensitive mutants. Consequently, the temperature-sensitivity suppressors re-couple supply and demand by restoring specific activity to native-like levels.

The severely reduced reaction rate, and reduced thermal stability of E189F may be caused by a misalignment of motif A brought about by propagation of the original β -strand distortion at position 189, strand to strand through the β -sheet, to the β -strand bearing position 64 and motif A. However, a hydrophobic pocket located on the same face of the β -sheet as the arginine 64 side chain may allow the R64W substitution to restore the nucleotidyltransferase signature region; Motif A, to an active conformation, without significant restoration of *in vitro* thermal stability. This could leave enough contortion in the β -sheet of the double mutant enzymes, to preserve most or all of the thermal instability that characterizes the E189F and E189K variants.

It is also notable that specific activity and thermal stability have demonstrated the capacity to be mutually independent properties of the tRNA nucleotidyltransferase variants characterized in this study, and in previous work (Shan *et al.*, 2008).

6.0 FUTURE WORK

Liquid culture growth tests, quantitative activity assays, and thermal stability measurements should be conducted for the E189R variant enzyme and corresponding mutant strain. E189R is the least characterized of the five ts mutants. There is no biophysical information on this protein to date. It would be interesting to determine the level of specific activity exhibited by this variant; high, intermediate, or low, and whether or not this level of activity is proportional to the growth rate for the corresponding strain as determined by liquid media cultures at 37°C. Comparing the specific activity data with more quantitative liquid culture growth rate data accumulated at 37°C for this strain, offers another opportunity to test whether or not the growth rate at 37°C is indeed proportional to specific activity. Such a relationship would support the hypothesis that growth rate, and thereby the temperature-sensitive phenotype, is mainly dependent on the specific activity of tRNA nucleotidyltransferase, and therefore its capacity to meet the demand for mature tRNA, at 37°C.

Liquid culture growth studies and quantitative activity assays of R64W, R64WE189F, and R64WE189K would allow for the specific activities of these variants to be more accurately characterized, and to determine whether or not these activity levels are better or worse than that of the native enzyme. The degree to which changes in activity level and/or thermal stability translate to changes in cell viability as determined by cell growth rate can then be more accurately assessed. Also, liquid culture growth studies and quantitative activity assays conducted on the R64E mutant and corresponding variant enzyme, would allow for a similar assessment of this strain, thereby providing an indication of how well glutamate is tolerated at position 64. However, viable counts should also be conducted for all of the strains mentioned above at 22°C and 37°C in order to determine cell viability accurately at both permissive and restrictive temperature.

Growth, biophysical, and activity studies should be conducted on the newly discovered putative ts suppressor mutants to determine if they also appear to suppress the ts phenotype in a fashion similar to R64WE189F and R64WE189K.

However, activity assays should be conducted on all of the variants and the native enzyme in order to determine V_{max} and K_m for each. Substrate binding studies for these enzymes should also be carried out with tRNA and the NTP substrates. The activity assays and binding studies together will establish the role that each of these factors play in determining the activity levels of the variants.

It is also important to explore the relationship between temperature-sensitivity, thermal stability and proteolysis. The degree of thrombin sensitivity should be characterized for the two variants (E189F and E189K) for which there is evidence of increased thrombin sensitivity. It would also be interesting to know if any of the other temperature-sensitive variants; E189H, E189Q, and E189R, are also thrombin sensitive, and to characterize this thrombin sensitivity if applicable. However, ultimately the level of proteolysis should be characterized by Western blot of tRNA nucleotidyltransferase from extracts of the various *Saccharomyces cerevisiae* mutant and wild-type cells, at the restrictive and permissive temperatures. These studies may also reveal differences in enzyme expression level between the wild-type and various mutant strains at the permissive and restrictive temperatures, if differences do indeed occur.

The temperature-sensitive phenotype and the suppressor phenotype should be characterized through microscopic studies of all available mutants. Such studies may help explain the differences in optical density observed in growth studies at 37°C, as well as provide insight into the role of cell death in the temperature-sensitive phenotype.

Another alternative temperature-sensitivity mechanism involves the potential loss of fidelity in the polymerization reaction at restrictive temperature. This mechanism can be explored by allowing activity

assays to proceed long enough to produce 76 nucleotide products, perhaps 10-15 min at 22°C and 37°C. Subsequently, the products can be PCR amplified and sequenced to determine the 3' trinucleotide ends produced, and their proportions.

Motif C is an attractive site for protein-protein interactions that may augment specific activity. A search for extragenic temperature-sensitivity suppressors may facilitate the discovery of novel protein-protein interactions.

It is likely that there are important changes in the β -sheet structure for the reasons delineated above. Fourier Transform Infrared Spectroscopy (FTIR) conducted on the native and variant enzymes would allow for changes in β -sheet content to be revealed, and is one of the best ways to elucidate these changes. However, the best way to reveal all of the structural changes that have occurred in the enzyme as a result of the substitution mutations would be to conduct X-ray diffraction studies on crystals of the native and variant enzymes.

7.0 REFERENCES

- Aebi M, Kirchner G, Chen JY, Vijayraghavan U, Jacobson A, Martin NC, Abelson J. Isolation of a temperature-sensitive mutant with an altered tRNA nucleotidyltransferase and cloning of the gene encoding tRNA nucleotidyltransferase in the yeast *Saccharomyces cerevisiae*. *J Biol Chem.* 1990 Sep 25; 265 (27) :16216-20. PubMed PMID:2204621.
- Augustin MA, Reichert AS, Betat H, Huber R, Mörl M, Steegborn C. Crystal structure of the human CCA-adding enzyme: insights into template-independent polymerization. *J Mol Biol.* 2003 May 16;328(5):985-94. PubMed PMID: 12729736.
- Ben-Aroya S, Coombes C, Kwok T, O'Donnell KA, Boeke JD, Hieter P. Toward a comprehensive temperature-sensitive mutant repository of the essential genes of *Saccharomyces cerevisiae*. *Mol Cell.* 2008 Apr 25; 30 (2) :248-58. PubMed PMID:18439903.
- Bennett-Lovsey RM, Herbert AD, Sternberg MJ, Kelley LA. Exploring the extremes of sequence/structure space with ensemble fold recognition in the program Phyre. *Proteins.* 2008 Feb 15; 70 (3) :611-25. PubMed PMID:17876813.
- Betat H, Rammelt C, Mörl M. tRNA nucleotidyltransferases: ancient catalysts with an unusual mechanism of polymerization. *Cell Mol Life Sci.* 2010 May; 67 (9) :1447-63. PubMed PMID:20155482.
- Chakshusmathi G, Mondal K, Lakshmi GS, Singh G, Roy A, Ch RB, Madhusudhanan S, Varadarajan R. Design of temperature-sensitive mutants solely from amino acid sequence. *Proc Natl Acad Sci U S A.* 2004 May 25; 101 (21) :7925-30. PubMed PMID:15148363; PubMed Central PMCID: PMC419533.
- Chou JY. Simian virus 40 mutants carrying two temperature-sensitive mutations. *J Virol.* 1976 Oct; 20 (1) :39-44. PubMed PMID:185417; PubMed Central PMCID: PMC354963.
- Creighton, T. E. (1989). Protein structure: a practical approach. IRL. Oxford University Press.
- Creighton, T.E. (1993). Proteins: structures and molecular properties. 2nd ed., W.H. Freeman and company, New York.
- De Lano, W.L. (2009). PyMOL Molecular Graphics System. De Lano Scientific. LLC. @ www.pymol.org
- Dieterle MG, Wiest AE, Plamann M, McCluskey K. Characterization of the temperature-sensitive mutations un-7 and png-1 in *Neurospora crassa*. *PLoS One.* 2010 May 18; 5 (5) :e10703. PubMed PMID:20502699; PubMed Central PMCID: PMC2872674.
- Hashimoto K, Kato Z, Nagase T, Shimozawa N, Kuwata K, Omoya K, Li A, Matsukuma E, Yamamoto Y, Ohnishi H, Tochio H, Shirakawa M, Suzuki Y, Wanders RJ, Kondo N. Molecular mechanism of a temperature-sensitive phenotype in peroxisomal biogenesis disorder. *Pediatr Res.* 2005 Aug; 58 (2) :263-9. PubMed PMID:16006427.
- Hoffmeier A, Betat H, Bluschke A, Günther R, Junghanns S, Hofmann HJ, Mörl M. Unusual evolution of a catalytic core element in CCA-adding enzymes. *Nucleic Acids Res.* 2010 Jul; 38 (13) :4436-47. PubMed PMID:20348137; PubMed Central PMCID: PMC2910056.

- Imamura A, Shimozawa N, Suzuki Y, Zhang Z, Tsukamoto T, Fujiki Y, Orii T, Osumi T, Wanders RJ, Kondo N. Temperature-sensitive mutation of PEX6 in peroxisome biogenesis disorders in complementation group C (CG-C): comparative study of PEX6 and PEX1. *Pediatr Res.* 2000 Oct; 48 (4) :541-5. PubMed PMID:11004248.
- Larkin MA, Blackshields G, Brown NP, Chenna R, McGgettigan PA, McWilliam H, Valentin F, Wallace IM, Wilm A, Lopez R, Thompson JD, Gibson TJ, Higgins DG. Clustal W and Clustal X version 20. *Bioinformatics*. 2007 Nov 1; 23 (21) :2947-8. PubMed PMID:17846036.
- Levinger L, Mörl M, Florentz C. Mitochondrial tRNA 3' end metabolism and human disease. *Nucleic Acids Res.* 2004; 32 (18) :5430-41. PubMed PMID:15477393; PubMed Central PMCID: PMC524294.
- Li F, Xiong Y, Wang J, Cho HD, Tomita K, Weiner AM, Steitz TA. Crystal structures of the *Bacillus stearothermophilus* CCA-adding enzyme and its complexes with ATP or CTP. *Cell.* 2002 Dec 13; 111 (6) :815-24. PubMed PMID:12526808.
- Murphy BR, Hosier NT, Chanock RM. Temperature-sensitive mutants of influenza A virus: transfer of the two temperature-sensitive lesions in the Udorn/72-ts-1A2 virus to the A2Hong Kong/123/77 (H1N1) wild-type virus. *Infect Immun.* 1980 Jun; 28 (3) :792-8. PubMed PMID:7399695; PubMed Central PMCID: PMC551020.
- Neuenfeldt A, Just A, Betat H, Mörl M. Evolution of tRNA nucleotidyltransferases: a small deletion generated CC-adding enzymes. *Proc Natl Acad Sci U S A.* 2008 Jun 10; 105 (23) :7953-8. PubMed PMID:18523015; PubMed Central PMCID: PMC2430343.
- Peattie DA. Direct chemical method for sequencing RNA. *Proc Natl Acad Sci U S A.* 1979 Apr;76(4):1760-4. PubMed PMID: 377283; PubMed Central PMCID: PMC383470.
- Peixoto AA, Hall JC. Analysis of temperature-sensitive mutants reveals new genes involved in the courtship song of *Drosophila*. *Genetics.* 1998 Feb; 148 (2) :827-38. PubMed PMID:9504928; PubMed Central PMCID: PMC1459814.
- Peltz SW, Donahue JL, Jacobson A. A mutation in the tRNA nucleotidyltransferase gene promotes stabilization of mRNAs in *Saccharomyces cerevisiae*. *Mol Cell Biol.* 1992 Dec; 12 (12) :5778-84. PubMed PMID:1448105; PubMed Central PMCID: PMC360517.
- Pickett FB, Champagne MM, Meeks-Wagner DR. Temperature-sensitive mutations that arrest *Arabidopsis* shoot development. *Development.* 1996 Dec; 122 (12) :3799-807. PubMed PMID:9012501.
- Sambrook, J., Maniatis, T., Fritch, E.F. (1989). Molecular Cloning 2nd Ed., Cold Spring Harbor Laboratory Press.
- Shan X, Russell TA, Paul SM, Kushner DB, Joyce PB. Characterization of a temperature-sensitive mutation that impairs the function of yeast tRNA nucleotidyltransferase. *Yeast.* 2008 Mar; 25 (3) :219-33. PubMed PMID:18302315.
- Steitz TA. A mechanism for all polymerases. *Nature.* 1998 Jan 15; 391 (6664) :231-2. PubMed PMID:9440683.

- Toh Y, Takeshita D, Numata T, Fukai S, Nureki O, Tomita K. Mechanism for the definition of elongation and termination by the class II CCA-adding enzyme. *EMBO J.* 2009 Nov 4;28(21):3353-65. Epub 2009 Sep 10. PubMed PMID: 19745807; PubMed Central PMCID: PMC2776095.
- Trotter EW, Berenfeld L, Krause SA, Petsko GA, Gray JV. Protein misfolding and temperature up-shift cause G1 arrest via a common mechanism dependent on heat shock factor in *Saccharomyces cerevisiae*. *Proc Natl Acad Sci U S A.* 2001 Jun 19; 98 (13) :7313-8. PubMed PMID:11416208; PubMed Central PMCID: PMC34665.
- Voet. D., and Voet. J.G. (1995). *Biochemistry*. John Wiley & Sons, Inc, Newyork.
- Weiner AM. tRNA maturation: RNA polymerization without a nucleic acid template. *Curr Biol.* 2004 Oct 26; 14 (20) :R883-5. PubMed PMID:15498478.
- Wong C, Sridhara S, Bardwell JC, Jakob U. Heating greatly speeds Coomassie blue staining and destaining. *Biotechniques.* 2000 Mar;28(3):426-8, 430, 432. PubMed PMID: 10723553.
- Xiong Y, Li F, Wang J, Weiner AM, Steitz TA. Crystal structures of an archaeal class I CCA-adding enzyme and its nucleotide complexes. *Mol Cell.* 2003 Nov; 12 (5) :1165-72. PubMed PMID:14636575.

8.0 APPENDIX

8.1 A GST-fusion protein purification protocol (*by Mark Goring*)

- 1) Prepare 5 ml cultures of YT medium @ 100 µg/ml ampicillin. Inoculate these cultures with the appropriate strain, and place them in the shaker incubator overnight at 37°C. Prepare 1.3 l cultures of YT medium @ 50 µg/ml ampicillin in Fernbach flasks. Use the 30 min liquid cycle to autoclave these 1.3 l cultures. Place these autoclaved cultures on a bench to cool overnight.

Note: All of the following steps must be conducted aseptically.

Add stock ampicillin to the 1.3 l cultures to establish a final ampicillin concentration of 50 µg/ml. Inoculate the 1.3 l cultures by adding 5 ml of overnight culture to each 1.3 l fernbach flask of fresh media. Incubate at 37°C and 225 rpm until OD₆₀₀ 0.4-0.5. This may take approximately 2.5 hrs.

- 2) Add stock IPTG to 1.3 l cultures to a final concentration of 1 mM. Incubate the cultures at 18°C and 225 rpm overnight for 16 hrs.

Note: All of the following steps do not need to be conducted aseptically.

- 3) Place the cultures on ice and pellet the cells by repeated centrifugation for 15 min at 6000 rpm and 4°C in a JA-10 rotor. Store final pellet at -80°C until ready to purify protein. The empty weight of the centrifuge bottle used to store the final pellet, and the weight of centrifuge bottle with the pellet should be obtained so that the weight of the pellet can be estimated.
- 4) Allow the pellet to defrost on ice for 30-60 min. Add a volume of lysis buffer to the pellet that is numerically equal to the estimated mass of the pellet in grams. Add 50 µl of Amresco bacterial protease inhibitor cocktail for every 4 g of pellet mass as well. Suspend the pellet by vortexing and shaking. Lyse cells using the french press by passing the sample through 3 times. **Remember to keep the lysate on ice whenever possible.**
- 5) Centrifuge the lysate at 18 000 rpm for 40 min in a JA-20. Carefully transfer only the supernatant to a clean centrifuge tube, and repeat the centrifugation using the same conditions. Transfer this twice centrifuged supernatant to a clean tube, again being careful not to transfer any cell debris with it. **Remember to keep the lysate on ice whenever possible.**
- 6) Load the column by pouring the twice centrifuged cell lysate onto the beads, and seal the column. Fasten the agarose bead column containing the cell lysate onto the rotary mixer using rubber bands, and allow it to rotate overnight at 4°C.

- 7) Place the column up right and allow the beads to settle by gravity for 30 min.
- 8) Use a bulb to force out the remaining cell lysate, leaving no more than a few millimeters of lysate above the surface of the beads. This is done in order to ensure that the beads are never directly exposed to air. **Such exposure should be guarded against at all stages of use, or storage of the beads.**
- 9) Connect the pump to the column and set it up to wash the loaded beads at a pump setting of 3 mls/min. A total volume of 500 ml of 1xPBS @ pH 7.3 should be used to wash the beads. However, the entire flow-through should be collected in alternating fractions of 5 ml and 50ml in clean falcon tubes, starting with a 5 ml fraction. This should amount to 19 falcon tubes in total. The first and last 5 ml fractions, as well as several 5 ml fractions in between, should then be chosen for sampling in order to assess the protein content in the flow-through from the beginning to the end of the wash, e.g. fractions 1, 3, 7, 9, 11, 15, 17, and 19. 16 μ l aliquots of each chosen fraction should then be examined by SDS-PAGE. If the final lane (corresponding to fraction 19) is clear, continue with the purification. If not, the wash should be continued and assessed by SDS-PAGE once again in order to determine wash effectiveness.
- 10) Pump out all of the remaining wash buffer using a bulb. Fill the column with elution/cleavage buffer (50 mM Tris-HCl + 140 mM NaCl + 15 mM glutathione + 2.5 mM CaCl₂ @ pH 8.0) and elute slowly by pumping out the elution/cleavage buffer using a bulb. Collect 16 ml of eluate in 1 ml fractions, and test fractions 1, 3, 5, 7, 9, 11, 13, and 16 for protein content by SDS-PAGE.
- 11) Pool the most concentrated fractions, and quantify the total protein content in the pool using a Bradford assay. Save 50 μ l of the pooled protein on ice in the cold room in order to help assess the progress of protein cleavage at a later step. Transfer the pooled protein to a 6-8 kDa dialysis tube, and add a mass of thrombin that is 1000 fold less than that of the total protein content in the pool. Seal the 6-8 kDa dialysis tube and place it, along with a large stir bar, into 4 l of cold Tris-HCl/NaCl buffer (50 mM Tris-HCl + 140 mM NaCl @ pH 8.0). Dialyze for approximately 24 hrs. **4 l dialysis buffers should be prepared the day before and left to chill overnight in the cold room. Final pH adjustments can be made the following day. This is especially true for Tris-HCl buffers which require the pH to be adjusted while at its working temperature; which is 4°C in this case.**
- 12) Assess the proportion of protein cleaved by SDS-PAGE after the 24 hr incubation @ 4°C. To do this run a 16 μ l aliquot of the thrombin treated protein pool, and use 16 μ l of the protein saved in step 11 as the control in this assessment. If the proportion of cleavage appears to be high enough i.e. >90%, continue with the following steps of the purification. If cleavage should be continued, add more thrombin according to the proportion of cleavage observed; usually 10 μ l is enough, and place the dialysis tube back into the Tris-HCl/NaCl buffer overnight.
- 13) Transfer the pooled sample to 50 kDa dialysis tubing, seal and place the tube into 4 l of cold 1xPBS @ pH 7.3 to dialyze at 4°C overnight. Repeat the dialysis the following day by placing the

dialysis tube into fresh 1xPBS to dialyze overnight. The dialysis in 1xPBS is conducted in order to remove glutathione and thrombin, as well as to change the buffer and pH.

- 14) Regenerate the beads in the column. Place the column on a stand at room temperature, and allow it to warm for a couple of hours. Allow solutions of 25 mM Glutathione, 1% Triton X 100 (v/v), 70% ethanol (v/v), and 1xPBS @ pH 7.3 to warm to room temperature as well. Ensure that there is only a few millimeters of fluid remaining above the beads, and then add 3 ml of Gdn-HCl (which is always kept at room temperature). Suspend the beads in this volume by gently rocking the column back and forward. Allow the suspended beads to stand for a few minutes, and then pump out the Gdn-HCl until only a few millimeters remain above the beads. Fill the column with 1xPBS and suspend the beads in it. Pump out the 1xPBS using a bulb, again until only a few millimeters remain. Repeat this step with 1xPBS twice more, evacuate the column until only a few millimeters remain above the beads, and add 3 ml of 25 mM glutathione. Suspend the beads in this volume, and let it stand for a few minutes. Evacuate the column until only a few millimeters of glutathione remain above the beads, and then repeat the 1xPBS wash. Treat the beads with 3 ml of Triton X 100, and repeat the 1xPBS wash in the same manner. However, the 1xPBS wash should be conducted a total of 4 times instead of 3 times at this point. Finally, treat the beads with 3 ml of 70% ethanol, and conduct the wash with 1xPBS in a similar fashion. The column can then be filled half way with 1xPBS and connected to the pump in the cold room. Set up the pump to rinse the beads at 3 ml/min with 500-600 ml of cold 1xPBS @ pH 7.3. The beads are now regenerated and rinsed.
- 15) Load the pooled sample onto the regenerated and rinsed beads of the column, and use a bulb to push out the protein into a clean vessel, e.g. falcon tube or small flask. Reload the protein sample onto the beads in the column, and repeat the cycle 5-15 times. Use SDS-PAGE to judge the progress of GST-tag removal. Take small samples (50 µl) of the protein after several cycles. Conduct an SDS-PAGE analysis of the protein sample in order to access the level of GST remaining in the sample. If sufficient GST has been removed from the protein pool, the protein can be stored. If unacceptable levels of GST remain, continue cycling the protein. The beads can even be regenerated once again, and the cycles repeated if necessary.
- 16) Pump the protein out of the column using a bulb until only a few millimeters remain above the beads. Microcentrifuge the entire protein sample at 14 000 rpm and 4°C for 5 min in order to pellet any debris. Collect the supernatant into a clean falcon tube. Add ultrapure glycerol to the total volume of collected protein until a final concentration of 10% glycerol (v/v) is reached. Dissolve the glycerol into the protein solution by slowly pipetting up and down, taking care not to produce bubbles or foaming. The protein is now ready to be stored in small aliquots (50-200 µl), at -80°C.

8.2 Raw protein thermal denaturation profile data

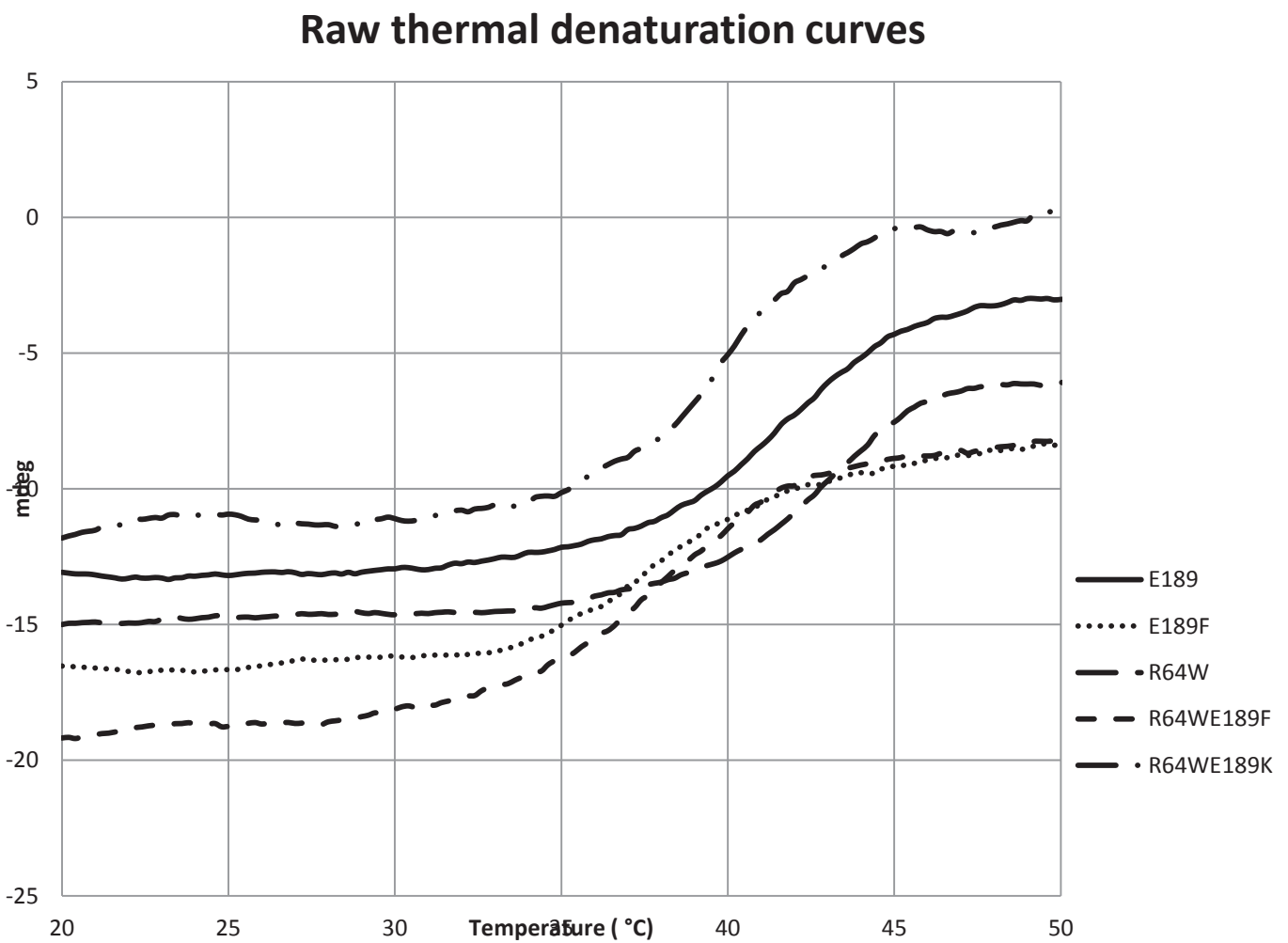


Fig. 8-2: Raw protein thermal denaturation profile data.

8.3 Equation used to develop the ‘fraction unfolded vs. temperature’ protein thermal denaturation curve

After smoothing the protein thermal denaturation curve with the Means Movement algorithm, the following linear equation (1) was used to convert the raw ellipticity data (θ), into fraction unfolded; F , in a spreadsheet.

$$(1) \quad F = 1/\Delta\theta_T \times \theta - \theta_i/\Delta\theta_T$$

F is the fraction of protein unfolded, θ is ellipticity measured in mdeg, and $\Delta\theta_T$ is the total change in ellipticity between the initial and final temperatures of interest; $\Delta\theta_T = \theta_f - \theta_i$. θ_i is the ellipticity value at the start temperature of interest (20°C for this study), and θ_f is the final ellipticity value at the end temperature of interest (50°C for this study).